AARHUS UNIVERSITY

UNIVERSITY OF COPENHAGEN

Technical University of Denmark

DTU

GEUS

AALBORG UNIVERSITY
DENMARK

Radical Innovation

Results of the Radical Innovation Sprint 2017

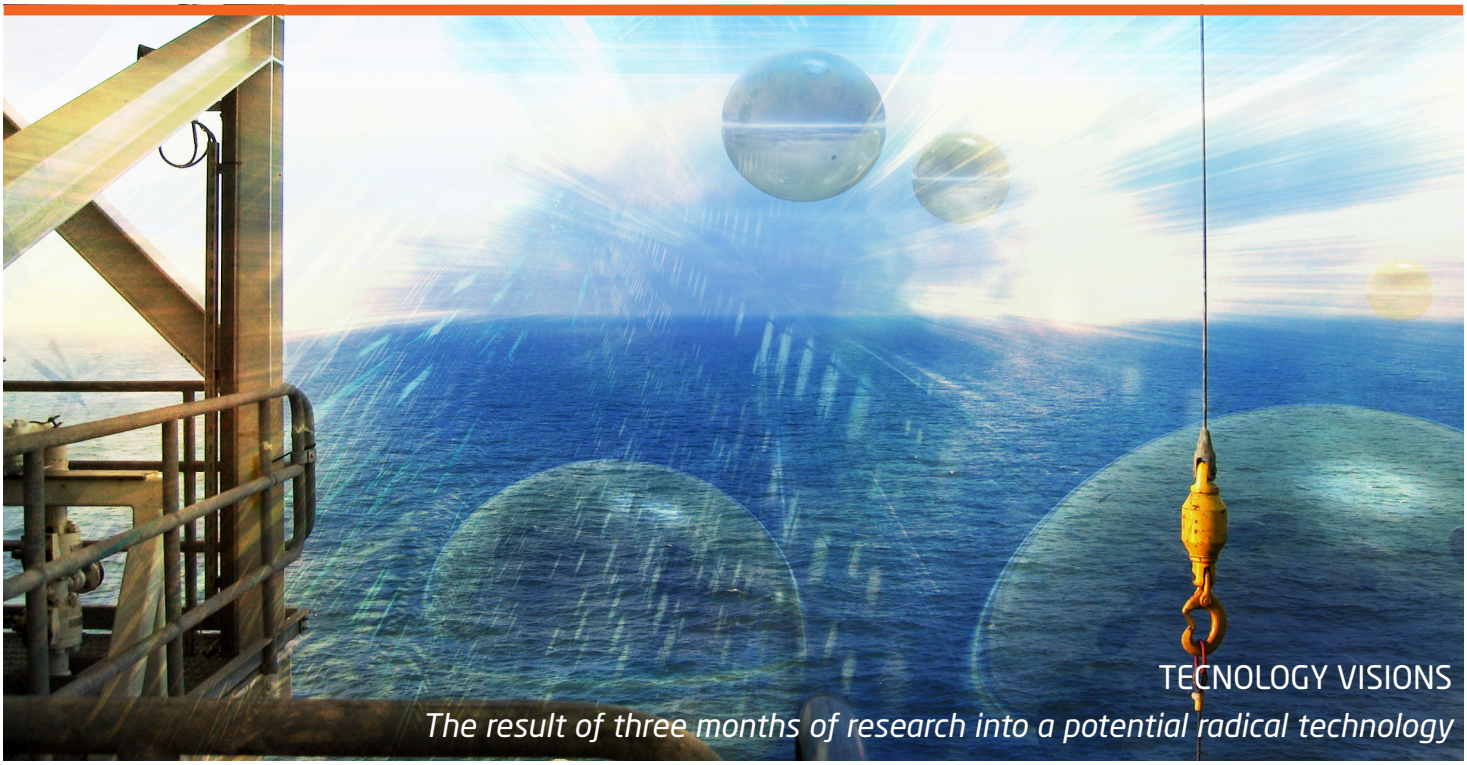

Centre for Oil and Gas - DTU
The Danish Hydrocarbon Research and Technology Centre

Are you longing for radical thinking?
Go seek the crazy thoughts
Some will grow into visions
others will fade away
The skilled will fail very quickly
leaving the rest to come
Start the radical movement
then the success will come

K. Scott

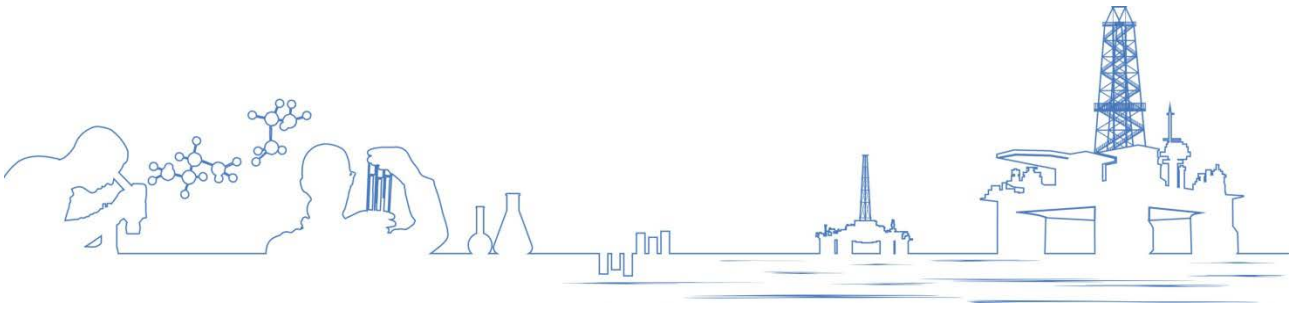

Preface

This book presents the results of the first DHRTC Radical innovation sprint, which was conducted over a 3 months period from September to December 2017. The book provides an overview of the technology visions and results of three months research effort into 10 ideas, which were funded. Further 2 ideas are under evaluation for patenting and one is omitted for commercial reasons and they can therefore not be published.

Defining if an idea is radical is not a simple task, what seems radical to one person may seem utterly incremental to another – it all depends on context. In order to ensure a solid selection process we have asked an assessment committee with representatives from academia and from the oil industry to advice on the selection of ideas. All ideas that have been funded have a radical aspect to some or all the members of the assessment committee. This radical aspect could be anything from a detail (e.g *Deep Reach Through Acid Encapsulation and Wormhole Propagation*), a new research approach (e.g. *Are there common genes for MEOR under pressure?*) or an entirely new idea (e.g. *Next generation liquid-repelling surface for improved oil flow*).

The result of working a radical idea is frequently a discovery of **why** this idea will **not** work - often when the idea fail in the first research test. Such discoveries are very important learnings that are a necessary part of any innovative process – radical or not. Without numerous such 'negative' research learnings we would probably rarely arrive at truly radical solutions. A steep learning curve where you spot the dead ends early is essential for a radical success. Therefore, at DHRTC we are grateful for all the research learnings presented in this book.

The oil and gas industry is technologically a relatively conservative industry, which has traditionally been inclined to stick with the technologies that are known to work. At DHRTC we expect that, partly for that reason, there may be many ideas that, even though they may appear radical to the O&G industry, are part of everyday practice in other areas of research or industries. An example of this is robot and sensor technologies which are widely used in e.g. the car industry, but which has just not really made it into the O&G industry yet. At DHRTC we believe that such technology fits that just need to be identified are abundant, and that often a three months workover may be enough to move a technology sufficiently forward for it to get the attention of the O&G industry.

DHRTC thanks all who submitted ideas for the radical sprint in 2017 and we hope that they and others will support the concept by submitting new radical ideas for the 2018 DHRTC radical sprint. Finally DHRTC would like to thank the members of the assessment committee for their effort in identifying the right ideas.

Lars Simonsen

R&D Director, DHRTC

Content

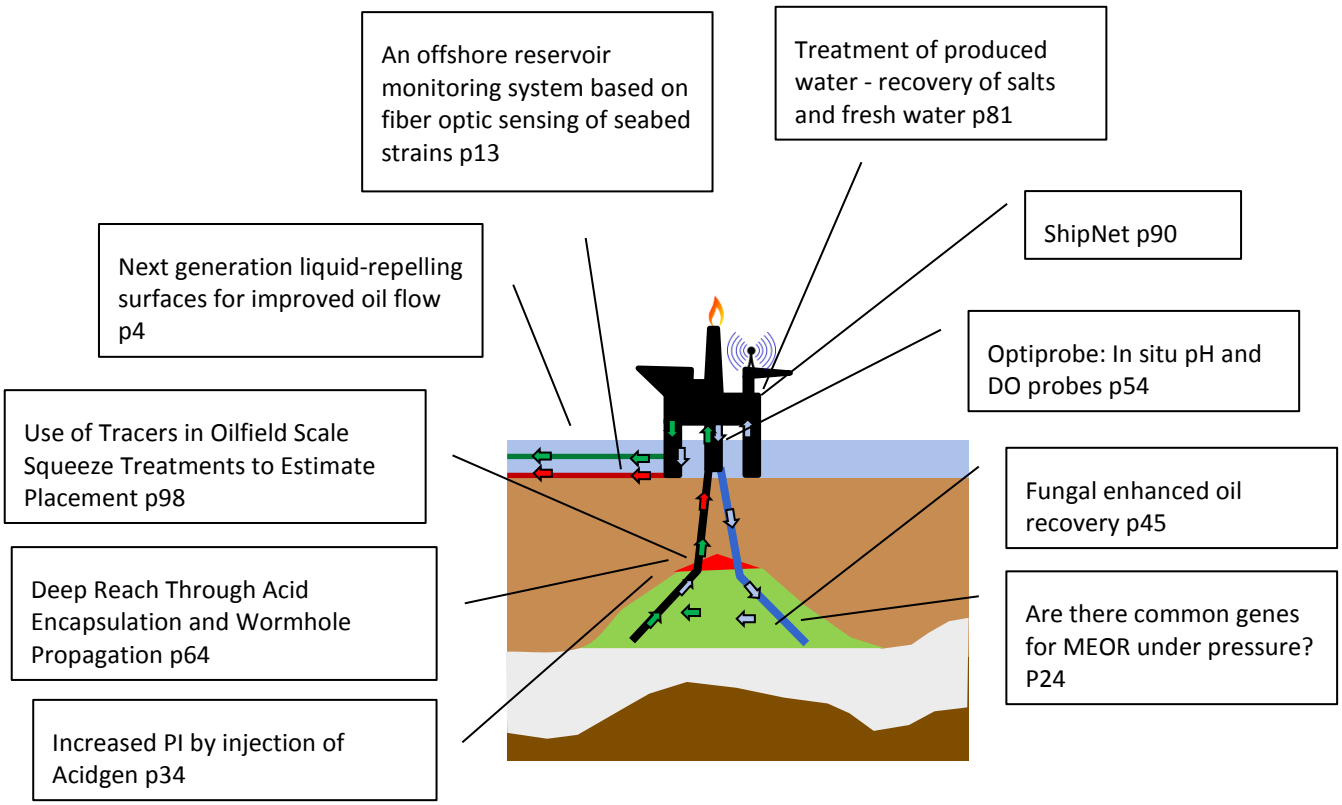

Introduction

Lene Hjelm Poulsen and Kristine Wille Hilstrøm, DHRTC, DTU

In the spring of 2017 DHRTC made their first call for radical ideas. The call resulted in 53 ideas of which 13 ideas were selected for funding of a three month research sprint to mature the idea. 2 of the ideas are under evaluation for patenting and one is omitted for commercial reasons and thus it is why only 10 of the ideas that are presented in this book.

Given the complexity of evaluating potentially very radical ideas it was decided to engage with a number of external specialists from academia and from the industry to assist inthe evaluation process. The assessment committee consisted of two oil and gas industry professionals, two researchers from the DHRTC network and one private consultant with more than 30 years of oil and gas industry experience. The committee was given the task of ranking all incoming idea proposals in three categories based on a set of selection criteria's and two definitions of radical innovation. All 53 ideas were fully anonymized prior to being evaluated.

The selection criteria's were:

- Is the idea radical?[1]
- How clear is the idea?
- How relevant is the idea?
- How dramatically could the idea impact the Danish oil and gas industry?
- How likely is it that the idea is matured successfully?
- What is the realistic time frame for the proposed sprint research in your opinion?

Based on a written recommendation from the assessment committee DHRTC sanctioned that 13 potentially radical ideas received funding for a three month research sprint.

The research was carried out in the fall between 1st of September to 1st of December 2017. During this time the ideas were matured by trying to envisage a technology vision and by conducting initial research in order to validate the potential of the idea e.g. testing likely showstoppers. The deliverables were a report (app. 10 pages), a presentation and an elevator pitch which for all projects were submitted to DHRTC 1st of December 2017.

By the end of the sprint the ideas were divided into three categories:

[1] The following definitions of radical innovation were applied:
Radical Innovation: radical innovation results from discontinuous change – that is, the innovation could not result from a linear extrapolation or progression from the initial conditions [1]
Radical Innovation,…., is novel, surprising and different in approach or composition. Scientific inventions belong to this category. Often radical innovation is based on the convergence of several different kinds of knowledge [2]

1) Ideas that potentially are patentable,

2) Ideas that are a technical success and which potentially have a line of sight to application in the oil and gas industry

3) Ideas that can be considered a valuable research learning.

Three ideas are categorized as potentially patentable, and these ideas are currently being screened for patenting. These ideas are consequently not published in this book. The funding by DHRTC of the radical sprint is a one-off financing and all researchers can freely seek funding for further maturation of their ideas

References

[1] The Open University, OpenLearning ((2006) Radical Innovation, www.open.edu/openlearn/money-management/management/technology-management/radical-innovation.

[2] shortened version after Darsø, L. (2011) Innovationspædagogik - kunsten at fremelske innovationskompetence. Samfunds Litteratur 192, s 27.

Next generation liquid-repelling surfaces for improved oil flow

Johannes Franz & Tobias Weidner, Aarhus Universitet

Abstract

Pipelines are the very heart of crude oil production, from the oilfield over processing, service to delivery. However, oil flow within pipelines is determined by friction at the material surface. We develop next generation liquid-repelling surfaces to optimize oil flow by drag reduction. Reduced friction within pipelines would allow faster pump rates. Moreover, our liquid-repelling surfaces are self-cleaning and may protect pipelines from scale formation, biofouling and corrosion, which could be key to prolong maintenance intervals or even extend the lifetime of pipelines. Therefore, we established an experimental approach to perform flow experiments. The originally proposed soot-based surfaces were not able to withstand oil impalement during flow experiments. Instead, we developed a different approach mimicking liquid-infused slippery surfaces from pitcher plants. With a well-defined pillar model system, we determine the optimal structure size for a stable water lubricant layer during oil flow has. Moreover, an extensive outlook is given about future directions for this topic.

Technology vision

What can the technology do? What are the technical advantages in oil production, what can be achieved by reducing surface friction and describe how this can lower costs!

Oil flow within pipelines is determined by friction at the material surface. Inspired by nature, we develop next generation liquid-repelling surfaces to optimize oil flow by drag reduction. (Figure 1). Moreover, liquid-repelling surfaces may protect the pipeline surface from scale formation, biofouling and corrosion, prolonging maintenance intervals.

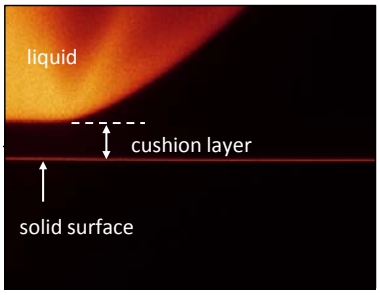

FIGURE 1 | Approach for liquid repelling surfaces. Transferring natural liquid-repelling mechanisms to pipeline surfaces.

What does the technology look like when it is installed / used in oil and gas production in the North Sea?

Basically, this is a few micrometer thin coating on the inner surface of a pipeline, which is neither visible by eye nor does it substantially decrease the diameter of the pipeline.

How to implement / install the technology?

For the nano-structures, it will be possible to install the coatings in post-production processing in a very convenient, self-assembling way. Therefore, on site implementation should also be possible by flushing pipelines with the respective chemicals, although thoroughly cleaned pipeline surfaces might be a precondition for successful layer formation.

What actions can be taken when the technology is installed?

This depends on the shear rates in the pipeline and the chemical composition of the flowing liquid. Since the chemically synthesized and self-assembled structure is per se stable, a low maintenance coating is possible. However, the lifetime of the lubricant layer remains to be determined in long-term experiments.

How can the technology be maintained/ repaired if it breaks down?

The coating consists out of two parts, i.e. the chemically synthesized structure and the lubricant layer. Defects in the structure can be very easily repaired by repeating the synthesis. This can be done, for instance, by flushing the pipeline with the chemical solution. The lubricant layer can also easily be renewed by rinsing the chemical structure with the lubricant solution. We can already show that gas bubbles are not a problem for the lubricant stability. However, since first wetting is crucial, contamination from crude oil impaling into the layer might compete with the lubricant solution. This has to be checked in future experiments.

Validation of technology

Validated during sprint

Which part of the technology has been validated?

The originally proposed soot-based surfaces were not able to withstand oil impalement during flow experiments (Figure 2). Instead, we developed a different approach using slippery surfaces (Figure 3). Pitcher plants have leaves known as pitfall traps. Moistened by condensation or nectar, the rim of the pitcher is slippery causing insects to fall into the trap. We mimic nature and copy those surface properties to develop liquid-infused slippery surfaces for industrial application. We show that those surfaces are indeed a promising approach to achieve drag reduction being able to repel both, oil and water and being mechanically stable during oil flow.

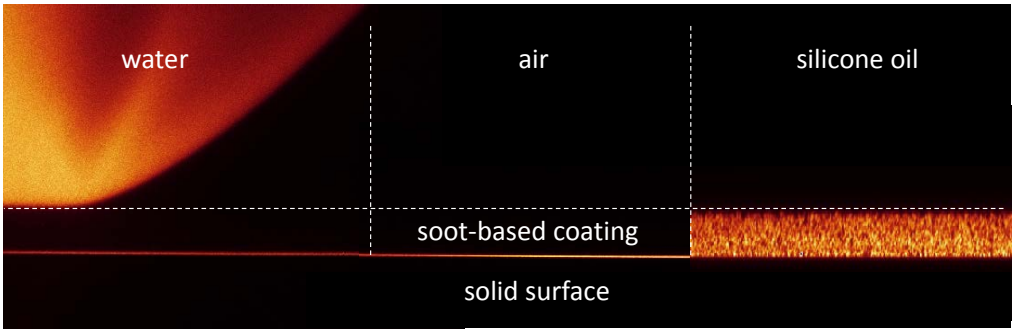

FIGURE 2 | Oil impalement into soot-based superamphiphobic surfaces.

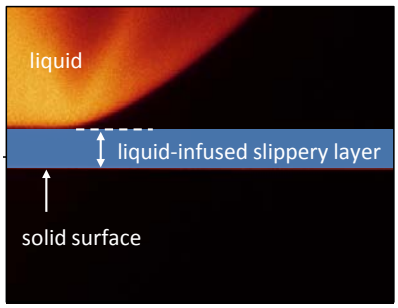

FIGURE 3 | Liquid-infused slippery surfaces. Applying the surface properties of pitcher plants to pipeline surfaces to generate liquid-infused slippery surfaces.

How was this part of the technology validated?

We developed an approach to perform and monitor flow experiments. The three major hurdles were continuous pressure generation, building a robust flow cell and establish an experiment to measure the effects of liquid flow on solid surfaces. We purchased a high performance Plug and Play flow control system (Figure 4), which provides fast flow changes (40 ms settling time, 9 ms response time) and pressure stability (0.005%) in microdevices. Pressure is supplied by a compressor and controlled by a flow controller (Elveflow OB1 MK3). The valves allow a maximum pressure of 2 bar and can be exchanged by valves with higher specifications if necessary in future experiments.

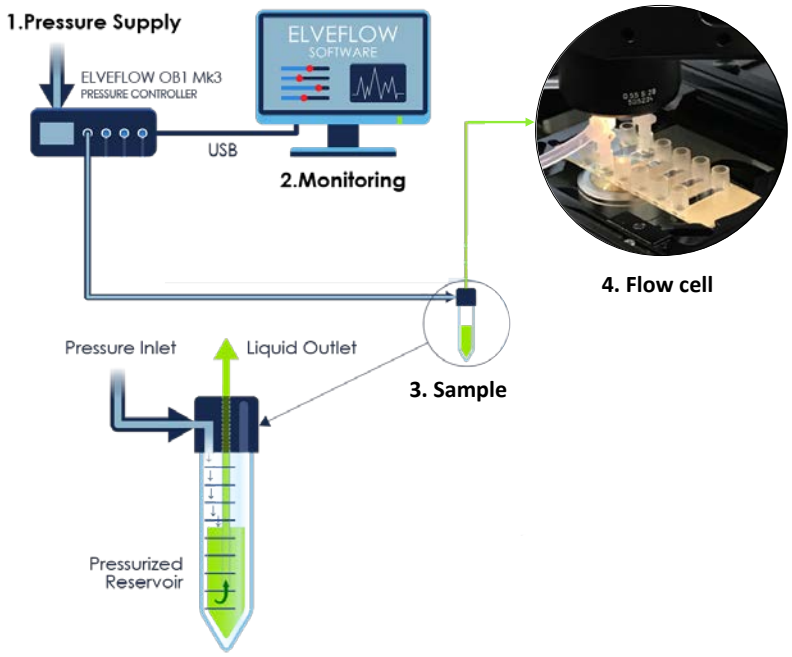

FIGURE 4 | Elveflow system. Cartoon representations of (a) a single amphipathic glycerophospholipid and (b) a cross section of glycerophospholipids self-assembled into a lipid bilayer. Taken and modified from elveflow.com.

The pressure is used to push a liquid from the pressurized reservoir through a flow cell. Here, we used bottomless 6 channel slides (ibidi sticky-Slide VI 0.4, Figure 5a and b; the dimensions of each of the channels are 3.8×18×0.5 mm (W×L×H)) with a self-adhesive underside to which functionalized substrates can be mounted. To seal the flow cells properly the substrates were mounted with a clamp, which applies homogeneous force (1.2 kN) and creates optimal adhesive bond. This prevents flow cell leakage up to the maximum pressure of 2 bar (Figure 5c).

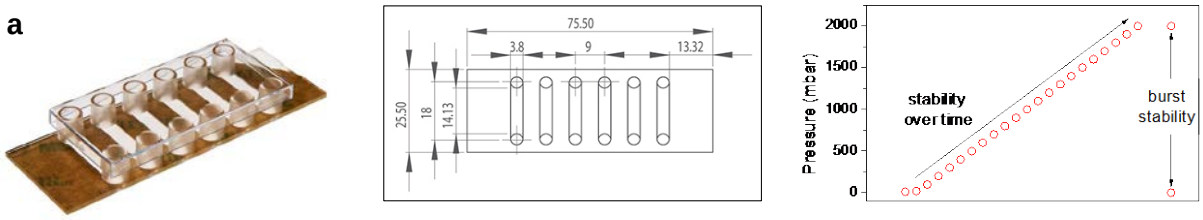

FIGURE 5 | The flow cell. (a) Image of the flow cell. (b) Technical drawings of the flow cell. (c) Test runs to determine pressure stability of the flow cells. Images (a) and (b) taken from ibidi.com.

Flow was monitored by laser scanning confocal microscopy (LSCM, Figure 6). Images were taken using an inverted Leica TCS SP8 SMD microscope with a HCX PL APO 40x oil or 63x water objective, respectively. Due to the small inner diameters of the tubing, silicone oil with low viscosity (5 cSt) was used for flow experiments.

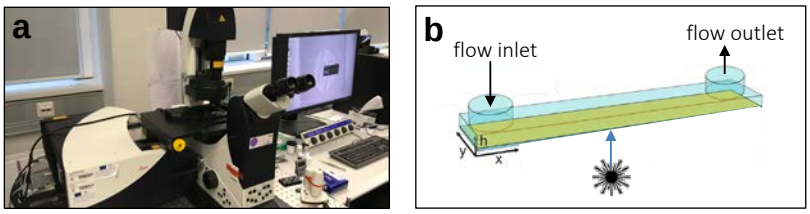

FIGURE 6 | LSCM. (a) Photo of the confocal microscope used for this project. (b) Cartoon of the application of the technique to the flow cell (only one channel shown).

To develop slippery liquid-infused surfaces, we use a well-defined pillar model system to determine the optimal structure size for a stable water lubricant layer during oil flow. Samples were prepared by lithographic patterning using SU-8 (Figure 7).

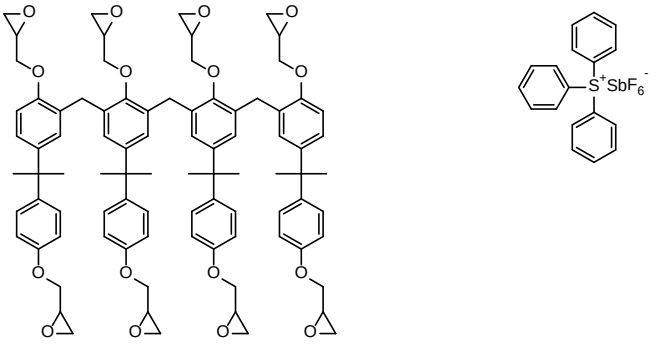

FIGURE 7 | Description of SU-8. Functionalized polymeric epoxy (a) and a triarylium-sulfonium salt (b).

The main component of the photoresist is a highly functionalized polymeric epoxy with 8 epoxy groups. Those molecules are not capable of starting the chemical reaction during UV irradiation. Therefore, a triarylium-sulfonium salt is added acting as a photosensitizer for photoacid generation. Upon exposure, cross-linking proceeds in two steps: After acid formation during the exposure process, acid-initiated epoxy cross-linking is thermally driven (Figure 8).

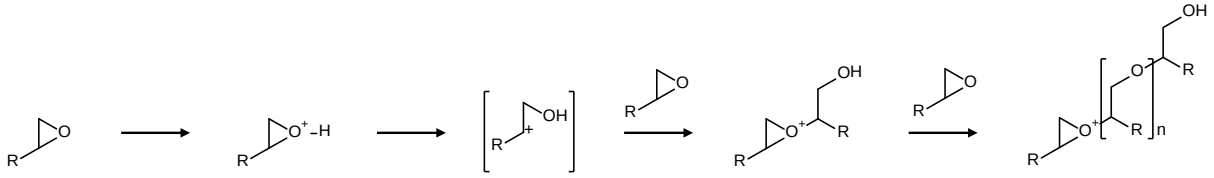

FIGURE 8 | Cross-linking of SU-8. When the photosensitizer is exposed to UV irradiation, a strong acid is produced that initiates and catalyzes the cross-linking reactions. Cross-linking occurs when an epoxy group becomes available near a carbocation. The reaction mechanism is described for one epoxy group.

Here we show how confocal imaging was used to determine the optimal surface structure size for the formation of a stable aqueous lubricant layer during oil flow. In Figure 9, different micropillar arrays are shown. The flow channels were first filled with water, then with air and finally with silicone oil. In contact with air, the water stayed in all cases in between the pillars. However, after flushing the sample with

silicone oil, we found a sweet spot of pillar size and pillar distance, which allows the formation of an aqueous lubricant layer during oil flow. For all the other samples, the water was replaced by the silicone oil.

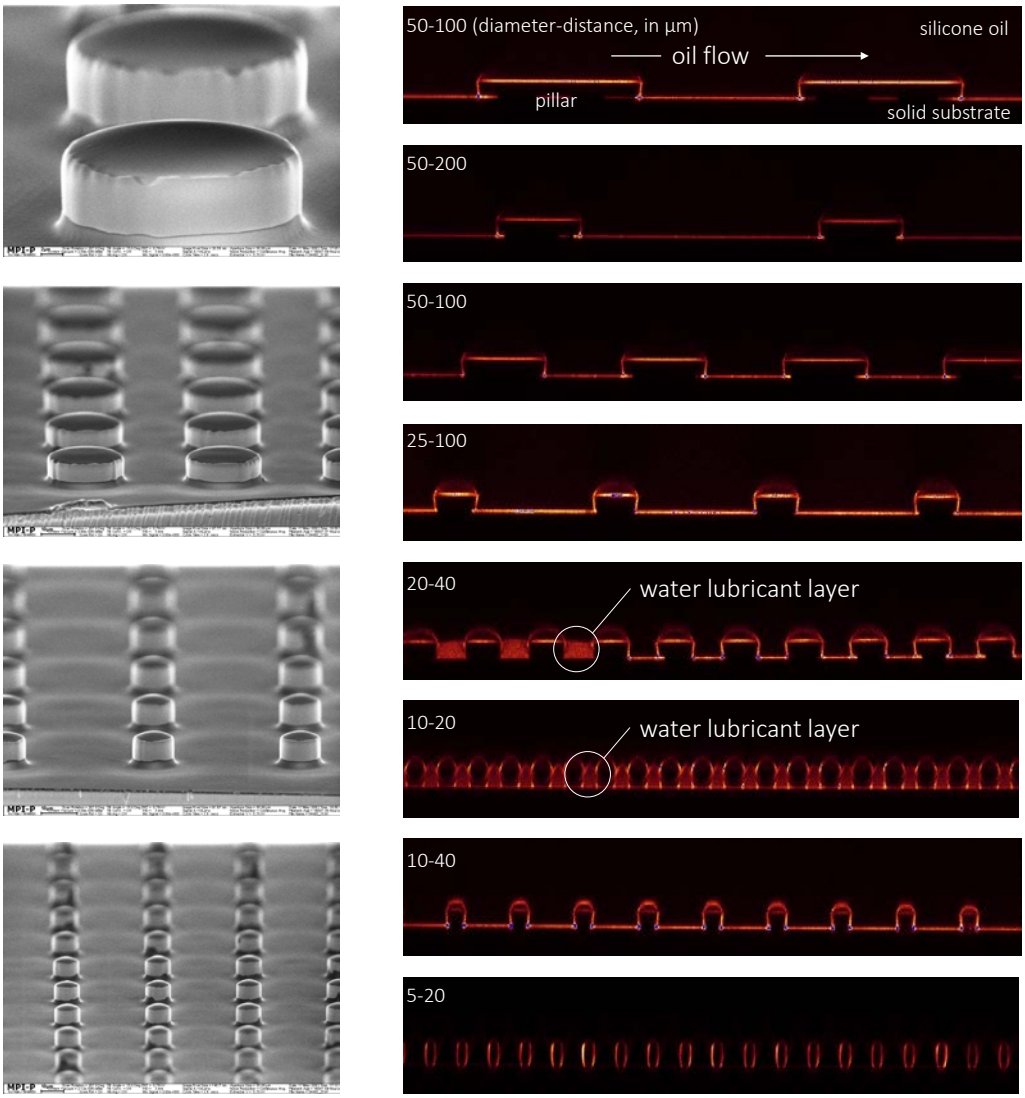

FIGURE 9 | Structure size determination for lubricant layer formation in micropillar arrays. (left) SEM images. (right) .LSCM taken in the xz-plane during silicone oil flow. SEM images courtesy of Doris Vollmer.

Flow experiments were performed to test the stability of the lubricant layer over time and in alternating environments, i.e. gas phase and oil flow (Figure 10). The lubricant layer turned out to be not affected, which is promising for reliable operation in industrial application.

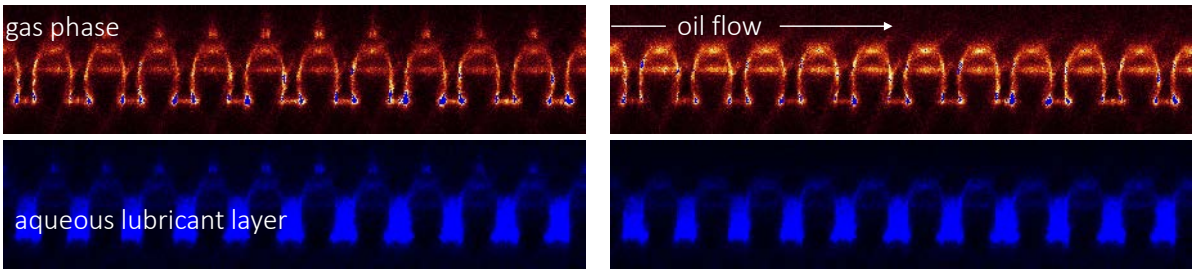

FIGURE 10 | Stability of the lubricant layer with alternating environment. Flow experiments monitoring the lubricant layer in the xz-plane over time and in alternating environments, i.e. gas phase and oil flow.

What are the conclusions of the validation?

The micropillar surfaces demonstrate the feasibility of a slippery liquid-infused surface modification in presence of an oil flow. However, the lithographic procedure for pillar formation is not applicable on site in pipelines. Therefore, we suggest another approach using nanofilaments (see "proposed way forward"). However, the micropillar array are great model systems to further investigate surface interactions (see "what is next in line").

Proposed way forward

The nanofilaments are sponge-like, liquid-infused structures (Figure 11) and act exactly in the same way like the micropillar arrays described in the previous section, but are formed by self-assembly (Figure 12) and, therfore, also applicable in pipelines.

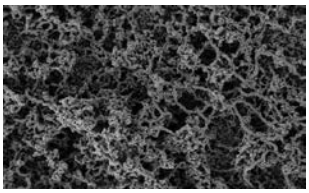

FIGURE 111 | Liquid-infused nanofilaments. (left) SEM image of the synthesized nanofilaments. (right) Cartoon illustrating the liquid-infusion with the nanofilaments acting like a sponge. SEM image courtesy of Doris Vollmer.

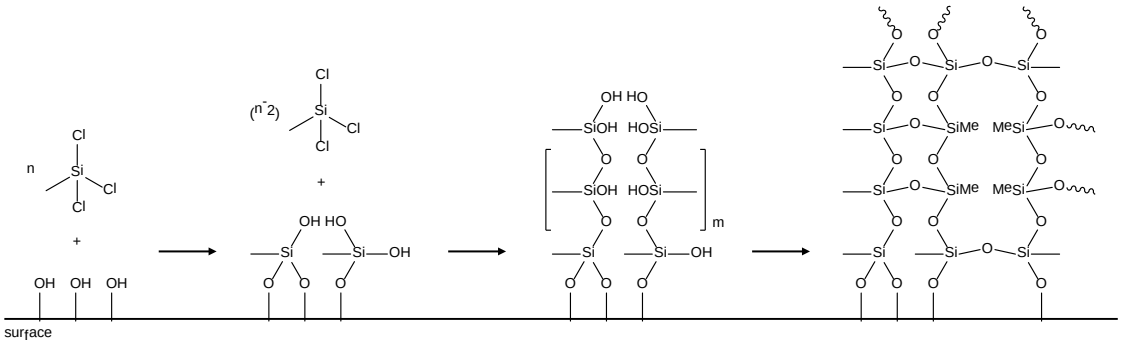

FIGURE 22 | Rreaction scheme for the formation of nanofilaments.

What is next in line to be validated? How can this be validated?

The micropillar arrays are very good model systems to further study surface interactions and hydrodynamics. With different coatings promoting either water or oil infiltration, a wide range of issues in oil industry can be addressed (Figure 13).

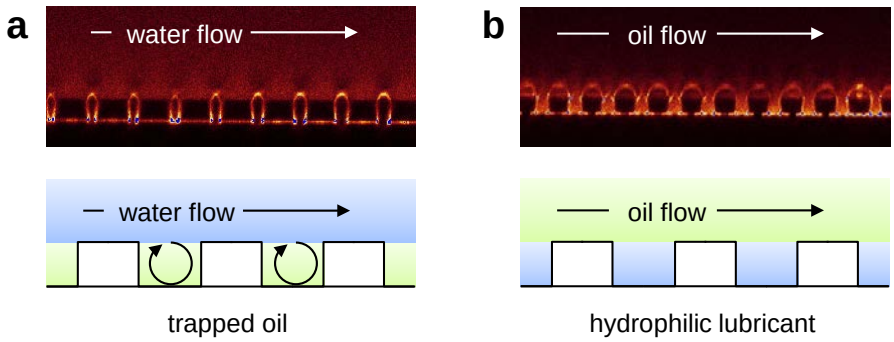

FIGURE 13 | Applications of the micropillar arrays. Using oil lubricant layers to develop new strategies for oil extraction from porous materials or (b) aqueous lubricant layers to improve oil flow capabilities.

For instance, tracer particles in the lubricant layer can be used to gather information about the hydrodynamics in the lubricant layer. Here, surface structure can be altered to either improve the lifetime of the layer to reduce recoat intervals or reduce the lifetime of the lubricant layer, promoting impalement and systematically investigate new approaches for effective oil extraction from porous materials. Figure 14 shows LSCM images of first experiments performed with polystyrene tracer particles in a water solution. The particles appear as small dots in reflection, fluorescence and transmission channels. Also, we note a strong propensity of the tracer particles to stick to the walls of the micropillars, which is shown by the orange circles around the micropillars in Figure 15b. More experiments using other tracer particles should be conducted. However, first flow experiments in presence of the tracer particles were also performed (Figure 15). Interesting to note is, that the tracer between the pillars do not move at all, whereas particles in the liquid flow above the pillars appear as a “meteor shower”, crossing the image faster than the time resolution of the microscope. However, the time resolution could be significantly improved in the future by collecting data in resonant mode of the microscope and scarifying image resolution.

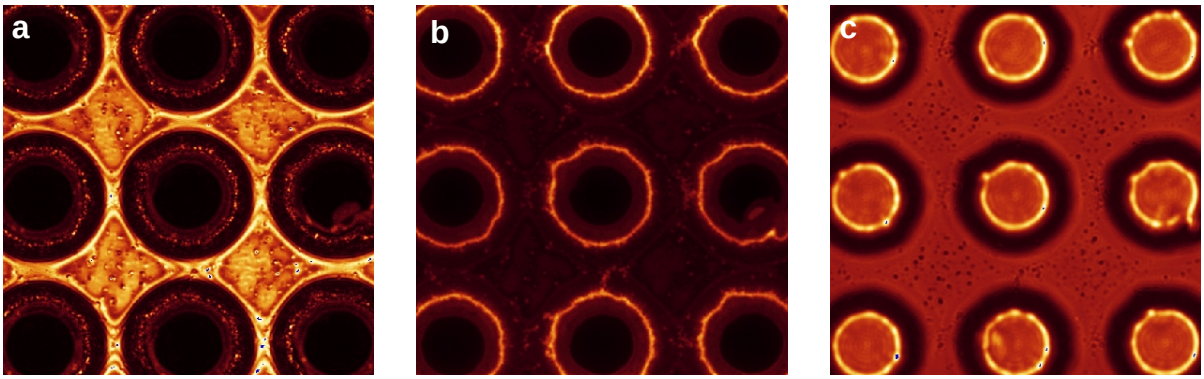

FIGURE 34 | Test run with tracer particles. LSCM images of a micropillar array in the xy-plane in (a) reflection, (b) fluorescence or (c) transmission channel. The polystyrene tracer particles are visible in each channel in the interpillar space.

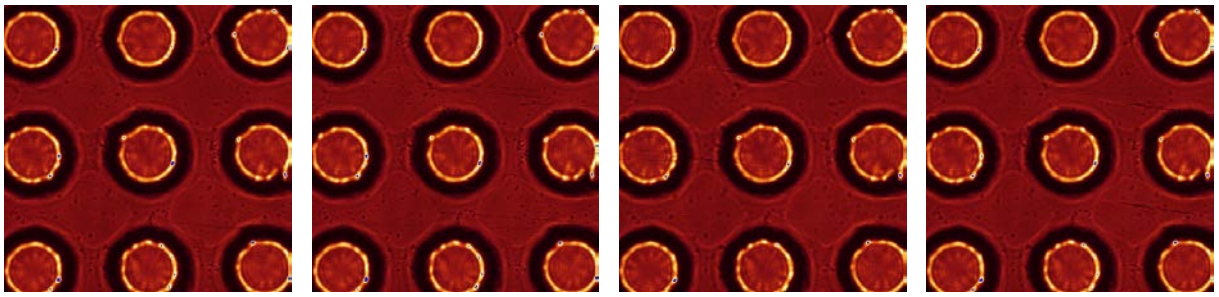

FIGURE 45 | Flow experiment with tracer particles. Snapshots taken from the transmission channel in the xy plane during a flow experiment. Tracer particles in the interpillar space are stationary, whereas the particles above the pillars move very quickly and appear as a "meteor shower".

Does it depend on other technologies?

In this RIS we used laser scanning confocal microscopy (LSCM) for flow experiments. In follow-up projects, the developed approach can be used to look at surface wetting capabilities and flow patterns since both turned out to have a major effect on the macroscopic properties of the superamphiphobic properties.

Moreover, we want to combine confocal imaging with state-of-the-art surface science techniques (Figure 16) to investigate degradation of the liquid-repelling surfaces and changes in surface chemistry on both, the macroscopic and the molecular level. Sum frequency generation (SFG) spectroscopy provides vibrational spectra of interfacial molecules to investigate molecular orientation during oil flow. X-ray photoelectron spectroscopy (XPS) can be used to track changes in surface chemistry after oil flow, e.g. biofouling or self-cleaning capabilities. Also changes in thickness of the surface modifications due to oil flow can be determined. Both techniques are part of our expertise.

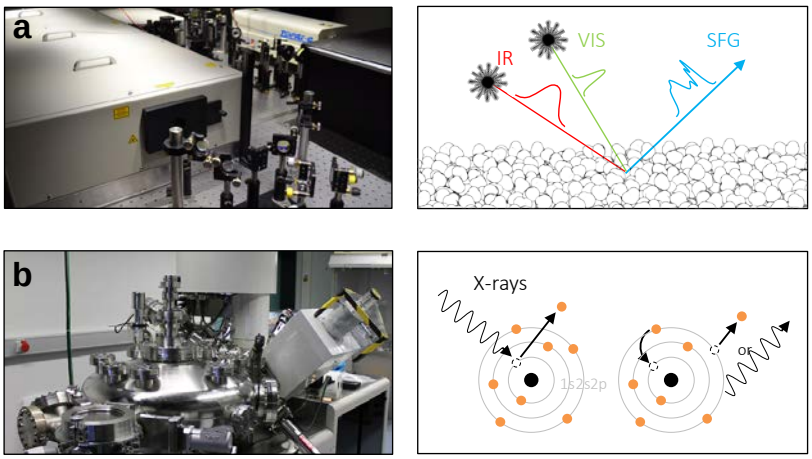

FIGURE 16 | Techniques for future experiments. (a) Sum frequency generation (SFG) vibrational spectroscopy and (b) X-ray photoelectron spectroscopy (XPS).

Final conclusion

Liquid-infused slippery surfaces are a promising approach for pipeline surface modification. However, especially the lifetime of the lubricant layer and its stability in contact with more complex fluids remains to be investigated.

An offshore reservoir monitoring system based on fiber optic sensing of seabed strains

Eyal Levenberg and Ivanka Orozova-Bekkevold (DTU Civil Engineering), and Kristian Nielsen (DTU Photonics Engineering)

Abstract

One of the problems affecting mature fields in the North Sea is seabed subsidence due to reservoir depletion. Seabed subsidence can directly affect integrity of production facilities. Severe subsidence, as in the case of the Ekofisk field, can lead to platform sinking below the sea level and, subsequently, to very high repair costs or possibly to a complete platform replacement. Subsidence is an issue also in the Tyra field, and it may become a problem in other fields as depletion is ongoing. Fluid injection is a widely used method to boost production and/or maintain reservoir pressure in order to mitigate compaction and subsidence. Both reservoir depletion and fluid injection operations induce seabed deformations. The deformation pattern potentially holds useful information about production efficiency and reservoir management, which could be captured by careful and continuous monitoring of seabed strains. Current technologies for monitoring offshore seabed deformations only provide point or line readings. The idea that this sprint project explores is achieving nearly full-field and continuous monitoring of seabed surface deformations by means of distributed fiber optic sensors. The objective of the study was to theoretically assess whether current fiber optic sensing technology is sensitive enough to detect production-induced seabed strains originating at a 2000 m deep reservoir.

1. Technology vision

The Danish gas fields in the North Sea are produced by natural depletion with gas/fluid expulsion and related compaction as drivers [***1***]. Often, reservoir compaction is translated into seabed subsidence, which has a direct adverse effect on production facilities. Such subsidence, as in the case of the Tyra gas field, is of the order of 200 mm per year. To a lesser extent, seabed subsidence is also observed in oil fields such as Dan. Initially, the Dan field was produced by natural depletion - with water injection initiated only after 8 years of production. Despite water injection, seabed subsidence has continued, indicating that the compaction drive remained active. Modern developments, such as the Halfdan Field, have parallel injection and producer wells resulting in near-zero seabed subsidence. Nevertheless, pressure differences between injector and producer wells may have caused minor deformations of the seabed - leading to minor positive and negative vertical displacements at the different Halfdan platforms. It is reasonable to assume that loss of pressure support

caused by short circuits between injector and production wells might have been the reason for the observed deformations. To the best of our knowledge, these displacement ripples have yet to be thoroughly investigated.

The technology vision proposed in this project is to develop a reservoir monitoring system based on reading seabed deformations by the means of distributed fiber optic strain sensing technology, with fiber optic cables coupled to the seabed. The idea is conceptually shown in Figure 1. The sketch on the left is an overhead view of a production field (e.g., Tyra), showing a single-cable distributed fiber optic sensor system deployed around a platform. The shown meshing is geared towards reading radial and tangential strains w.r.t. a cylindrical coordinate system positioned at the bottom of the platform. Redundancy is assured by loops periodically returning to the platform. Thus, a damaged loop can be skipped by splicing operations taking place on the platform - without expensive underwater gear. In practice, the deployment pattern must be tailored to the production setup with fiber orientations corresponding to the anticipated principal strain directions. The center (middle) image in Figure 1 shows a Fugro seabed trencher - a semi-robotic device that can potentially deploy a fiber optic cable according to a desired pattern [***2***]. This device buries a cable at a depth of about two meters below the seabed thus ensuring mechanical coupling with the surrounding soil medium. Such burial depth also provides protection against fishing trawls and isolation from storm effects. The estimated cost of such deployment is about 2.5 million DKK per kilometer. The sketch on the right hand side of Figure 1 illustrates how fiber optic cables can be brought to the platform deck through a J-tube in order to be connected to a fiber optic interrogator which consists of a delicate laser source and receiver optics [***3***].

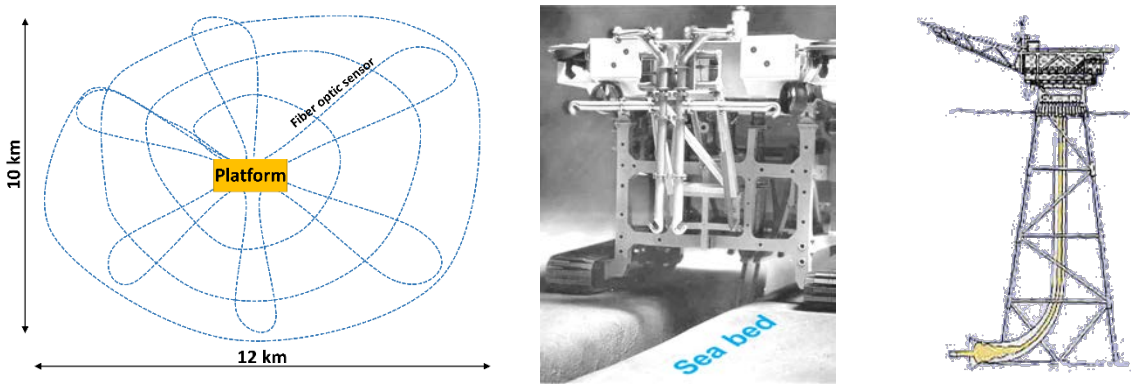

Figure 1: Possible deployment pattern for a fiber optic sensor around an offshore platform (left), Fugro seabed trencher for sensor embedment (center), and J-tube for bringing fiber optic cables onto the platform (right).

Fiber optic strain sensing is an established technology, commonly employed for monitoring Civil Engineering facilities [***4***]. Fiber optic sensors have also been employed in the oil and gas industry, as point strain sensors [***5***] or along pipes [***6***]. A recent survey of fiber optic sensing applications within the oil and gas industry can be found in [***7***]. Ideally, the monitoring system should be deployed and activated before the start of production. For already producing fields (such as in the North Sea), a fiber optic monitoring system

deployed after the start of production will sense only events/changes subsequent to installation. In either situation, the proposed system offers several potential benefits: (i) help in monitoring and prediction of reservoir compaction and related subsidence, (ii) provide indication on possible location of short circuits between injection and production wells, (iii) monitor and/or predict the changes in the gap between the deck of the platforms and the sea surface, (iv) provide additional input to 4D seismic surveys, (v) monitor potential smart water that can increase the compaction drive, (vi) monitor induced seismicity due to production activities, and (vii) monitor post-production deformations to accommodate any future environmental inquiries by the authorities. These benefits lead to better decisions on production, re-development, and end-of-field life strategies. By very nature, the system has an advantage over pipeline surveys which provide only information along a line, with readings that are susceptible to pipe corrosion, pipe failure, submarine storms, etc. Furthermore, when a reliable technology arises, capable of reading fiber strains at a very fast rate of the order of 10 kHz, the deployed cables can be utilized as geophones. In this case, considerable price reduction in acquiring 4D seismic data is anticipated [***8***].

Fiber optic strain sensing is based on the so-called Brillouin scattering effect wherein the light intensity in the fiber locally modifies the density of the solid, resulting in scattering and frequency shift [***9***]. Optical detection systems currently available on the market for distributed strain sensing operate with standard telecommunications optical fibers. One example of a relevant interrogator is OZOptics' Foresight™ series of fiber optic Distributed Strain and Temperature Sensors (DSTS). This device uses stimulated Brillouin scattering to independently measure changes in both strain and temperature along the length of an optical fiber. Temperature readings are needed to annul temperature-related strains. The maximum sensing length for this system is 100 km (fiber length can be 160 km) with a resolution of 0.1 microstrains and accuracy of ±2 microstrains. If desired, the spatial resolution can be as short as 5 cm. The device is of the size a desktop computer with a cost of about 1 million DKK.

2. Validation of technology

The main objective of the current work was to carry out an in silico feasibility study of whether current fiber optic sensing technology has the measurement ability in terms of resolution and accuracy to detect production-induced seabed strains. Such assessment is a first and necessary step before any further development because the associated strains are expected to be very small.

2.1. Analytic Modeling

An existing analytic theory for computing mechanical responses due to deep deformations was employed as a basic modeling tool [***10***]. The theory considers (see Figure 2) a weightless, isotropic, homogeneous, and linear elastic layer with thickness H and material properties E (Young's modulus) and ν (Poisson's ratio), which is infinite laterally. Herein, this layer represents the overburden, i.e., the entire strata overlaying a reservoir. Initially, the medium is assumed to be undeformed and stress-free, with both top and bottom boundaries completely flat (dash-dot lines), i.e., any existing stresses due to self-weight are taken as initial

conditions and therefore annulled. Next, an axisymmetric blister-like displacement field is imposed at the bottom of the layer, forcing the lower boundary to deform vertically, without inducing shear stresses at the interface (solid line).

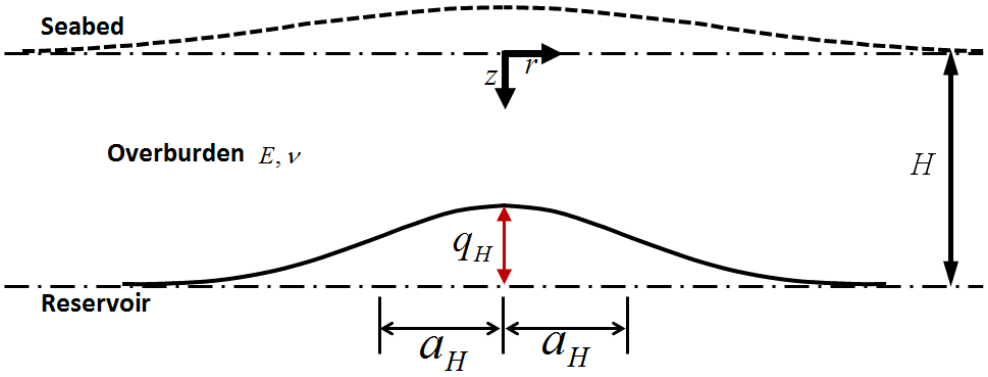

Figure 2: Illustration of basic model definitions.

The modeling allows for calculating all mechanical responses (i.e., stresses, strains, and displacements) inside the layer as well as at the top - corresponding to the seabed level. To facilitate the formulation, a cylindrical coordinate system is included in the Figure, with its origin placed at the top of the undeformed layer, the depth z-axis drawn into the medium, and the radial r-axis ($r \geq 0$) parallel to the top boundary. The imposed displacement field at bottom is denoted by u_z^H, mathematically expressed as an axisymmetric Gaussian:

$$u_z^H(r) = q_H e^{-(r/a_H)^2/2} \tag{1}$$

where r is the radial coordinate, q_H is the peak displacement occurring at $r = 0$, and a_H represents the location where the curvature of $u_z^H(r)$ changes sign (i.e., inflection point). Both q_H and a_H have units of length; a_H must be positive, while q_H can be either positive or negative to indicate downward or upward deformation (respectively). The particular form of Equation 1 was chosen because it can serve as a radial basis function for representing any other deformation shapes - not necessarily axisymmetric [***11***]. This modeling flexibility is needed when simulating, e.g., the effects of a producer-injector array.

The mechanical responses at the top of the layer (where $z = 0$) are calculated from the following equations:

$$\sigma_r^0 = -E \int_{m=0}^{\infty} \left\{ \left[mJ_0(m\rho) - \frac{J_1(m\rho)}{\rho} \right] \begin{Bmatrix} [A+C]e^{-m} \\ +B-D \end{Bmatrix} + 2\nu m J_0(m\rho)\left[Ce^{-m} - D \right] \right\} dm \tag{2}$$

$$\sigma_\theta^0 = -E \int_{m=0}^{\infty} \left\{ \frac{J_1(m\rho)}{\rho} \left[Ae^{-m} + Ce^{-m} + B - D \right] + 2\nu m J_0(m\rho)\left[Ce^{-m} - D \right] \right\} dm \tag{3}$$

$$u_z^0 = -H(1+\nu)\int_{m=0}^{\infty}\left\{J_0(m\rho)\left[Ae^{-m} - C(2-4\nu)e^{-m} - B - D(2-4\nu)\right]\right\}dm \quad (4)$$

$$u_r^0 = H(1+\nu)\int_{m=0}^{\infty}\left\{J_1(m\rho)\left[Ae^{-m} + Ce^{-m} + B - D\right]\right\}dm \quad (5)$$

where σ_r^0, σ_θ^0, u_z^0, and u_r^0 denote (respectively) radial stress, tangential stress, vertical displacement, and radial displacement; m is a unitless integration parameter. The superscript zero indicates that these responses are calculated at $z = 0$. Moreover, $\rho = \rho(r) = r/H$ is a normalized (dimensionless) radial coordinate, $J_0(\cdot)$ and $J_1(\cdot)$ are Bessel functions of the first kind of order zero and one (respectively), and A, B, C, and D are each a dimensionless function of m. The latter are obtained from enforcing the problem boundary conditions; they are explicitly listed in [***12***]. Seabed strains, expected to be read by the fiber optic sensors, are derived from the stresses in the usual way:

$$\varepsilon_r^0 = \frac{\sigma_r^0 - \nu\sigma_\theta^0}{E} \quad \text{and} \quad \varepsilon_\theta^0 = \frac{\sigma_\theta^0 - \nu\sigma_r^0}{E} \quad (6)$$

where ε_r^0 and ε_θ^0 denote the strain in the radial direction and tangential direction (respectively). Note that these strains are not affected by the overburden modulus because it cancels-out when inserting the stress expressions from Equations 2 and 3.

Two scenarios are considered hereafter. The first deals with simulating the conditions of depletion-induced subsidence, for example in the case of gas production. The second deals with monitoring a stimulated field consisting of an array of producers and injectors. For both cases it is assumed that the strain monitoring system is deployed and activated at some point in time after the start of production operations, and therefore detects only subsequent events.

2.2. Simulation of depletion-induced subsidence

The model is first utilized for simulating depletion-induced subsidence over a large area. The overall compaction at top reservoir (equivalent to the bottom of the overburden) is idealized as being axisymmetric according to Equation 1. The assumed model parameters are: (i) overburden thickness $H = 2000\,\text{m}$, (ii) Poisson's ratio of medium $\nu = 0.26$, (iii) width of Gaussian representing displacement pattern at the reservoir top $a_H = 1000\,\text{m}$, and (iv) peak reservoir compaction $q_H = 300\,\text{mm}$ representing an annually expected value.

Model calculation results are shown in Figures 3 and 4. Figure 3 presents the vertical displacement fields at top reservoir (bottom charts depicting u_z^H) and at the seabed level (top charts depicting u_z^0). It can be seen that the induced displacement is attenuated at the seabed. The peak vertical displacement drops from 300 mm (assumed at top reservoir) to about 180 mm at seabed (top of overburden). Also, the deformation pattern

(i.e., subsidence bowl) is somewhat wider at the surface. Figure 4 presents the corresponding seabed strains in the radial (bottom charts) and tangential (top charts) directions. It can be seen that radial strains (ε_r^0) change sign from positive (compression) to negative (tension) while the tangential strains (ε_θ^0) are only compressive. The strain levels in both directions are of the order of 50 microstrains, i.e., within the resolution and accuracy limits of current fiber optic sensing technology – and therefore detectable.

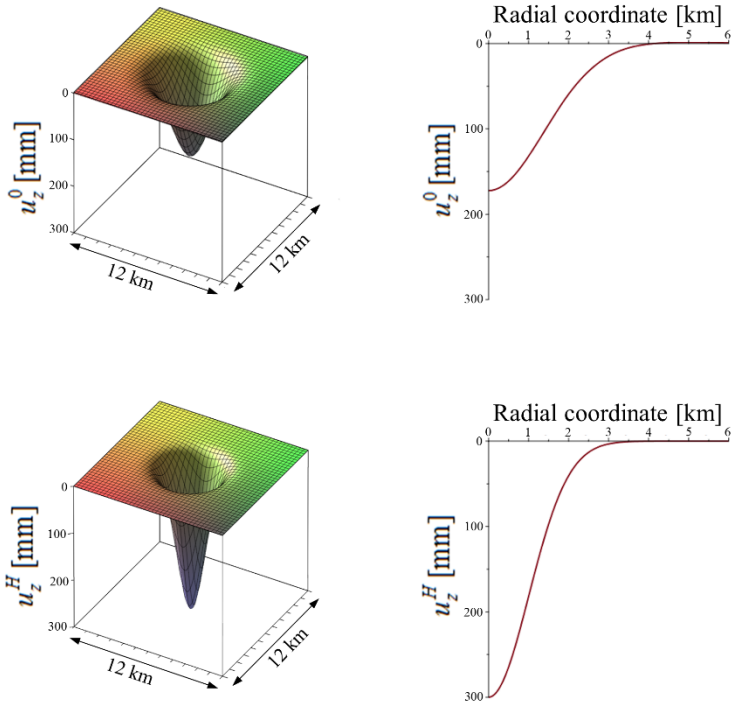

Figure 3: Vertical displacement field in the axisymmetric case; reservoir (bottom charts) and seabed level (top charts).

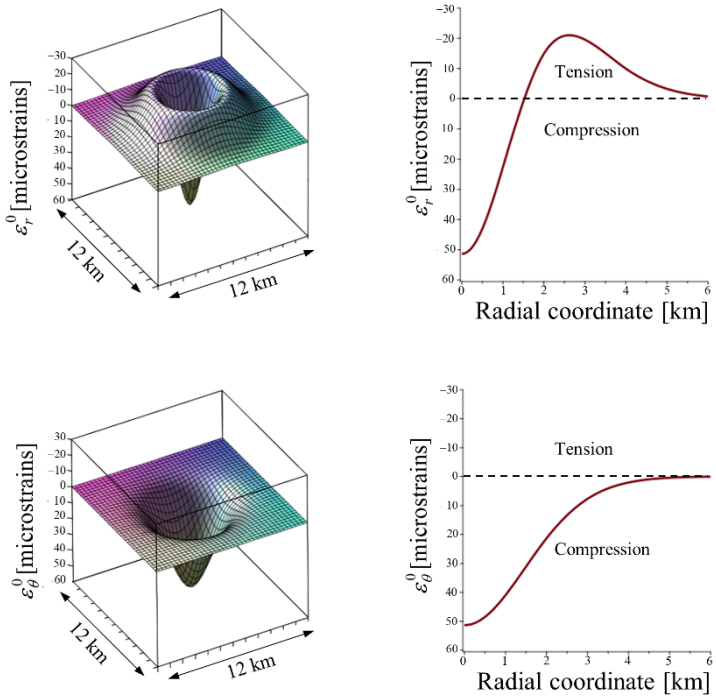

Figure 4: Seabed strain distributions in the axisymmetric case; radial (top charts) and tangential (bottom charts).

2.3. Simulation of injector-producer array

The second considered case simulated a virtual injector-producer array consisting of 3 producers (denoted as $P_1 ... P_3$) and 4 injectors (denoted as $I_1 ... I_4$). The array is arranged as shown in Figure 5 (left hand side) with L denoting length and W denoting spacing between injectors and producers. A Cartesian coordinate system is employed in this case, with the y-axis oriented parallel to the wells, the x-axis pointing in the transverse direction, and the z-axis (not shown) pointing downward towards the earth's core. A proposed pattern for fiber optic sensor deployment, matching the geometry of the injector-producer array (and the expected principal strain directions), is shown on the right hand side of Figure 5. As can be seen, the pattern includes several loops, generally oriented in the directions of the x and y axes. As in Figure 1, redundancy and ease of maintenance is enabled by periodically returning the fiber to the platform to enable splicing in case of a damage loop.

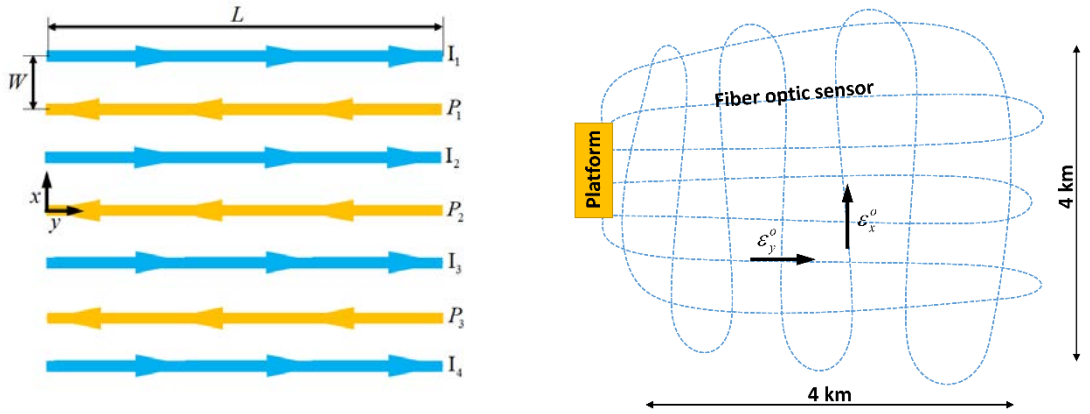

Figure 5: A virtual injector-producer array (left) and a possible fiber deployment pattern (right).

Under operation, the injector-producer array in Figure 5 imposes vertical deformations at the bottom of the overburden (top reservoir) - depression in the vicinity of the producers and heaving in the vicinity of the injectors. Such deformation pattern can be approximated mathematically by the following expression:

$$u_z^{IP} = \frac{A}{2}\cos\left(\frac{\pi x}{W}\right)\left(\begin{array}{l}\left(\begin{array}{l}H(x-0.5W)-H(x+0.5W)\\+H(x-1.5W)-H(x+1.5W)\end{array}\right)H(sL+y-L)\\+\left(\begin{array}{l}H(x+0.5W)-H(x-0.5W)\\+H(x+1.5W)-H(x-1.5W)\\+2H(x-3.5W)-2H(x+3.5W)\end{array}\right)H(y-L)\\-2\left(\begin{array}{l}H(x-3.5W)\\-H(x+3.5W)\end{array}\right)H(y)\end{array}\right) \qquad (7)$$

where u_z^{IP} is the vertical displacement magnitude at the reservoir level at an arbitrary location/point identified by coordinates x and y. The parameter A denotes the displacement amplitude induced by either an injector or a producer, and $H(\cdot)$ is the Heaviside step function. The parameter s can range between zero and unity; it is introduced to represent a shortcut event between injector wells I_2 and I_3. If this condition occurs, the heave amplitude caused by I_2 and I_3 is reduced by 50% along a length of sL. At the same time, the depression along P_2 becomes limited to a length $L(1-s)$. In other words, when $s=0$ the injector-producer array is fully operational, and when $s>0$ a partially operational situation is simulated. A full shortcut between I_2 and I_3 is simulated when $s=1$.

Assuming that a strain monitoring system is installed at the seabed when the array is fully functional ($s=0$ condition), subsequent strain readings will reflect deformations caused by any shortcut event, i.e., the difference between $u_z^{IP}(s>0)$ and $u_z^{IP}(s=0)$. This situation is illustrated in Figure 6. The top 3 charts provide plots of u_z^{IP} for different s values. The bottom three charts depict the corresponding displacements (at top reservoir) that generate strains at the seabed level. The common parameters for preparing the charts were: $W=200\,\text{m}$, $L=2\,\text{km}$ and $A=1\,\text{m}$. The correctness of the latter value should be a subject of further study given that the real peak displacement magnitude near the injectors and producers it is not known. The

vertical axes in the charts in Figure 6 are graphically distorted (×50), so that the deformation pattern can be noticed.

Figure 7 shows the estimated seabed strains corresponding to the three cases in Figure 6 (bottom three charts), i.e., for the three different s values (0.25, 0.50, and 0.75). The top three charts depict seabed strains in along the x-axis direction (ε_x^0) and the bottom three charts depict seabed strains along the y-axis direction (ε_y^0). As it can be seen, the peak-to-peak strain magnitudes are of the order of a few tenths of a microstrain. These strain levels are similar in magnitude to the current resolution limits of fiber optic sensing (about 0.1 microstrains), and about an order of magnitude smaller than the accuracy limits of the technology (about ±2 microstrains).

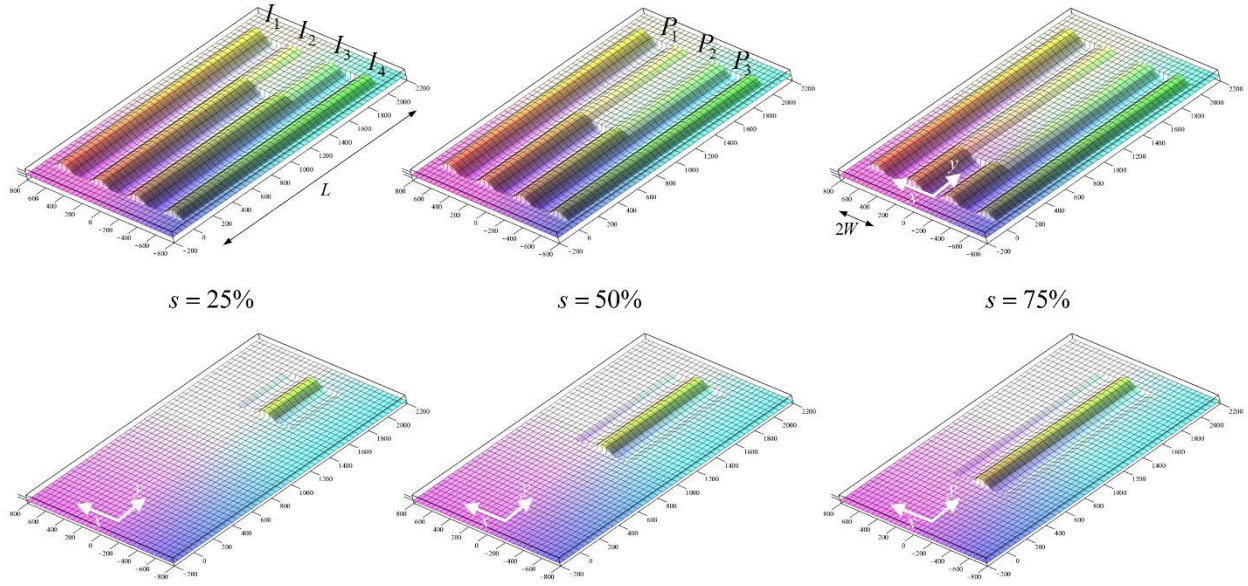

Figure 6: Simulating a partially-operational Injector-Producer array (refer to Figure 5). The top three charts represent the assumed displacement pattern for different shortcut lengths (expressed via the s parameter) according to Equation 7; the bottom three charts display the corresponding differences in displacements.

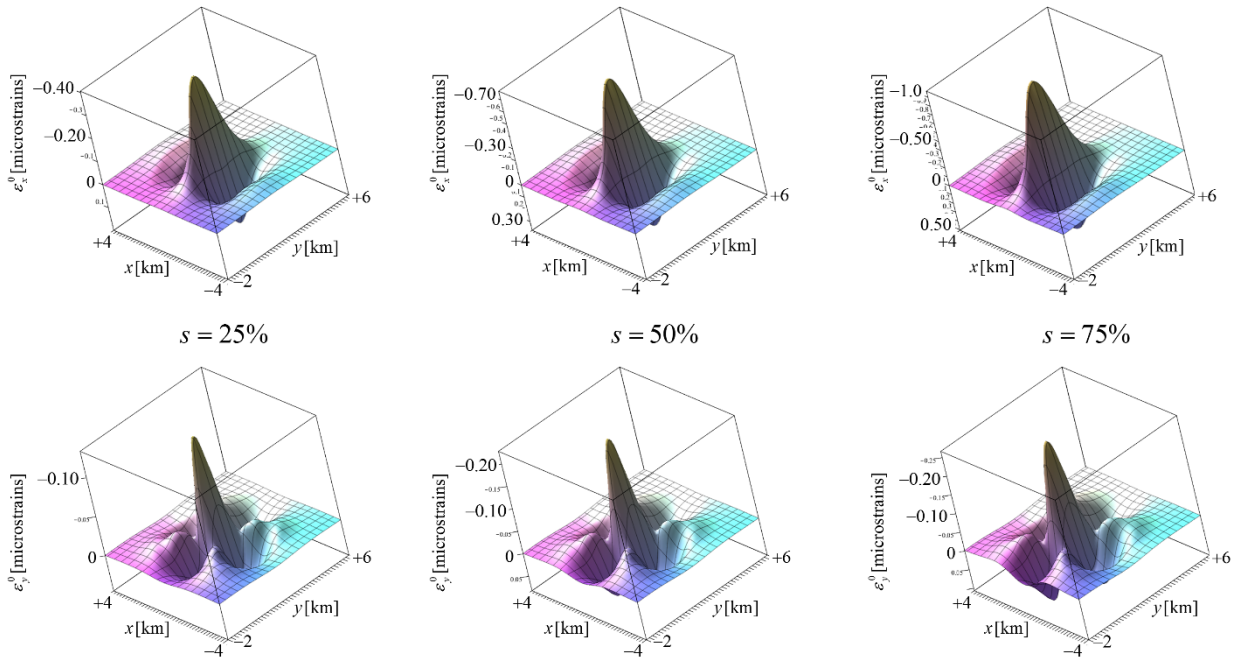

Figure 7: Calculated seabed strains in the x and y directions (see coordinates in Figures 5 and 6) corresponding to three different shortcut cases (refer to bottom charts in Figure 6).

3. Summary and conclusions

This work considered the idea of meshing the seabed near offshore platforms with fiber optic sensors as means of detecting deformations originating at the reservoir level. An analytic model was employed to estimate the magnitude and orientation of expected strains as a first-step feasibility study. Two separate cases were investigated: (i) monitoring the annual compaction of an entire field (see Figure 1), and (ii) monitoring the effects of shortcuts in an injector-producer array (see Figure 5). Based on the calculations, is it concluded that the expected seabed strain levels in the first case are detectable and measurable with current fiber optic sensing technology, while the strain levels in the second case are very small, within the resolution limits of commercially available technology.

3.1. Proposed way forward

The idea proposed in this study appears very promising and practical, and it is therefore suggested to invest further research resources in promoting its realization. The following is a list of recommended actions: (i) improve the modeling by incorporating actual/more detailed production data and compaction/subsidence measurements, (ii) improve the modeling by considering a stratified overburden, (iii) improve the modeling by considering more advanced material behavior e.g., time-dependent properties and permanent deformation properties, (iv) investigate the expected displacements induced by an injector-producer array, (v) construct a scaled-down controlled field experiment where optic fibers are physically deployed, and a buried actuator mechanically simulates reservoir displacements, (vi) develop an inverse analysis scheme that accepts as input fiber readings, and provides as output information about the reservoir, (vii) investigate distributed fiber

optic sensor readings in combination with other instruments such as geophones and tilt-meters, (viii) investigate physical deployment issues, and (ix) perform cost-effectiveness analysis.

References

[1] Danish Energy Agency (2013), "Oil and gas production in Denmark (and subsoil use)," Online report accessed November 20, 2017: https://ens.dk/sites/ens.dk/files/OlieGas/oil_and_gas_in_denmark_2013.pdf.

[2] Fugro Inc., "TSM Q1400 Trenching System," Online link accessed November 20, 2017: youtube.com/watch?time_continue=7&v=cFxlwWPm4f0.

[3] Online image link accessed November 27, 2017: http://pipelineencyclopedia.blogspot.dk/2010/07/j-tube.html.

[4] Barrias, A., Casas, J.R., and Villalba, S. (2016), "A review of distributed optical fiber sensors for civil engineering applications," Sensors, Vol. 16/748, pp. 1–35.

[5] Yanlin, W., Bi Xiangjun, B., Sheng, F., Yingxin, M., and Qianjin, Y. (2011), "Subsidence monitoring of offshore platforms," Procedia Engineering, Vol. 15, pp. 1015–1020.

[6] Inaudi, D. and Glisic, B. (2010), "Long-range pipeline monitoring by distributed fiber optic sensing," Journal of Pressure Vessel Technology, Vol. 132(1), pp. 011701(1)–011701(9).

[7] Daniel, J.S., Maida, J.L., and Skinner, N.G. (2017), "Adapting optical technology to dynamic energy prices: fiber-optic sensing in the contemporary oil field," SPIE Proceedings Vol. 10208: Fiber Optic Sensors and Applications XIV, Anaheim, California, United States.

[8] Maas, S.J. and Buchan, I. (2007), "Fiber optic 4C seabed cable for permanent reservoir monitoring," Proceedings of the International Symposium on Underwater Technology and Workshop on Scientific use of Submarine Cables Related Technologies, Tokyo, Japan, pp. 411–414.

[9] Galindez-Jamioy, C.A. and López-Higuera, J.M. (2012), "Brillouin distributed fiber sensors: an overview and applications," Journal of Sensors, Article ID 204121.

[10] Levenberg, E. (2013), "Analysis of pavement response to subsurface deformations," Computers and Geotechnics, Vol. 50, pp. 79–88.

[11] Goshtasby, A. and O'Neill, W.D. (1993), "Surface fitting to scattered data by a sum of Gaussians," Computer Aided Geometric Design, Vol. 10(2), pp. 143–156.

[12] Levenberg, E. (2015), "Intrinsic roughness mitigation of pavements on expansive soils - an analytic investigation," International Journal of Pavement Research and Technology, Vol. 8(3), pp. 167–171.

Are there common genes for MEOR under pressure?

Alberto Scoma, Kasper Urup Kjeldsen, Aarhus University

Abstract

Oil degradation is a common biological process for several microorganisms. Genes, enzymes and pathways that regulate the activation of hydrocarbons, the transport inside the cell, the degradation and/or modification of the hydrocarbon to serve microbial cell needs are relatively widespread among bacteria. Recently, this applicant isolated the first hydrostatic pressure (HP) adapted, oil degrading microorganisms. The aim of the present project was to sequence the genome of these bacteria to investigate whether a common set of genes existed which explained why such bacteria were consistently predominating under increased HP in the presence of solid hydrocarbons as sole carbon source. This information has the potential to highlight specific microbial functionalities explaining how microbial oil degradation occurs in deep-sea environments subjected to pressure. In particular, the project aimed at understanding whether a specific set of genes is required for HP-adapted bacteria degrading oil, with the latter an interesting information for processes of industrial interest such as microbially-enhanced oil recovery (MEOR) in pressurized environments (e.g., deep oil reservoirs). Provided that the present ones are the first oil degrading cultures specifically enriched to grow under HP, the information gained through this project could also be of relevance for 1) the numerous microbial activities normally occurring in deep oil reservoirs (e.g., those leading to scaling, souring, corrosion); 2) the numerous microbial activities carried out by bacteria inoculated into certain deep oil reservoirs by means of water injection. We identified three potential genes of interest, involved in increased tolerance to a stress response (*AraC_binding*, *LON_Substr_bdg*) and capacity to modify hydrocarbons (*Acetyltransf_8*). However, their function is too general and taken together insufficient to be descriptive of a specific enzymatic set conferring a selective advantage. A cultivation-based approach would allow gene expression (i.e., transcriptomics) to indicate which genes are actually upregulated under deep, subseafloor conditions. This experimental set-up would build up on the knowledge gained through the present project (i.e., genome sequencing) and explain which functions are critical, for instance, to stimulate MEOR under HP.

Technology vision

The present project aimed at assessing the capacity for microbially-enhanced oil recovery (MEOR) in deep oil reservoirs based on the presence/absence of specific genes. Microbial activities leading to oil degradation in deep reservoirs occur at the interface with water once bacteria are supplied with nutrients. Deep oil reservoirs are also characterized by critical parameters for microbial life such as temperature and HP. While much is known about the effects of nutrients availability and temperature shifts, little to no information is available on the effects of HP on microbial oil degradation. Recently, research from this applicant suggested that under increased hydrostatic pressure (HP) as that occurring in deep sea environments microbial representatives and pathways in oil degradation are different as compared to those occurring in surface waters. In particular, bacteria dominant under HP are generally secondary degraders, that is, bacteria able to consume hydrocarbons and several other organic sources. On the contrary, surface waters contaminated with

oil are typically enriched in obligate oil degraders, that is, bacteria that apart from acetate and pyruvate consume exclusively hydrocarbons. Following enrichments at various HPs (surface to 30 MPa, equivalent to 3 km below sea surface level) using solid hydrocarbons (at ambient conditions) as sole carbon source (i.e., either eicosane or triacontane), bacterial isolation was attempted to collect individual species. This work produced 11 multispecies micro-colonies constituted by the same 8-9 bacterial species. By sequencing the metagenome of these bacteria, we aimed at revealing whether specific genes are required for oil degradation under increased HP.

This information could play a role in enhancing oil recovery. In case specific genes are required for MEOR to occur under HP, samples collected from deep oil reservoirs could be analysed to check whether such reservoir possesses the proper microbial functionalities for MEOR to occur. This would lay the basis to microbial physiology studies to understand how to steer this process at deep oil reservoirs conditions. The latter could also provide information on whether bacteria possessing this genetic property could be inoculated in the reservoirs. Steering of microbial communities to control oil reservoirs conditions is rather common in the oil and gas sector, as nitrate supply through water injection is used to quench sulphate reducing bacteria and prevent sulphide accumulation leading to souring, scaling and corrosion.

A practical development of this technology in the North Sea would entail multiple steps:

A. mapping of presence/absence of target genes in deep oil reservoirs; this would include mapping the geological features of oil reservoirs;
B. assessing whether MEOR is expected to enhance oil recovery in the target deep reservoir;
C. in case genes are present in the target reservoir, stimulation of MEOR by providing the necessary nutrients, chemicals and incubation time for the bacteria;
D. in case genes are absent, inoculation of known bacteria holding such genes along with nutrients and other chemicals necessary for bacterial activity.

Point C and D consider that the microbial physiology of such oil degraders has been investigated, therefore the exact response to all *in situ* oil reservoir conditions have been thoroughly assessed. Implementation of this technology would require intimate understanding of the mechanistic response to any of the deep oil reservoir's *in situ* condition (alone and in combination with other factors), which would allow modelling bacterial activity.

In the present project, to validate whether a common gene set exists explaining the prevalence of secondary degraders at increased HP, we selected a number of genes known to be:

1) HP responsive;
2) involved in hydrocarbon activation, transportation, modification, degradation;
3) involved in biosurfactant production.

Testing points 1 to 3 would provide a clear case to show a genetically-based response to HP and oil. However, a negative response may also be expected. The occurrence of different microbial communities involved in hydrocarbon degradation due to HP may be explained not by the presence of specific genes, rather by the capacity of such genes to be expressed at a given time. The latter activity is described by transcriptomic rather than genomic studies, and is much more labour intensive. While very interesting to answer the question of what rules MEOR under HP, the latter experiments cannot be addressed within the present project frame.

Validation of technology

Owe to the overwhelming information that can be gained by genome analysis, the comparison of different genomes is a time consuming, labour intensive work which may require several months, particularly when dealing with several genomes at a time. Putting forward a hypothesis is thus essential to make this analysis effective.

Preliminary evidences motivating the DRTHC project proposal. The preliminary evidence motivating the present project was that obligate oil degraders were inhibited by HP while growing bacteria in complex microbial enrichments for several months. On the other hand, HP favoured the predominance of secondary oil degraders, that is microbial 'generalists' able to degrade many sources of carbon, including oil. Following an intense work of isolation, we were able to narrow down the complex microbial enrichments growing under HP to multispecies micro-colonies of 2-3 bacterial species. These bacterial species typically belonged to the genera *Halomonas*, *Vibrio*, *Thalassospira* and *Pseudoalteromonas*. The reason why single microbial species could not be retrieved is still unclear, but may rely on 1) the compensative capacity of different species to collaborate to gain survival; 2) the solid nature of the hydrocarbon supplied, possibly leading to cells' adhesion to oil particles. When pooling together again such multispecies micro-colonies to form a HP-adapted synthetic community (a microbial community whose representatives are known and belong to a common environment, which is here one under HP) these secondary degraders largely predominated once again under HP. However other 'satellite' genera were found in different proportions, according to the culture conditions, such as obligate oil degraders (e.g., *Thalassolituus*), piezophiles (e.g., *Photobacterium*), or fermentative bacteria (e.g., *Clostridium*). This natural differentiation into a core community surrounded by different satellite members is most interesting to set the special properties and functionalities of the core community (Fig. 1).

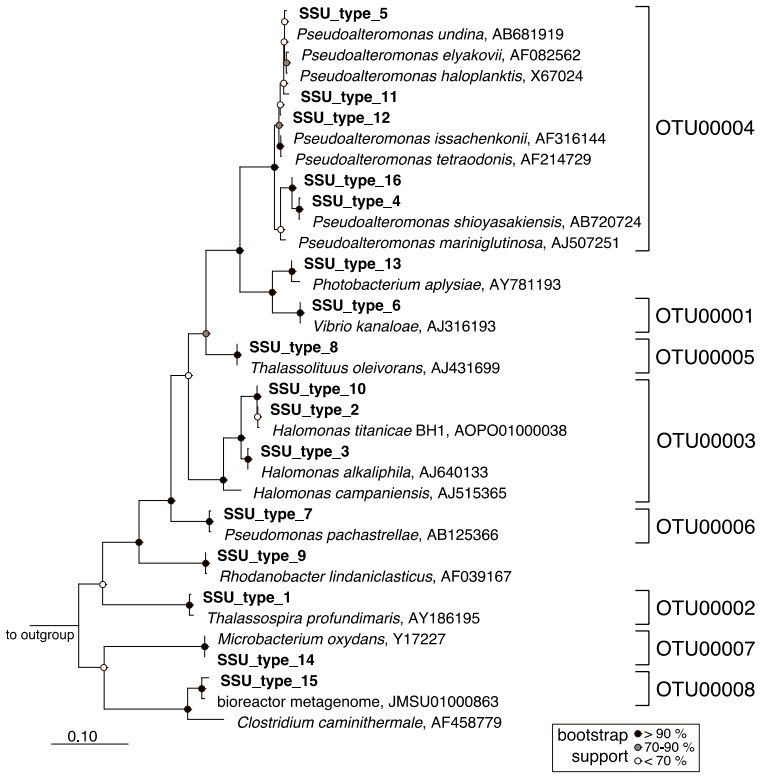

Figure 1. Phylogenetic 16S rRNA tree representing the multispecies micro-colonies (left, SSU_type) as compared to the HP-adapted synthetic communities (right, OTU). *The SSU_types represent the microbial representatives present in the initial multispecies micro-colonies, while the OTUs indicate the main Operational Taxonomy Units (that is, bacterial representative) growing in the HP-adapted synthetic communities. The tree indicates that throughout the continued experimentation (from multispecies micro-colonies to synthetic communities), the supposedly unfit secondary degraders* Halomonas, Thalassospira, Vibrio *and* Pseudoalteronomas *are constantly found, matching the exact 16S rRNA sequence.*

How does HP shape microbial hydrocarbon metabolism? The research hypothesis of this DHRTC project. We selected the genomes of the most recurrent bacterial species belonging to the core community predominating under HP (the secondary degraders

Halomonas, *Thalassospira* and *Vibrio*) and compare it to the satellite member which is an obligate oil degrader but fails to grow under HP (i.e., *Thalassolituus*). Comparison of their genomes was focused on the known genes responsible for hydrocarbons metabolism and pressure resistance as they constitute the two main conditions of the present experimental set up. However, the research was extended to another function that is 'surfactant biosynthesis', which might explain microbial biocatalysis in oil-containing environments. Biosurfactants are produced by certain microbial species as a response to an excess of oil to 1) prevent cell damage to the toxicity of high hydrocarbon concentrations; 2) solubilize hydrocarbons in water favouring accessibility by the cell and their consumption as carbon source. The list of selected genes is presented below, with a general indication of their function (Table 1).

Table 1. Target gens selected for comparison of the HP-adapted, solid hydrocarbon-degrading microorganisms. *A general description of the function of each gene is reported, along with the Pfam (Protein Family), that is, the family of proteins generated by such genes. The latter indicates the actual enzymatic functionality hold by the genes.*

Adaptation	Gene	Function	Pfam
Hydrocarbons	katEF	catalysis of peroxide	Catalase
Hydrocarbons	sodAB	superoxide dismutase	Sod_Fe_N
Hydrocarbons	sodAB	superoxide dismutase	Sod_Fe_C
Hydrocarbons	alkB	fatty acid desaturase	FA_desaturase
Hydrocarbons	cheW	chemotaxis	CheW
Hydrocarbons	fadL/todX	FadL outer membrane protein transport family	Toluene_X
Hydrocarbons	ompW	OmpW fatty acid transport	OmpW
Hydrocarbons	pagP	pagP	PagP
Hydrocarbons	P450	cytochrome P450	p450
Hydrocarbons	gntR	alkane degradation regulation	GntR
Hydrocarbons	araC	alkane degradation regulation	AraC_binding_2
Hydrocarbons	araC	alkane degradation regulation	AraC_binding
Hydrocarbons	araC	alkane degradation regulation	HTH_AraC
Hydrocarbons	tetR	alkane degradation regulation	TetR_N
Hydrocarbons	tetR	alkane degradation regulation	TetR_C
Hydrocarbons	merR	alkane degradation regulation	MerR
Hydrocarbons	amoC	ammonia/methane/hydrocarbon monooxygenase	AmoC
Hydrocarbons	amoB	monooxygenase B subunit	Monooxygenase_B
Hydrocarbons	fadB	beta oxidation	3HCDH
Hydrocarbons	fadB	beta oxidation	3HCDH_N
Pressure	ftsZ/A/K	GTPase that polymerizes to form a fstZ ring playing part of cell division	FtsZ_C
Pressure	trwB	plasmid transfer protein similar to the F0F1-ATPase	TrwB_AAD_bind
Pressure	sulA	inhibitor of ftsZ	SulA
Pressure	RecA	nucleases processing single-stranded DNA	RecA
Pressure	RecBCD	nucleases processing single-stranded DNA	Exonuc_V_gamma
Pressure	ssb	single-stranded DNA binding proteins	SSDP
Pressure	lexA	autoproteolytic activity	LexA_DNA_bind
Pressure	toxR	inner membrane proteins, environmental sensors	ToxS
Pressure	rseA	part of the rpoE operon, they anchor the inner membrane proteins	RseA_N
Pressure	rseA	part of the rpoE operon, they anchor the inner membrane proteins	RseA_C
Pressure	lon	protease related to sulA	LON_substr_bdg
Pressure	lon	protease related to sulA	Lon_C
Pressure	hsp	heat shock protein	HSP90
Pressure	hsp	heat shock protein	HSP70
Pressure	hsp	heat shock protein	HSP20
Pressure	hsp	heat shock protein	HSP33

Pressure	csp	cold-shock domain	CSD
Pressure	dnaJ	putative cellular thermometer; stress response	DnaJ
Pressure	dnaJ	putative cellular thermometer; stress response	DnaJ_C
Pressure	clpP	CLP protease	CLP_protease
Pressure	ompAF	OmpA/F	OmpA_like
Pressure	ompCF	OmpC/F	Porin_1
Pressure	ompH	OmpH	OmpH
Pressure	lamB	LamB (maltoporin)	LamB
Pressure	fabF	enzyme L-ketoacyl-ACP syn- thase II, an enzyme catalyzing cis-vaccenic acid (fatty acids unsaturation)	ketoacyl-synt
Pressure	fabF	enzyme L-ketoacyl-ACP syn- thase II, an enzyme catalyzing cis-vaccenic acid (fatty acids unsaturation)	Ketoacyl-synt_C
Pressure	mutT	MutT/NUDIX	NUDIX
Surfactants	acyltransferase	acyltransferases	Acyltransferase
Surfactants	acetyltransferase	acetyltransferase	Acetyltransf_1
Surfactants	acetyltransferase	acetyltransferase	Acetyltransf_2
Surfactants	acetyltransferase	acetyltransferase	Acetyltransf_3
Surfactants	acetyltransferase	acetyltransferase	Acetyltransf_4
Surfactants	acetyltransferase	acetyltransferase	Acetyltransf_5
Surfactants	acetyltransferase	acetyltransferase	Acetyltransf_6
Surfactants	acetyltransferase	acetyltransferase	Acetyltransf_7
Surfactants	acetyltransferase	acetyltransferase	Acetyltransf_8
Surfactants	acetyltransferase	acetyltransferase	Acetyltransf_9
Surfactants	acetyltransferase	acetyltransferase	Acetyltransf_10
Surfactants	glucosyltransferase	includes glucosyltransferases	Glyco_transf_8
Surfactants	ABC transporter	ABC transporter	ABC_tran
Surfactants	vhb	globin (O_2 transport)	Globin

The presence/absence of these genes in the selected genomes is reported in Fig. 2. The analysis will use the genes absent in *Thalassolituus* (the obligate degrader inhibited by HP) as a negative control, explaining their relation to survival under HP conditions using solid hydrocarbons as sole carbon source.

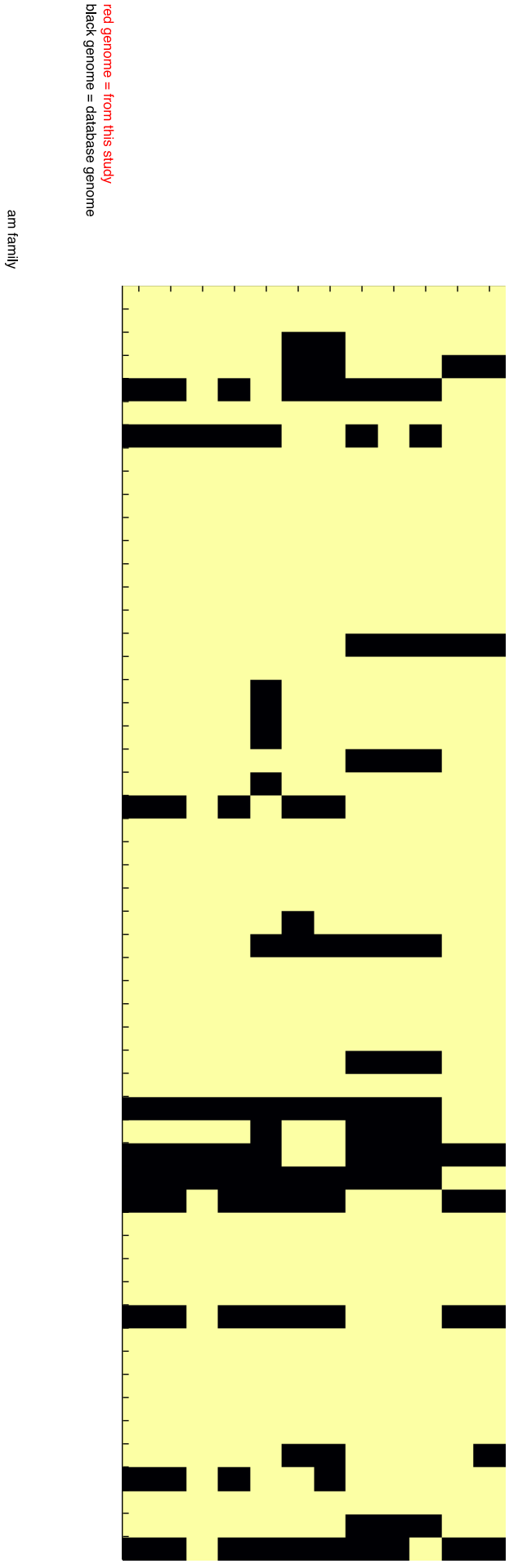

Figure 2. Heat-map representing the presence/absence of the target genes indicated in Table 1 in the selected genomes. *Black squares indicate absence of the gene (therefore, lack of the capacity to perform that specific function and dependence on other bacteria, where and if possible, for survival), while yellow indicates presence. Bacterial genome nominatives are indicated in red and black: the red nominative is the genome of the actual bacterial species that we possess, while the black nominative indicate the genome of the closest bacterial member known in the literature. As a result, black and red genomes belonging to the same member (e.g.,* Vibrio*, last two columns in Fig. 2) are very similar, but may different in few specific cases (e.g., Acetyltransf_8).*

Hydrocarbons. Both *Thalassolituus* genomes miss the *AraC_binding*, *AraC_binding2* and the *catalase* gene. In particular, *AraC_binding* is present in all the other genomes, making this an interesting function to investigate. On the contrary, the catalase is largely absent in all the other genomes too and will not be considered.

***AraC_binding*.** AraC is a regulator of the alkane degradation pathway. The expression of the bacterial genes involved in alkane assimilation is tightly regulated. Alkane-responsive regulators ensure that alkane degradation genes are induced only in the presence of the appropriate hydrocarbons. Many microorganisms contain several sets of alkane degradation systems (Rojo, 2009), each one being active on a particular kind of alkane or being expressed under specific physiological conditions (e.g., HP, temperature, oxygen availability). AraC-like gene sequences have been found linked to oil metabolism. In *Acinetobacter*, the AraC-family-related AlkR is induced by different *n*-alkanes. This regulator controls the expression of two genes: *alkMa* and *alkMb*. Both *alkR* and *alkM* are essential for growth on alkanes as sole carbon sources (Ratajczak et al., 1998): *alkMa* responds to solid, long-chain alkanes >C22, while *alkMb* responds to alkanes between C16 and C22. This information is very relevant, as the solid

hydrocarbons supplied throughout the whole experimental phase (enrichment, isolation and synthetic community testing) was either C20 or C30. Interestingly, neither acetate (one of the few non-oily substrates commonly degraded by obligate oil degraders) nor hexadecanol (an intermediate of C16 degradation) induce *alkMa* or *alkMb* (Tani et al., 2001). Both *alkM* genes encode a terminal alkane hydroxylase, which catalyses the first step of alkanes degradation by inserting an oxygen atom into the linear alkane chain to eventually form a fatty acid, a metabolizable substrate for the cell. This 'alkane-activating' mechanism is the first step in microbial alkane degradation, and absence or impairment of such function entailed cell inability to access the only carbon source available in our experimental set up.

However, *Thalassolituus* largely predominates when long-chain hydrocarbons are supplied as unique carbon source under ambient pressure. The absence of a regulator such as the *AraC_binding* gene may indicate a reduced capacity to support long-chain degradation under specific circumstances (e.g., HP) rather than the incapability of growing on long-chain hydrocarbons in general. For instance, the aforementioned alkane hydroxylase regulated by AraC, alkM, is an integral-membrane hydrocarbon hydroxylase. The latter are anchored to the cell membrane as they physically pass through it with single or multiple domains (Fig. 3).

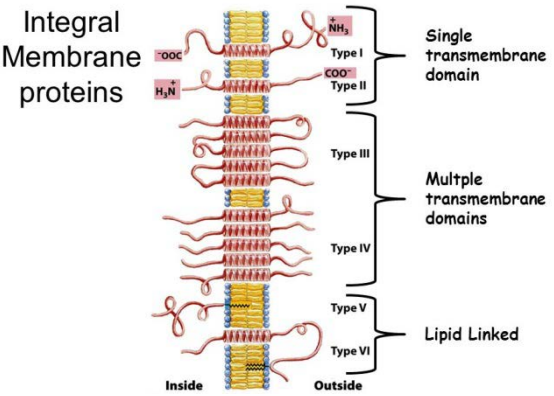

Figure 3. Different types of integral membrane proteins (from Lehninger Principles of Biochemistry, Fifth Edition, 2008. W.H. Freeman and company).

Maintenance of cell membrane fluidity is a primary problem under increased HP. HP is generated by the addition of 'more mass within a same volume'. On a biological level, this entails a compressing effect which reduces the cell membrane fluidity, therefore its capacity to keep homeostasis by 1) regulating the fluxes of metabolites inside/outside the cell; 2) maintaining transmembrane enzymes functional. The importance of cell membrane regulation under HP is highlighted by the multiple copies of the ATPase genes present in pressure-resistant bacteria (Vezzi et al., 2005). The transmembrane ATPases are, literally, little engines generating ATP, the energy-currency of the cell, of pivotal importance in cell metabolism. However, cells can counterbalance the 'compressing' effect imposed by HP in several ways. The absence of an AraC regulator supporting the expression of a long-chain alkane-activating enzyme appears as a relevant candidate in support of *Thalassolituus* impaired growth under HP while supplied with solid hydrocarbons. While not preventing its capacity to grow, this feature may however explain its loss of competitiveness in complex microbial communities. In this scenario, the obligate oil degrader *Thalassolituus* would be unable to regulate the expression of the transmembrane, alkane-activating enzyme alkM, which gives access to the only carbon source available. In *Thalassolituus*, an impaired activity of alkM due to HP would limit its capacity to thrive when long-chain hydrocarbons are supplied. Consequently, *AraC* gene availability in all the other secondary degraders may explain at least in part their capacity to grow.

Pressure. There are several missing genes in *Thalassolituus* in relation to pressure. Those absent in our strain Thalassolituus_T3 but present in others are *LON_Substr_bdg* and *LamB*. The latter is absent also in other genomes. Of these, only Thalassospira_T4 represents a genome of a microbe actually present in our experiments (the black entries refer to a database, see Fig. 2 legend). However, *Thalassospira* is commonly found in micro-colonies together with *Halomonas* species T4, T2 and C2, which possess this function. Therefore, this gene is also considered.

***LON_Substr_bdg*.** This gene encodes the ATP-dependent protease La (LON) substrate-binding domain protein. ATP-dependent Lon proteases are conserved in all living organisms and catalyse rapid turnover of short-lived regulatory proteins and many damaged or denatured proteins. The lack of this gene would imply the reduced capacity by the cell to remove non-functional proteins. One notable case related to HP concerns cell division, during which the enzyme FtsZ polymerizes to form a ring which is involved in the physical separation of one cell into two new cells. In *Escherichia coli*, HP inhibits FtsZ polymerization resulting into long, filamentous, undivided cells. Aertsen and Michiels reported that an *E. coli* mutant lacking Lon proteases displayed hyperfilamentation after a short (15 min) HP treatment (100 MPa, equivalent to 10 km below sea surface level). These values are different from the ones applied during our enrichment, isolation and synthetic community testing since we used much longer incubations (10-14 days) but lower HP (from 10 to 30 MPa). Normally, the FtsZ polymerization is inhibited by the gene *SulA* (which is present in *Thalassolituus*, Fig. 2). Generation of an *E. coli* double mutant containing lon sulA no more displayed filamentous cells under the same conditions, indicating that proper FtsZ activity, therefore proper cell division, is conducted under the regulation of lon proteases. Confirmation of such an impairment in *Thalassolituus* is most interesting and would require target experiments with pure cultures.

Together with HSP70 and CLP_protease (both present in all genomes in Fig. 2), Lon proteases are preceded by a promoter region which is sensitive to HP as much as to heat-shocks. Variation in temperature or pressure would therefore enhance the expression of these genes, whose activity is to prevent cell damage, or aid recovery after such stresses. In *E. coli*, a HP of 75 MPa mildly induced the expression of these genes, with a substantial expression observed at 150 MPa, both very high HPs above what experience in deep oil reservoirs in the North Sea. However, the level of heat or pressure necessary to induce a response differed among mutants (Abe, 2007). While it is hard to set a threshold valid for any bacterium, or define the capacity for such genes to effectively repair a damaged cell, it is relevant to note for the present DHRTC project's objective that deep, sub-seafloor reservoirs are subjected to both high temperatures and HP. The concomitant application of multiple stressors has been not studied extensively in the literature, particularly when related to HP along with another parameter. A full set of functional genes targeting cell damage might very well be necessary to cope with life in deep, sub-seafloor conditions at oil reservoirs.

***LamB*.** The LamB glycoporin family encode a maltoporin, that is a transmembrane enzyme (i.e., a porin) predicted to facilitate the passage of mono-, di-, and oligosaccharides, nucleic acids, and proteins across the bacterial outer membrane (Lång and Ferenci, 1995). The presence of the *LamB* gene along with a variety of fatty acid biosynthetic genes was considered a selective advantage to survive cell membrane stress in a naphthalene-degrading *Alteromonas* (Math et al., 2012). This consideration is based on the fact that transporters are the first target for HP stress owe to membrane stability, and because they allow import of available metabolic intermediates from outside the cell, preventing energy investment by cell for their biosynthesis. However, in the present case, the lack of a maltoporin in an obligate oil degrader is likely due to its inability to degrade sugars.

Surfactants.

The only gene absent in *Thalassolituus* and present in all other genomes is *Acetyltransf_8*.

***Acetyltransf_8*.** Acetyltransferases (or transacetylase) are a type of transferase enzyme that transfers acetyl groups. Acetyltransferases are normally related to biosurfactant-related metabolic pathways or hydrocarbon modification (e.g., production of wax esters and triacylglycerols, Kalscheuer and Steinbüchel 2003). Acetyltransferases are many, and the exact role of any of these is hard to assess without specific experiments (e.g., mutants deprived of target genes compared to double mutants where such genes are reintroduced).

Metaproteomic analysis of the synthetic communities revealed that HP significantly upregulated glycerol metabolism in cultures supplied with solid hydrocarbons (unpublished data). This suggests that HP might impact hydrocarbon metabolism by favouring hydrocarbon modification and storage of intracellular metabolites rather than leading to hydrocarbon complete oxidation. The lack of one acetyltransferase out of many (Fig. 2) does not suffice to validate this hypothesis. However, it is interesting to note that while *Acetyltransf_8* is present in all the other genomes here investigated, it is widely absent in obligate oil degrading genera (i.e., *Oleispira*, *Thalassolituus*, *Neptunomonas*, *Cycloclasticus*) or species (i.e., *Marinobacter hydrocarbonoclasticus*), and it is only present in three *Alcanivorax* species (http://pfam.xfam.org/family/acetyltransf_8#tabview=tab7).

Validated during sprint

Which part of the technology has been validated? We searched for a common gene set explaining why secondary oil degraders predominate under HP when solid hydrocarbons are supplied as sole carbon source in place of obligate oil degraders. The research was based on a number of target genes considered of relevance to thrive under these conditions, such as genes involved in hydrocarbon metabolism, pressure-responsive genes and genes related to biosurfactant production.

How was this part of the technology validated? We conducted a presence/absence comparison between the aforementioned target genes in the genome of a HP-sensitive negative control (*Thalassolituus*) and HP-adapted microbes (*Halomonas*, *Vibrio*, *Thalassospira*).

What are the conclusions of the validation? Of the selected target genes, we found that only few could indicate a significant difference explaining improved microbial catalysis under oil-containing deep-sea HP. These conditions point to an increased tolerance to a stress response (*AraC_binding*, *LON_Substr_bdg*) or capacity to modify hydrocarbons (*Acetyltransf_8*). However, these seem insufficient to be descriptive of a specific enzymatic set conferring a selective advantage.

Proposed way forward

What is next in line to be validated? A thorough analysis of how these genes are expressed under the specific deep, sub-seafloor conditions is needed. Presence/absence of genes (genomic analysis) does not *per se* suggest that such genes are actually expressed (transcriptomic analysis) under the desired conditions. MEOR under HP may be impaired by a general incapacity on the part of bacterial cells to express some specific genes.

How can this be validated? A new series of synthetic community experiments should be performed, incubating cultures under conditions resembling deep oil reservoirs in terms of HP, temperature and hydrocarbon. Cultures should be incubated for a number of days, after which gene expression analysis should follow. Negative, HP-sensitive controls available in culture collections (*e.g.*, *Alcanivorax*) should be incubated to confirm the pattern observed with the present synthetic cultures.

Does it depend on other technologies? Gene expression analysis (transcriptomics) is an expensive but affordable technique. At the Dept. of Bioscience of Aarhus University, all the required equipment is available to run this analysis. Hence, this information would not depend on other technologies. However, some genes may yield proteins with an unknown function. Understanding these proteins' functionality would require a more intensive effort. However, narrowing down the research to (few) unknown proteins would likely reveal novel enzymatic activities in an extreme yet defined environment such as deep, sub-seafloor oil reservoirs. Owe to the public unawareness of these proteins function, gaining this information would then turn into a critical advantage.

Transcriptomic analysis would also require cultivation techniques to simulate *in situ* conditions of temperature and HP. However, these facilities are used on a daily basis by this applicant within the *Self Healing Cement* project.

Final conclusion

We investigated whether a common gene set exist explaining the microbial requirements for MEOR under HP by sequencing the genome of the first HP-adapted, solid hydrocarbon degraders. We selected a number of potentially interesting genes and highlighted three related to stress response and hydrocarbon modification. While being related to the relevant process under study, their function appears to be too general and their comprehensive impact on cell metabolism too limited to explain the observed HP impact on microbial metabolism. The highlighted genes do have an impact on microbial hydrocarbons degradation, but it remains unclear how they can confer a selective advantage in deep-sea environments. Another approach would thus be required to 'select' the genes of interest. This would entail cultivation of the HP-adapted microbes under *in situ* conditions and analysis of the most expressed genes. This functional approach would clearly highlight which genes are actually necessary under the relevant conditions. All the required facilities (DNA sequencing, bioinformatics, HP and high temperature bioreactors) are used on a daily basis at the Dept. of this applicant. These experiments would however require another project to be executed.

References

Abe 2007. Biosci. Biotechnol. Bioenv. 71(10):2347-2357.

Tani et al 2001. Bacteriol. 183:1819–1823.

Rojo 2009. Env. Microbiol. 11(10):2477–2490.

Vezzi et al. 2005. Science 307:1459–1461.

Lång and Ferenci 1995. Biochem. Biophys. Res. Commun. 208:927–934.

Math et al. 2012. PlosOne 7(4):e35784.

Kalscheuer and Steinbüchel 2003. J. Biol. Chem. 278:8075–8082.

Increased PI by injection of Acidgen

Helle Foged Christensen, Geo and Finn Engstrøm, Mærsk Oil and Gas AS

Abstract

Long horizontal wells in chalk reservoirs need in general to be stimulated in order to produce at commercial rates. The objective for the stimulation is to remove drilling induced permeability impairments around the well bore and/or to reduce the effects of the converging flow lines around a well bore. Stimulation of chalk wells is often done by injecting HCl into the wellbore which may increase the well bore radius (matrix wash), generate worm holes (CAJ) or generate fractures (acid fracturing). Common for all 3 methods is that they will generate a partly water filled zone around the well bore/wormholes/fractures that at least initially or permanently will impede the inflow due to a relative permeability effect. The methods will likely not stimulate evenly along the well bore, due to the fast reaction of between calcite and HCl that does not allow the HCl to penetrate deep.

Injection of a slow reacting acid would allow the acid to penetrate into the matrix around the wellbore and would likely produce a more even stimulation. The effect of Acidgen on chalk has been tested in a previous project (Chemweak/JCR-7) where it was found that Acidgen can be injected at room temperature without reacting with the chalk matrix. After being heated to reservoir temperature it will convert into formic acid plus alcohol and evenly increase the porosity in the affected zone.

The objective of this project was to investigate the effect of Acidgen on water filled reservoir chalk - especially to study the effect on the absolute permeability. The results demonstrated that Acidgen can be injected into reservoir chalk and will homogeneously increase both matrix porosity and matrix permeability. The minimum change in permeability can be predicted from the poroperm trend for the chalk. The injection of Acidgen may in some cases increase the permeability by more than a factor 10 in case the Acidgen removes the calcite cement in stylolites. The injection of a 30% Acidgen slug may increase the matrix permeability by a factor 2.

A comparison of permeability effect of the injection of 15% Acidgen into the matrix and the effect of an acid-wash by 15% HCl demonstrated that for the same acid volume, a more negative skin is generated by the Acidgen compared to the HCl.

The results of the project demonstrated that Acidgen injection in some cases could be a better alternative than HCl injection with respect to decrease of skin effect. Acidgen injection also hold the possibility of chang-ing the relative permeability in a zone around a well bore / fracture in a chalk reservoir as Acidgen likely remove the outermost layer on the calcite particles and thus remove the effects of any previous coating.

Technology vision

The inflow/injectivity potential of an oil well in low permeability reservoirs like the North Sea chalk is signifi-cantly controlled by the permeability in the zone around the wellbore. The effective permeability around the well bore can be negatively affected by the drilling/completion process. Chalk wells are therefore commonly stimulated by acid wash, acid injection and fracking including complex and expensive well completions. The objective for the stimulation/fracking is to improve the productivity/injectivity of the well and to remove/reduce any drilling induced damage.

The primary stimulation techniques for carbonates include the injection of HCl into the well bore. The injection of HCl will effectively increase the wellbore size and generate some worm holes, but will have limited positive effect on the matrix properties, as the acid reacts nearly instantaneous with the carbonate (the acid is therefore not injected into the matrix pores). The injection of the HCl may cause a reduction of the matrix permeability around the well bore, as the spent acid is pushed into the matrix around the bore hole and worm holes, generating a negative (lower PI/II) relative permeability effect.

The basic hypothesis/technology vision behind this project is that if an acid can be injected into the chalk in an inactive state and then be activated when the acid is within the matrix pore space, it will be possible to acid stimulate the matrix in a zone around the wellbore. This will likely increase PI/II of the well, generate a more even flow pattern into the well bore and reduce the risk of bypassing oil between worm holes/fractures.

The stimulation of the matrix pore space around a wellbore with acid in the pore space can, in addition to increase porosity/permeability, also be expected to remove any coating of the carbonate grains. This could make it possible to manipulate the surface properties of the chalk matrix by co-injection of surface active chemicals. A change of the surface properties of the matrix may allow modifying the relative permeability and capillary pressure properties of the matrix. This may reduce the water-cut.

In a previous project (Chemweak in JCR-7) it has been demonstrated that Acidgen (a formic acid precursor) can be injected into the chalk matrix in a cold state and then turn into a strong acid by being heated-up to reservoir temperature, dissolving part of the chalk matrix.

The objective with this Sprint project is to demonstrate the effect of Acidgen injection into chalk with respect to change of matrix porosity/permeability and thereby the potential for increasing the PI/II of a chalk well.

The injection of the Acidgen into a well bore will likely take place at the end of the drilling phase, before the running of the casing and may allow the treatment of the entire well length in one go. The effect of the Acid-gen injection will develop while the casing is run and the well is completed. The Acidgen injection technique may thus provide a cheaper stimulation technique, compared to the currently used. It may also reduce some of the matrix damage introduced by the current acid stimulation techniques and have the potential to modify the matrix properties around the wellbore. Acidgen injection may thus provide a cheaper and potentially more efficient stimulation technique, compared to the currently available. The Acidgen injection technique may also open-up for modifying the surface properties of the chalk around a well bore and thus open-up for modifying the relative permeability which could ultimately act as a filter reducing the water cut.

Validation of technology

The first step in the validation of the Acidgen injection technology (this project) is to prove the feasibility of the injection of cold Acidgen into chalk at reservoir condition (stress), activate the Acidgen by heating the chalk samples to reservoir temperature and observe the change in the matrix porosity and matrix permeability. The feasibility of Acidgen injection is considered validated, in case the Acidgen will increase the overall porosity/matrix permeability of chalk in a predictable manner.

The validation of the Acidgen injection method was performed by selecting 6 reservoir chalk samples from the Dan field (cleaned plugs), load the samples to reservoir stress, saturate the samples with water, record the liquid permeability, inject Acidgen into the samples at room temperature, heat the samples to 90 ^{o}C and allow it to react with the chalk matrix, cool the samples and replace the spent acid with water, record the liquid permeability, reduce the stress on the samples and finally record the unstressed sample porosity. The performed tests included some variation in base sample permeability and the Acidgen concentration was varied.

The test data allow a full evaluation of the porosity/permeability effect of injection of Acidgen at reservoir condition into water bearing chalk, but the project has not provided data on the effect of oil in the matrix. Nor has the effect of the acidization on the calcite particle surfaces been studies in details (e.g. by SEM).

Laboratory Testing and Test results

The selected test program (stress and temperature) is based on typical reservoir conditions in the Dan Field.

Selection of plugs for testing

A total of 10 plugs, previously used for CCAL, were received for the Acidgen project. It was decided to select the 6 plugs for testing on the basis of their absolute permeability, cf. Figure 3-1.

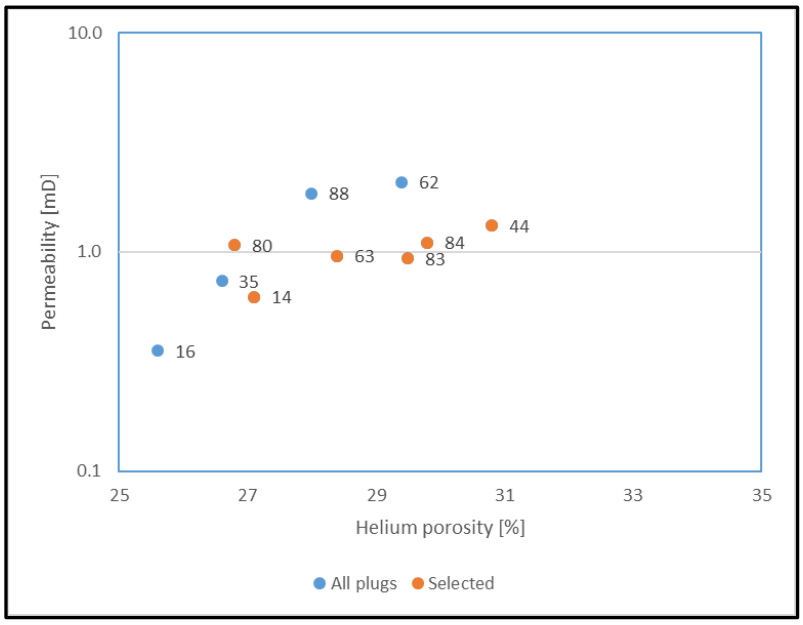

Figure 3-1 Porosity/permeability plot for all plugs received

Test set-up

The triaxial test set-up consists of a conventional Hoek cell with the end pistons fitted for acoustic measurements. External axial deformations are measured using two LVDT's (Linear Variable Differential Transformers) and by the displacement measured by the load frame itself. Pore pressure transducers are mounted at both the top and bottom outlet from the specimen.

A heating device is fitted around the Hoek cell and isolated at the sides. Further, isolating material is placed at the top and bottom pistons to prevent heat transfer from the cell through the pistons to the load frame (cf. Figure 3-2. The temperature is measured inside the Hoek cell by a PT100 needle placed in the hydraulic oil close to the Hoek membrane.

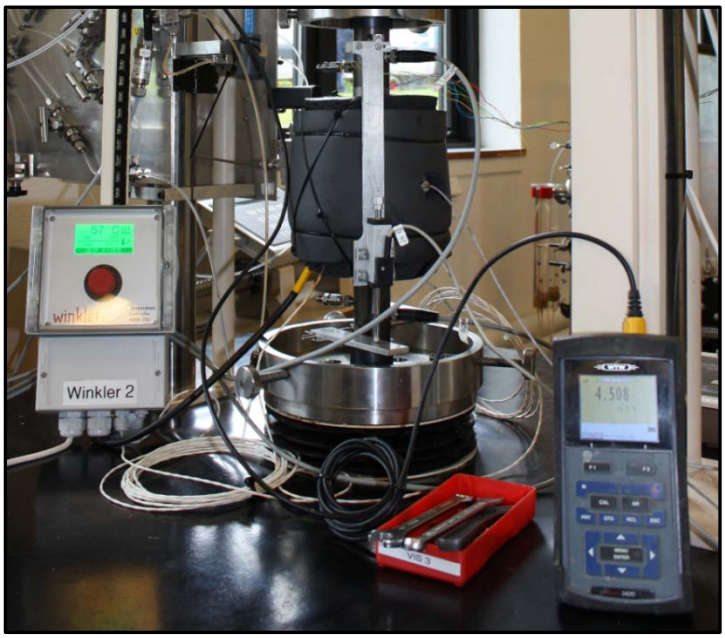

Figure 3-2 Hoek cell with heating device and control unit

The specimen is installed with a layer of fibertex on top of top and bottom filter plate (to prevent jetting during the injection phase).

Test program

The test program comprises the following test phases (single stage injection):

1. Initial loading in dry state to estimated field stress level (σ_v, σ_h) = (11.6, 5.3) MPa
2. Creep phase
3. Saturation and permeability measurements at 3 differential pressure levels
4. Drying the specimen for 2 days at 90 °C
5. Cool down phase
6. Inject Acidgen at selected injection rate and given concentration. The aim is to inject 1 PV in 30 minutes
7. Activate Acidgen by heating to 90 °C for 1 day
8. Cool down phase
9. Flush out Acidgen 3 PV
10. Permeability measurements at 3 differential pressure levels
11. End test including measurement of the He-porosity after the Acidgen injection.

For the multi stage test (plug 44) the first phase includes step 1 through 10 followed by a drying phase for 2 days. The specimen is then unloaded, the Hoek cell is rotated and the specimen is loaded to field stress again, following steps 1 through 11. The purpose of the rotation is to avoid dissolution at the inlet end due to double injection of Acidgen.

An overview of the test program is found in *Table 3-1*. The Table shows the plug no., the Helium porosity before test from SCAL, the injected Acidgen concentration, the injection rate and the state of the specimen at injection.

Table 3-1 Overview of test program

Plug no.	Helium porosity [%]	Specimen length [cm]	Acidgen concentration	Injection rate [cm^3/hr]	State at Acidgen injection
14	27.1	5.085	10 %	30	Dry
44	30.8	3.697	20 %*	25.7	Dry
63	28.4	3.275	5 %	25.7	Dry
80	26.8	3.047	10 %	20	Dry
83	29.5	5.230	20 %	35	Dry
84	29.8	3.226	15 %	25.6	Dry

*2 times 10% - Test programme step 1 to 10 was run and the core plug dried in the Hoek cell. The Hoek cell was rotated and test programme step 1 to 11 was then run.

First Pass Analysis of Results

The changes in absolute liquid permeability are listed in Table 3-2. The table shows the plug no., the CCAL porosity before testing, the used Acidgen concentration, the absolute permeability measured at field stress before (Kperm1) and after Acidgen treatment (Kperm2) and the increase in absolute permeability in %.

Table 3-2 Permeability changes

Plug no.	$ø_{before}$ [%]	$Ø_{after}$ [%]	Acidgen conc. [%]	k_{perm1} [mD]	k_{perm2} [mD]	k Increase in [%]
14	27.1	26.4	10	0.42	0.36	-14 %
44	30.8	30.3	20*	0.64	0.66	+3 %
				-	1.02	+59 %
63	28.4	28.5	5	0.52	0.64	+17 %
80	26.8	26.7	10	0.51	10.1	+1880 %
83	29.5	30.3	20	0.66	0.58	-12%*
84	29.8	30.0	15	0.76	0.84	+11 %

*2 times 10% - see comments below Table 3-1.

Table 3-2 illustrates that Acidgen injection in general has increased the liquid permeability slightly for the majority of the tested samples and increased the liquid permeability by nearly a factor 20 for one of the 6 samples (cf. Figure 3-3). The sample porosity from before/after testing (Table 3-2), sample dimension during testing (LVDT-measurements) and recorded sample dimensions/weight before/after testing are illustrated, however, that samples had compacted during testing and sample porosity was affected by temperature. A more complex analysis (Section 3.5) was therefore required in order to correctly infer the effect of Acidgen on permeability.

Figure 3-3 Photo of plug 80 w. stylolites, after test

Detailed Analysis of the Results

The initial analysis of the results demonstrated that the porosity after the tests was not in general larger than before as expected due to the acidization. The lower-than-expected post Acidgen injection porosity is likely due to compaction of the samples during the testing. The changes in the porosity during the rock mechanics testing of the samples were therefore investigated in details and the "exact" porosity at the time of permeability measurement before/after Acidgen injection was estimated both from the LVDT-measurements during testing and the measured porosity before/after testing. The LVDT-porosities was anchored in the recorded porosities before/after and LVDT-readings where converted to porosities assuming a constant sample diameter during the test. The results summarized below and illustrated on Figure 3-4.

- Tested chalk samples was truly matrix permeability dominated chalk samples (limited fracture permeability)
- 1 cm^3 1% Acidgen solution will dissolve 0,0058 cm^3 calcite. The uncertainty is around 5%. The calcite solubility of Acidgen was defined from data in the Chemweak project (JCR-/). A 20% Acidgen solution will thus dissolve the same amount of calcite as a 15% HCl solution. Acidgen is thus only 73% as efficient as HCl per volume.
- Acidgen will increase the size of all the matrix pores/pore throats and will increase the matrix porosity in line with the volume of Acidgen in the pore space. This was illustrated by CT-scanning in the Chemweak project (JCR-7)
- The change in the matrix porosity/permeability induced by the Acidgen in the pore space will in general follow the poroperm for the chalk, but may also significantly (factor ~20) increase the matrix permeability in case the stylolites in the sample is parallel with the direction of the permeability measurement.
- Total permeability enhancement for a 30% Acidgen injection could be in the order of a factor 2 for the matrix and a factor 20 if the Acidgen have "cleaned" some stylolites. The effect of 30% Acidgen injection is based on the estimated change of porosity by a 30% Acidgen injection converted to a change in permeability using a standard poroperm model for chalk.

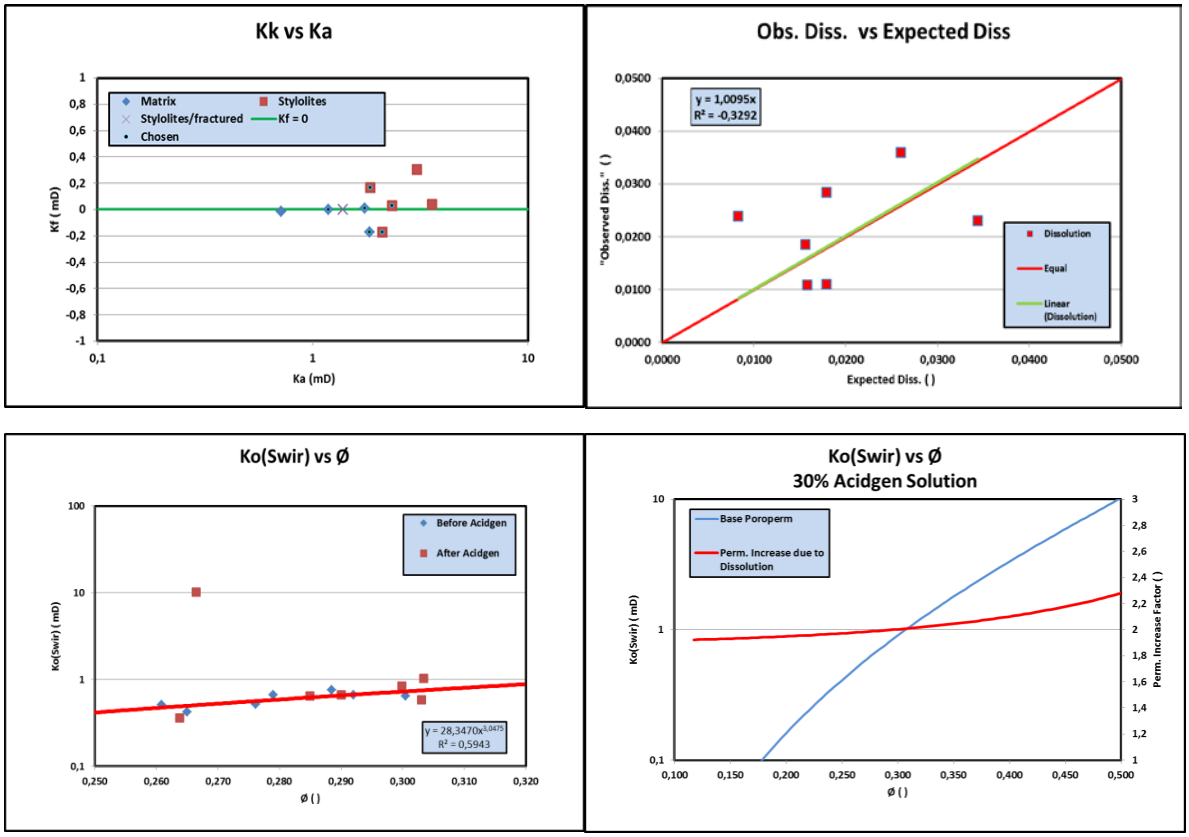

Figure 3-4: Primary Results

Possible PI/II Effect of Acidgen Injection

The possible effect of an Acidgen vs HCl acidization has been tested by estimating the expected skin after injecting 20% Acidgen or 15% HCl into a chalk well bore. 20% Acidgen and 15% HCl was chosen as a test case as 20% Acidgen will dissolve the same amount of calcite as 15% HCl for the same amount of solution. In the estimation of skin it was assumed that HCl will increase the borehole, while Acidgen will increase the porosity around the bore hole. The skin was estimated as function of acid solution volume in bbls/ft of 6" well bore and for 5 different cases:

- Water filled chalk or no effect of water block or Krw(Sor(w))f=1)
- Full waterblock or Krw(Sor(w)f = 0,3)
- Acidgen generate on average a factor 4 increase in the permeability due to cleaning of fractures and full water blocking (Krw(Sor(w)f = 0,3)
- Acidgen generate on average a factor 10 increase of the permeability due to cleaning of fractures and full waterblocking (Krw(Sor(w)f = 0,3).
- Acidgen generate on average a factor 4 increase of the permeability due to cleaning of fractures and no waterblocking (Krw(Sor(w)f = 1).

The results of the analysis are illustrated on Figure 4-1.

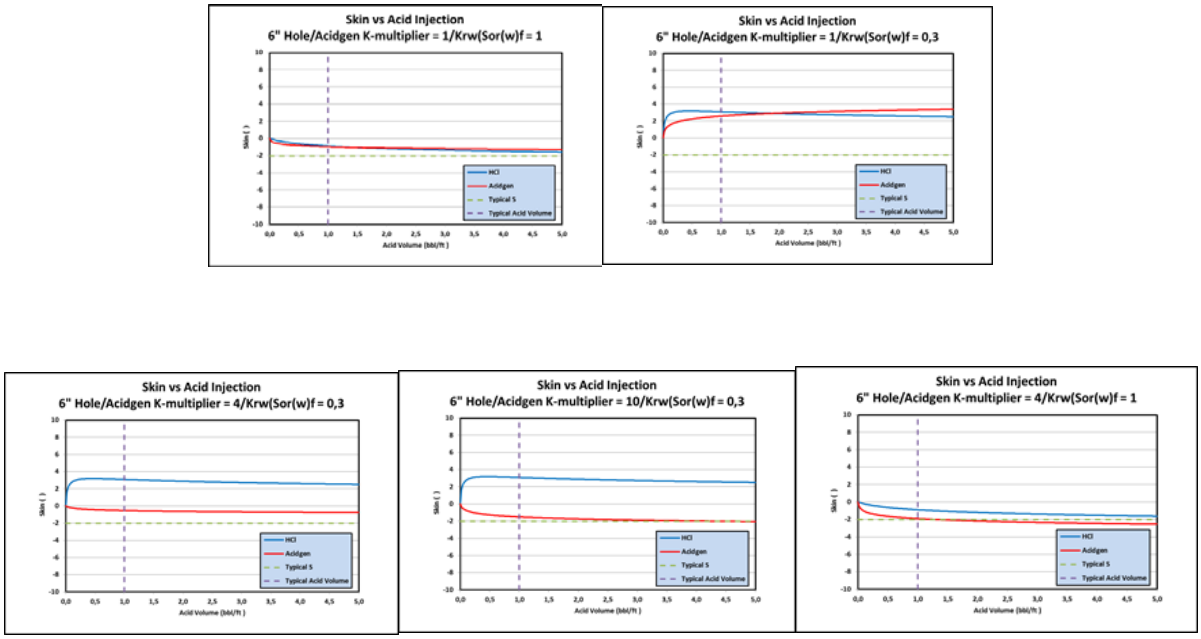

Figure 4-5: Skin Effect of Acidgen and HCl injection

The primary observation of the analysis is that:

- Acidgen injection may produce an equal or lower skin compared to standard HCl injection for the same amount of injected fluid if the effect of worm holes/fractures created during HCl injection is ignored.
- Acidgen injection can generate a -2 skin in case the effect of water blocking is limited after some time and the average permeability enhancement due to cleaning of small scaled fractures is a factor 4. Alternatively, in case the effect of water blocking is included, then a factor 10 increase in the permeability due to fracture cleaning is required.

As the permeability enhancement on average in the performed 6 tests was in the order of 3-4 it follows that it is not unrealistic to expect that Acidgen injection may be able to generate a -2 skin in a homogeneous manner along a well bore and thus could be able to deliver a well bore stimulation that is similar to e.g. a CAJ-stimulation where the stimulation effect likely is more variable along the well bore.

Summary of Observations

The performed limited test program has demonstrated:

- Acidgen injection may improve the matrix porosity/permeability in chalk. The injection of 20% Acidgen to a depth of 1 ft around a 6” wellbore may increase the PI by 30-40% based on the change in porosity/permeability, but may in reality be more, as the Acidgen may also remove some mud cake or less due to a relative permeability effect.
- The increase in effective permeability due to Acidgen injection could be in the order of a factor 10 in case the Acidgen injection remove calcite cement from e.g. stylolite associated fractures.

- Acidgen injection will likely remove the outer layer on the calcite particles in chalk in a homogeneous manner and thus remove the effects of any coating on the grains associated with diagenesis or deposition from the pore fluid (e.g. oil) and thus leave the calcite particles with pure calcite surfaces.

The limited test program has thus supported the basic project hypothesis, but further work/studies are required before the full effect and cost of Acidgen injection as a stimulation method can be established.

Proposed Way Forward

The following topics should be studied further:

- **Effect of relaxation near the wellbore wall (as opposed to compaction) and radial strain?**
  The 6 tests have been carried out at constant stress, which is a conservative estimate of the stress state near a wellbore. A test series with constant strain conditions is suggested
- **Does Acidgen injection alter the relative permeability and/or the wettability?**
  In case Acidgen injection alters the wettability of the grains affected, this may further enhance the PI and could provide a method to lower water cut. The effect of the acidization by Acidgen on the calcite particle surfaces shall also be studied – e.g. by SEM.
- **Permeability changes when injecting in a two phase system (oil/water saturated chalk)?**
  The 6 tests have been carried out by injecting in dry chalk, the relative perm effects when injecting in oil or oil/brine saturated chalk should be quantified
- **Effect of washing out the Acidgen residue with oil or water?**
  Some data on the washing out process is provided, but the effect of washing out with oil should be studied
- **Effect on the oil/water ratio and the fluid properties in the near-wellbore regime?**
  Further modelling is required to quantify the oil/water ratio and fluid properties around the injection well – including a study of the possibility of modifying the matrix properties in a manner that can act as a filter that could reduce the water production by holding the water back in the formation
- **Effect of hole size on the skin effect?**
  Further modelling of the effect on skin reduction as function of hole size – including a study of the most efficient use of 1 bbl of acid. The modelling may demonstrate that the Acidgen injection may improve the effect of the Fishbone technique.
- **A parametric study of the effect and cost of Acidgen** injection with the objective of defining how an Acidgen injection can provide the maximum increase in NPV compared to other stimulation techniques.

Final conclusion

The limited test program has demonstrated that:

- Acidgen injection will likely not have any negative effect on the chalk poroperm in the form of plugging of the pore space by spent Acidgen or dissolved calcite
- It may increase the local matrix permeability around a wellbore by up to a factor 2 for a 30% Acidgen solution and locally up to a factor 20 by increasing the permeability of existing stylolites

- It is likely that Acidgen injection has the potential of removing any existing coating/deposits on chalk particles and thus returns all the chalk particle surfaces to naturally water wet calcite. If the injected Acidgen solution include agents like Silan that can change the wettability of the calcite surfaces it may be possible to tailor the properties of the chalk matrix close to the well bore such that the near well bore region may act as a filter. The filter effect could be an effect of a modification of the relative permeability. This could open-up for a reduction of the water inflow into chalk wells.

The test program has thus in general confirmed the underlying hypothesis. Future work should be aimed at designing the maximum effect and to study the economic/practical optimum for the application of the stimulation method.

References

From the JCR-7 Chemweak Project:

1. Report A1: Homogeneous dissolution of outcrop chalk samples. GEUS report, Claus Kjøller & Lykourgos Sigalas
2. Report A2: Homogeneous dissolution of reservoir chalk samples (GEUS), including SEM report (UiS)
3. Report B1: SEM report (University of Stavanger)
4. Report C1: Stevns chalk, specimen preparation. Geo job no. 36983, dated 2014-02-21
5. Report C2: Stevns Chalk treated AcidgenTM, preliminary assessment, Triaxial compression tests, Geo job no. 36983, dated 2014-08-20
6. Report D1: Back calculation of Chemweak laboratory tests, IsamGeo report

Fungal enhanced oil recovery

Simon Knutsson, Aalborg University, Department of Chemistry and Bioscience

Morten Poulsen, Danish Technological Institute – DTI Oil & Gas

Jens Laurids Sørensen, Aalborg University, Department of Chemistry and Bioscience

Abstract

A substantial amount of oil remaining in oil reservoirs after primary and secondary production are not readily producible using conventional methods. For this purpose, alternative methods like microbial enhanced oil recovery (MEOR) needs to be developed. In this study we explored the potential of utilizing biosurfactant-producing fungi for MEOR purposes through community mapping of fungi-communities in crude oil, condensate and pipeline pigging solid, and isolation and characterization of fungi present in the samples. Our study reveals that fungi are present in the crude oil produced and that they were able to produce water surface tension-lowering compounds with surfactant properties. In the future, we envision that this knowledge can be used to modulate the fungal community in oil reservoirs to favor the presence of the most potent surfactant-producing fungi.

Technology vision

More than two thirds of the oil ever found is still in the ground after primary and secondary production. To increase oil production, numerous strategies can be applied including Microbial Enhanced Oil Recovery (MEOR). Fungi are known to produce biopolymers, biosurfactants and crude oil-degrading enzymes. Biosurfactants are amphiphilic molecules harbouring both hydrophobic and hydrophilic properties [1]. Consequently, they preferentially partition in the oil-water interphase, reduce the interfacial tension and form oil emulsion in the oil-water interface [2, 3]. Biosurfactant-producing fungi thus pose potential candidates for enhancing oil recovery. Numerous biosurfactants have been isolated from fungi [4, 5], oil reservoir indigenous fungi can also be biosurfactant producers.

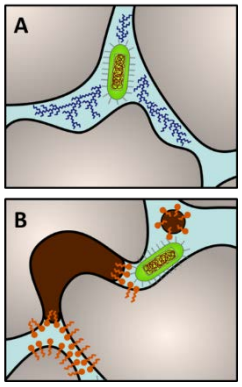

Figure 1. Conceptual model of effect of biopolymers (A) and biosurfactants (B) on oil production. Biopolymers increase the viscosity of the water phase and through this increase the sweeping effect of the water front. Biosurfactants reduce the interfacial tension and form oil emulsion in the oil-water interface thereby increasing oil production.

Fungal communities have traditionally been examined through isolation and cultivation using different media and growth conditions [6, 7]. In these culture dependant methods, slow-growing fungi often fail to

be isolated using standardized protocols, which limits the available information about fungal community composition at site of interest. However, recent technological advances in next-generation sequencing techniques targeting specific genomic regions from fungi [8, 9] enable culture-independent analyses of the fungal communities [10]. In-depth knowledge about fungi present will enable formulation of mediums for targeted and selective enrichment of potential biosurfactant-producing fungi.

The fungal kingdom is divided into seven phyla and include single celled organisms (yeasts) to larger multicellular organisms (filamentous). Yeast cells vary greatly in size (typically 3-15 µm) depending on growth conditions and genome size. Filamentous fungi form tubular, elongated, and thread-like (filamentous) structures called hyphae with a typical diameter of 4-6 µm. Filamentous fungi spread by forming various types of spores (2-20 µm) or by breaking off pieces of hyphae, which are dispersed to the environment.

Members of the fungal kingdom have been found in almost all environments on earth, including arctic areas and glaciers [11] and in areas with temperatures above 62 ˚C [12], although their reproductive spores can survive even more extreme conditions. We envision that fungi can be used for enhanced oil recovery by exploiting their potential for producing biosurfactants *in situ* or *ex situ*. *Ex situ* production is achieved through large scale production on land by choosing the most powerful producers that can be controlled in a production facility. *In situ* production of surfactants is achieved by stimulating production of biosurfactants by the fungi that are already present in oil reservoirs. To determine the potential of using this approach, a characterization of the fungal community and their biosurfactant-producing ability is therefore needed.

Carbonate reservoirs may exhibit varying properties with respect to permeability, porosity and liquid flow patterns. The Danish North Sea reservoirs are characterized by having average pore size around 1 µm (calculated from the Kozeny-Carman equation, [13]) with fractures and individual pores being considerably larger. It is therefore anticipated that fungal spores in sizes of few µm's hold the ability to pass through the reservoir. This observation is further supported by the finding of fungal DNA in crude oil samples; fungi either inherently present in the reservoir or originating from the brine injected to sweep the reservoir. Regardless, the isolation of fungi from a reservoir samples demonstrates that the fungi, if not active, at least are able to survive under reservoir conditions. In addition, the finding of a candidate organism able to produce surfactants under laboratory conditions, opens the possibilities for applying Fungal Enhanced Oil Recovery (FEOR) through several strategies:

1. Facilitate growth of already present organisms in the reservoir through supplementation of growth mediums, with the aim of producing surfactants *in vivo*. This likely will furthermore induce plugging of high-permeable pores by growth of hyphae and through this induce water conformance.
2. Introduce spores of fungi able to produce surfactants under anaerobic conditions to the reservoir, and subsequently activate and support their activity through nutrient supplementation. Besides the EOR effect from the biosurfactants this will, similarly to option 1, likely also lead to plugging of pores and through this induce conformity of water sweep.
3. Produce surfactants *ex vivo* for subsequent injection into the reservoir. Compared to the above this is considered a safer way to biologically enhance oil production, although also more costly process.

Validation of technology

Validated during sprint

The potential of using fungi for enhanced oil recovery was determined by two parallel tracks: 1) Profiling of the fungal community by a culture-independent approach using extracted DNA from oil reservoirs and 2) Determination of the ability to produce biosurfactants by fungi isolated from oil reservoirs.

The experiments were conducted with samples isolated from oil reservoirs from the North Sea collected by personal operating at oil rigs and stored at DTI at 4 °C under anaerobic conditions.

1. Experimental

1.1 Profiling the fungal community

To profile the fungi community in crude oil, DNA was extracted directly from crude oil samples and analysed with use of amplicon sequencing. In brief, genomic DNA was extracted from crude oil by centrifugation at 20.000 x g for 30 min. The supernatant was discarded and the pellet was processed with the FastDNA SPIN Kit for Soil (supplied by MP Biomedicals). The extracted genomic DNA from 17 samples was screened for fungi DNA with the use of PCR and internal transcribed spacer (ITS)-targeting primers and sequenced using the Illumina MiSeq platform.

1.2 Growth and identification of fungi

1.2.1 Isolation of fungi

Ten samples from oil reservoirs were collected. The samples were handled under sterile conditions in an N_2 atmosphere to minimize the risk of contamination and introduction of oxygen. The samples were plated onto three types of media: Potato dextrose ager (PDA) medium containing (per litre) 39 g PDA and 1 mL trace solution (5 g/L CuSO4•5H2O, 10 g/L ZnSO4•7H2O), Malt extract ager (MEA) medium containing (per litre) 20 g malt extract, 1 g peptone, 20 g glucose, 20 g ager and 1 mL trace solution and yeast pep-tone glucose (YPG) medium, consisting of (per litre) 10 g yeast extract, 20 g peptone, 20 g glucose, 20 g agar and 1 mL trace solution [14]. PD and MEA media contained both tetracycline and ampicillin for antibacterial selection.

For liquid samples (crude oil), 100 µL of sample was inoculated onto the petri dish, and for solid samples (picking debris) an inoculating loop was used to inoculate the samples. The plates were incubated under anaerobic and aerobic conditions at three different temperatures: 25 °C, 40 °C and 60 °C for up to 4 weeks or until growth was observed. Upon growth, fungi were transferred and isolated on new plates.

1.2.2 Identification of isolated fungi

DNA was extracted from the emerging fungi using DNeasy Plant Mini Kit (supplied by Qiagen, Germany) and the FastDNASPIN Kit for Soil (supplied by MP Bio-medicals) following the manufacturer's instructions. To identify the isolated fungi, polymerase chain reaction (PCR) was used to amplify the ITS region. PCR was run with the primers ITS1 (5'-TCC GTA GGT GAA CCT GCG G-3') / ITS4 (5'-TCC TCC GCT TAT TGA TAT GC-3') to amplify the ITS region, which should generate a product with the size of 524 bp. The reaction was carried out in a 25 µL volume containing 1x PCR HF buffer, 0,2 mM dNTP mixture, 0,5 µM of each primer, 0,02 U/µL Phusion polymerase and 1 µL template DNA. PCR amplification was performed as following: Initial denaturation at 98 °C for 30 s, followed by 35 cycles each of 98 °C for 10 s, 60 °C of annealing for 35 s, and a

1 min extension at 72 °C, final extension at 72 °C for 5 min. The PCR products were analysed for positive amplification with gel electrophoresis. Positive PCR products were subsequently purified with the Qiagen - QIAquick PCR Purification Kit and 15 µL purified PCR products (5 ng/µL) were sequenced by Eurofins Genomics (Germany). The resulting sequences were analysed with the unite database (unite.ut.ee) in order to identify the fungal strains.

1.2.3 Production and assessment of biosurfactants

Three different media were used throughout the study as production medium. The three media were as followed: PD (Potato dextrose), ME (Malt extract) and a minimal salt medium (MSM) containing (per litre) 40 g sucrose, 18.8 g yeast extract, 0.5 g sodium acetate, 0.1 g sodium benzoate, 0.5 g $MgSO_4 \cdot 7H_2O$, 3 g $(NH_4)_2SO_4$, 2 g KH_2PO_4, 0.9 g NaCl. Each media was duplicated and 2% vegetable oil was added to one duplicate as an additional carbon source. Biosurfactant production was tested from six different fungi (three isolated from oil reservoirs, three promising surfactants producing control strains from terrestrial sources: *Fusarium graminearum* OE::NRPS4, *Aspergillus fumigatus* and *Mucor* sp.), which was inoculated to each medium. 50 mL cultures in baffle flasks were incubated at 28 °C and 150 rpm in a shaker incubator for 7 days.

After 7 days of incubation, each sample was filtered through Miracloth filter paper. The flow-through were collected and acidified to pH 2 using 6 M HCl. The samples were kept at 4 °C overnight to precipitate biosurfactants. The samples were centrifuged for 10.000 x g for 30 min to pellet the biosurfactants and dissolved in 0,05 M bicarbonate pH 8,6. The samples where reacidified and centrifuged at 10.000 x g for 30 min. Pellets were resuspended in ethylacetate/methanol 5:1 to obtain the maximum yield of product [15]. The samples were centrifuged at 10.000 x g for 20 min to accelerate a phase separation. Each sample was checked for the phase separation. None separation was observed, leading to direct nitrogen evaporation. The samples were placed at 50 °C and evaporated with nitrogen for around 30 min until all solvent was evaporated.

To determinate biosurfactant production, each sample was resuspended in 500 µL demineralized water. Each sample was diluted to a 10x and a 100x dilution. The surface tension was measured with use of Drop Shape Analyzer DSA100 (KRÜSS) following the manufacturer's instructions. Each sample was measured in triplicates.

2. Results

2.1. Characterization of the fungal community in selected oil reservoirs

Seven of the evaluated 17 samples (#1-17) contained sufficient fungal DNA for profiling the fungal community (**Figure 2**). Most samples contained only 1-3 fungal species, while sample #2 was the most species rich with six different species.

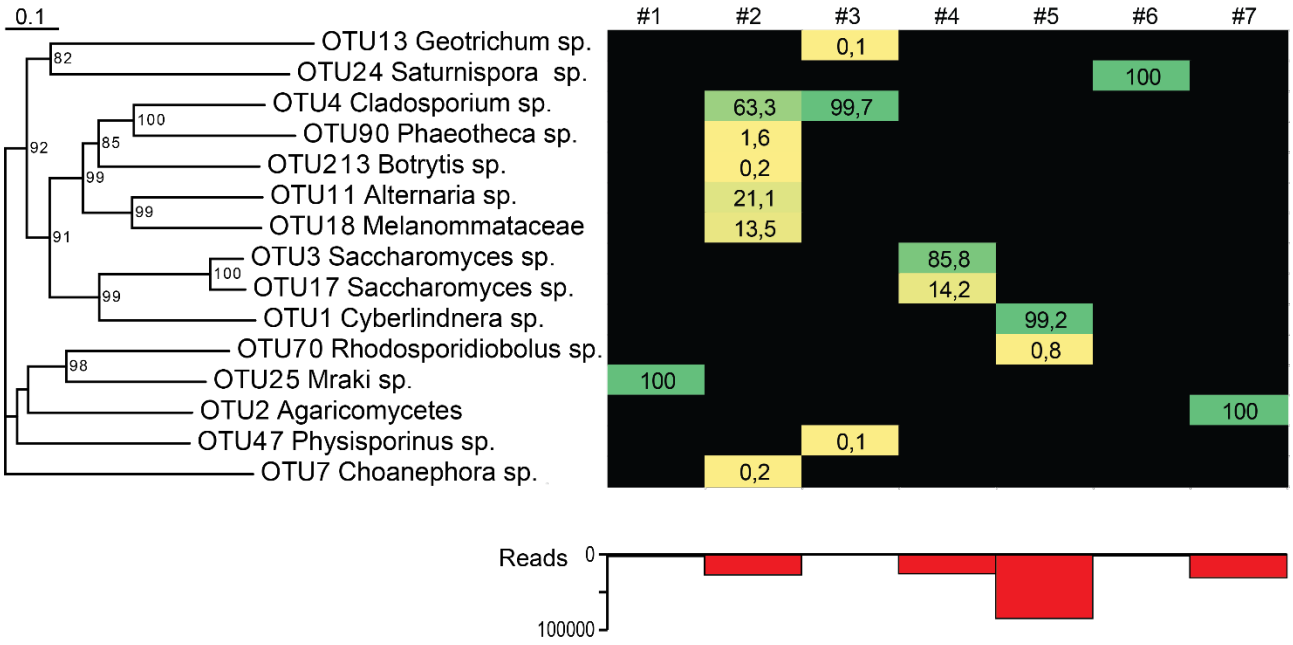

Figure 2. Identification of the fungal community in seven samples from oil reservoirs. The sequential order is determined by a phylogenic tree based on the obtained sequences analysed by fast Fourier transform (MAFFT) alignment and subsequent maximum likelihood with 100 bootstraps.

2.2 Isolation and identification of fungi and characterization of their biosurfactant potential

2.2.1 Isolation of fungi

During the study we managed to isolate six different fungi (exemplified in **Figure 3**), although three could not be sustained under laboratory conditions. The remaining three fungal strains (#2-k1, #2-k2 and 8-k1) were identified by sequencing part of internal transcribed spacer (ITS) region, which serve as a barcode for identification. The resulting analyses identified that the strains belong to the genera *Fusarium* (#2-k1), *Lecanicillium* (#2-k2) and *Aspergillus* (#3-k1).

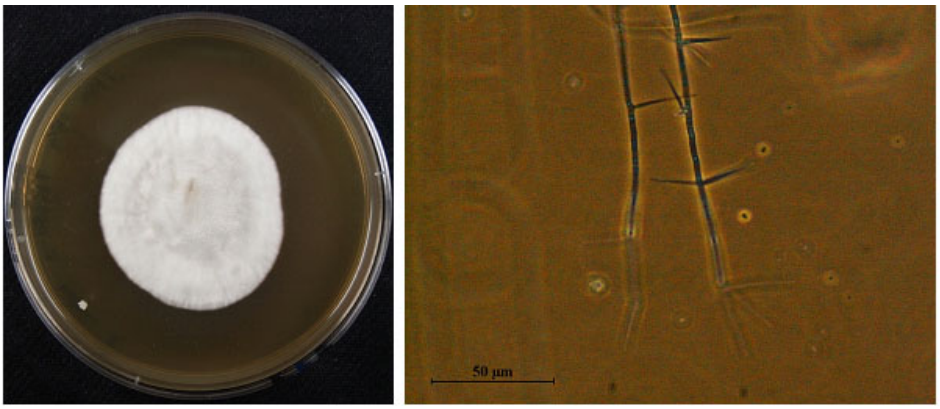

Figure 3. Example of a fungal strain (*Lecanicillium* sp. #2-k2) isolated from an oil reservoir sample. Left: Growth of an isolated fungi at a petri dish containing nutritional agar. Right: Microscopy picture of hyphae and spores from the same fungi.

2.2.2. Production of biosurfactants

The biosurfactant-producing properties were examined through a surface-tension assay where the ability of extracted secondary metabolites to reduce the surface tension of water was determined. The three isolated fungi and three control fungal strains cultivated on six different media (ME, PD and MSM ± oil) and excreted compounds were extracted and tested for ability to lower surface tension of water. The results showed that fungi grown in the ME and PD media caused the most overall change in the surface-tension crosswise all six fungi. *Fusarium graminearum* (OE NRPS4), which previously in our lab has been shown to have promising surfactant potential was found to be the most promising fungi to lower the surface-tension (**Figure 3**). The thermophilic *Aspergillus fumigatus* and *Mucor* were likewise tested as candidates for biosurfactant production. Both reduced the surface-tension. The fungi isolated from the oil samples (#2-k1, #2-k2 and 8-k1) were likewise analysed for surface-tension changes. For all three isolated fungi, a change in surface-tension in the undiluted samples and for some slightly in the 10x dilution was observed.

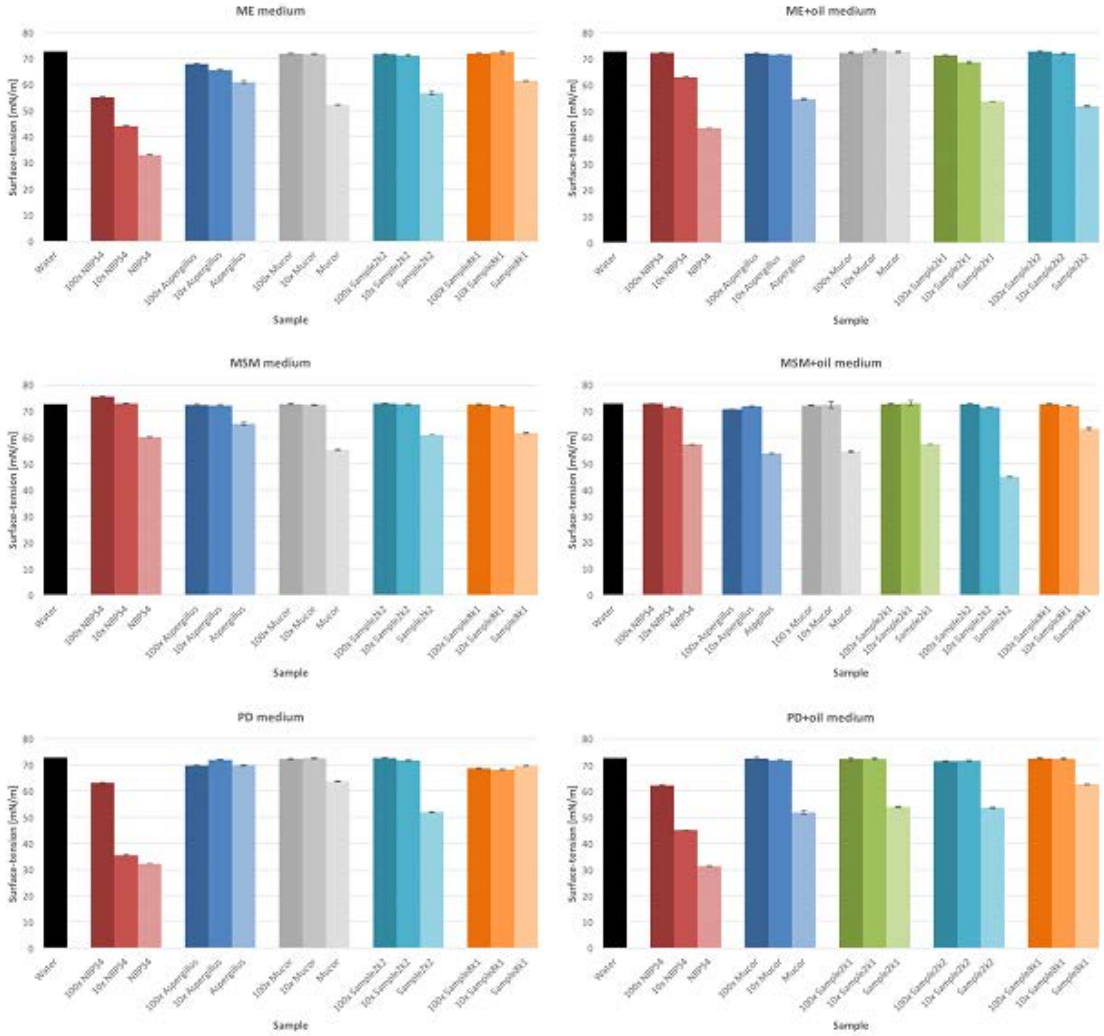

Figure 3. Measurement of surface-tension for *F. graminearum* (OE NRPS4), *A. fumigatus*, *Mucor*, and fungi isolated from oil sample (#2-k1, #2-k2 and 8-k1) in six different media. The black column is the surface-tension of water compared to the reference of value of 72,7 mN/m. At the y-axis is the surface-tension in mN/m and at the x-axis is each sample clustered with its dilutions.

The biggest change in surface-tension was observed at the PD+oil medium with *F. graminearum* (OE NRPS4) with a value of 31,27 mN/m. Compared to the reference of water this decrease corresponds to 41,43 mN/m. When looking at the undiluted samples among the other fungi, the surface-tension decrease to a surface-tension between 44,96 mN/m – 65,21 mN/m. Furthermore, is it observed that the sample from *Mucor* grown in ME+oil medium and the sample #8-k1 grown in PD medium did not decrease in surface-tension, which indicate that the decrease seen in other sample, is not caused by salts from buffers or other compounds from the media.

2.2.3. Study of optimal nutrition.

A growth study was conducted to examine the optimal nitrogen and carbon sources for growth. The effect of varying nitrogen and carbon source on growth rate for *Lecanicillium* (#2-k2) was examined using $NaNO_3$, NH_4NO_3 and $(NH_4)_2HPO_4$ as nitrogen source and sucrose, glucose and glycerol as carbon source (**Figure 4**).

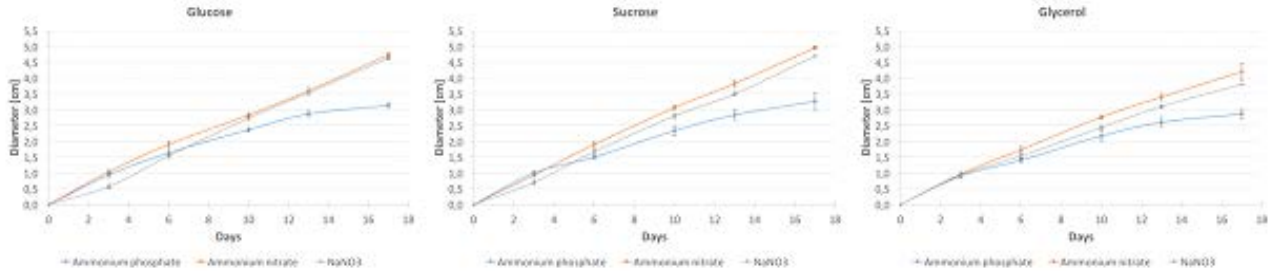

Figure 4. Growth curves for radial growth for *Lecanicillium* (#2-k2)

The growth was measured in triplicates for every 3-4 day. Ammonium nitrate was found to be the best nitrogen source, since it gave the best growth combined with every carbon source. The best combination of N- and C-source was found to be ammonium nitrate combined with sucrose. The diameter on the fungal, grown with sucrose/ammonium nitrate, was 4,97 cm (mean value of triplicates), for glucose/ammonium nitrate the diameter was 4,73 cm (mean value of triplicates) and for glycerol/ammonium nitrate the diameter was 4,2 cm (mean value of triplicates) after 17 days of growth.

Perspectives and proposed way forward

After decades of production, North Sea oil fields have matured and are now produced with increasing water cuts compared to oil recovery. Thus, despite substantial amounts of residual oil in place, conventional oil extraction strategies does not allow for production of these resources. It is anticipated that these mature oil fields holds particularly high potential for successful application of MEOR technologies, as fields will benefit markedly from changes in conformance of the water sweep, and changed oil-water interactions. However, to uncover the true potential of fungi for enhancing oil recovery, there is a need for addressing the following points:

Determination of MEOR potential and selection of approach

a. In-depth mapping of inherent and introduced reservoir fungi through evaluation of fungal diversity in crude oil samples retrieved from reservoirs with or without water breakthrough to pinpoint best candidates for fungal MEOR.
b. Extended efforts to isolate fungi from crude oil samples, and further mapping of their abilities to produce surfactants.

c. Lab-scale production and purification of surfactants for following evaluation of their ability to increase oil production.

Reservoir-simulation experiments and method optimization

a. Evaluation of fungal enhanced oil recovery under reservoir-simulating conditions using core flooding allowing for:
   i. Ranking of MEOR strategies regarding their potential for enhancing oil recovery.
   ii. Evaluation for potential HSE risks associated with technology implementation (reservoir souring, potential plugging and subsequent abandonment of well).
   iii. Determining overall feasibility of MEOR implementation based on production data.

Field simulation and definition of implementation strategy

a. Modelling of MEOR strategies to assess and determine optimal approach for field implementation by combining knowledge about MEOR mechanisms from laboratory evaluations and information, hereunder production data, flow dynamics, among others, from site under consideration.
b. Pinpointing requirements for strategy implementation and best practices for gaining optimal advantage from MEOR.

Final conclusion

Conclusions for experimental work

The culture-independent approach showed fungi are present in some the samples collected from oil reservoirs. Compared to samples normally examined from plant and soil samples the results showed that the fungal community is relatively poor in number of variable species. This could indicate a low number of fungal DNA present in the sample, which often cause few species to dominate the output. The results could also indicate that survival in oil reservoirs requires massive specialization and adaptation, which lowers the number of fungi able to grow under these conditions.

The culture-dependent approach showed that some fungi could be isolated from the oil reservoir samples, which again illustrate that fungi are present under these conditions. The isolated fungi were able to produce compounds, which could lower surface-tension of water and thus work as biosurfactants.

Together, these results indicate that fungi are present in oil reservoirs and that they contain potential to produce biosurfactants that can be used for enhanced oil recovery. Isolation and further study of the surfactants in question are suggested to be subject going forward.

References

1. Santos DKF, Rufino RD, Luna JM *et al* (2016): *International Journal of Molecular Sciences*, 17: 401.
2. Al-Sulaimani H, Al-Wahaibi Y, Al-Bahry S *et al* (2011): *Spe Journal*, 16: 672-682.
3. Sen R (2008): *Prog Energy Combust Sci*, 34: 714-724.
4. Amaral PFF, Coelho MAZ, Marrucho IMJ *et al*: **Biosurfactants from Yeasts: Characteristics, Production and Application**. In: *Biosurfactants.* Edited by Sen R, vol. 672; 2010: 236-249.
5. Mulligan CN (2005): *Environ Pollut*, 133: 183-198.
6. Hocking AD, Pitt JI (1980): *Appl Environ Microbiol*, 39: 488-492.
7. Abildgren MP, Lund F, Thrane U *et al* (1987): *Lett Appl Microbiol*, 5: 83-86.

8. Hertz M, Jensen IR, Jensen LO *et al* (2016): *Int J Food Microbiol*, 222: 30-39.
9. Naqvi A, Rangwala H, Spear G *et al* (2010): *Chem Biodivers*, 7: 1076-1085.
10. Guttman DS, McHardy AC, Schulze-Lefert P (2014): *Nat Rev Genet*, 15: 797-813.
11. Wang M, Jiang X, Wu W *et al* (2015): *Persoonia : Molecular Phylogeny and Evolution of Fungi*, 34: 100-112.
12. Maheshwari R, Bharadwaj G, Bhat MK (2000): *Microbiol Mol Biol Rev*, 64: 461-488.
13. Kruczek B: **Carman–Kozeny Equation**. In: *Encyclopedia of Membranes.* Edited by Drioli E, Giorno L. Berlin, Heidelberg: Springer Berlin Heidelberg; 2015: 1-3.
14. Frisvad J: **Media and Growth Conditions for Induction of Secondary Metabolite Production**. In: *Fungal Secondary Metabolism.* Edited by Keller NP, Turner G, vol. 944: Humana Press; 2012: 47-58.
15. Qazi MA, Kanwal T, Jadoon M *et al* (2014): *Biotechnol Progr*, 30: 1065-1075.

Optiprobe: In situ pH and DO probes

Knud Dideriksen and Thomas Just Sørensen

Nano-Science Center, Department of Chemistry, University of Copenhagen, Universitetsparken 5, DK-2100 Copenhagen Ø, Denmark. knud@nano.ku.dk

Abstract

pH and redox potential are two of the most important variables for understanding reactions in water alongside temperature and pressure. However, in situ measurement over extended periods is very complicated especially in high pressure, multiphase flow as in the oil and gas industry. Optical probes based on fluorescence overcome most critical limitations. A bioprocess pH and DO optical probe has already been developed by Thomas Just Sørensen. In competing probes, the fluorescent molecules decay rapidly in response to excitation by light. Using the existing probe geometry developed for biotech application, we demonstrated i) that the fluorescent molecules in our probes can be excited above 400.000 times without deterioration of probe performance; ii) that repeated cycling of the pH from 3 to 8, during which NaCl concentrations increases from 0 M to 0.42 M, does not change probe performance; and iii) that changes in fluorescence during 70 hours of continuous measurement are negligible. Furthermore, the optical probes are fully capable of measuring pH in seawater and in water from oil production containing crude oil. Immersion of the probe in crude oil prior to use did not affect measured signal, although it increased the probe response time (~5 minutes to stabilisation of response). Note, however, the response time was faster than that of the reference pH electrode. To optimise the probe geometry for long term operation in oil wells, the fluorescent molecules were attached directly on to two types of optical fibers targeting an integrated design. Tests showed that poly-methylmethacrylate fibers were not suitable, but that fluorescent molecules can be attached directly onto glass fibers to yield good fluorescence signal and response. We foresee that an optical probe with this integrated design will have a lifespan of years and be able to monitor pH in several off shore applications, when the probe design has been optimised. In particular molecule deposition with or without coating layers as well as substrate pre-treatment and post-treatment of the sensor have to developed further.

Technology vision

pH and redox conditions are two of the most important variables for understanding reactions in any aqueous environment. pH critically influences the solubility and growth rate of many solids (e.g., calcite, siderite, and Fe-oxides, [1,2] and dissolved oxygen (DO) directly affects corrosion rates.[3] From combined knowledge of pH and redox conditions, mineral stability can be predicted. Such information allows calculations of scale and corrosion product formation. Measurement of pH and redox potential is,

however, not straight forward. Electrodes require frequent calibration because of drift, ruling out long term in situ measurement. Furthermore, acid gas equilibria and formation of solids during ex situ measurement shift pH from its original value. Thus, traditional pH electrodes cannot provide accurate pH during oil production.

Our vision is to develop optical probes based on fluorescence that can be used for measurement of pH and DO in various water streams during oil production. Optical probes overcome many of the limitations associated with electrodes. They do not drift; they can be comparably easily implemented for in situ, real time measurement; and they are expected to be operational at higher pressure and temperature. An optical pH and DO probe has already been developed by Thomas Just Sørensen (University of Copenhagen, KU) targeting single-use application in the biotechnological industry. The current technology is developed for implementation in sterile polycarbonate vessels. It includes a sensor spot, which contain the fluorescent molecules in a polymer matrix and is in contact with the solution. The fluorescence is detected by optical fibers in close proximity to the sensor spot, so that light can be transmitted from spectrometer to spot and back (Fig. 1A). This means that transmission of light between the sensor spot and the optical fibers depends on the geometry of the setup and that the measured fluorescence is sensitive to physical disturbances. Such disturbances would almost certainly occur during long periods of measurement. For operation at the higher T/P conditions present in oil and gas wells, the probe requires modifications. These are best realised if the fluorescent molecules can be mounted directly on the optical fibers to produce an integrated probe (Fig. 1B). To protect the sensor material, this integrated probe would then be covered by an ultrahydrophobic, nanoporous polymer and mounted in a thermowell (see http://www.jms-se.com/thermowell.php for details) Our aim is that such a probe could be installed on facilities so that it either protrudes into the water flow or resides protected within a depression in the well side if minimisation of shear stress is required.

Based on discussions with Maersk Oil and Gas, we foresee that fully developed probes could be implemented at a range of water streams, including i) top sides of production wells, ii) on injection wells and iii) at production water treatment facilities. Our ambition is that fully developed probes have a lifetime in excess of the typical frequency of maintenance at the facility where it is mounted, so that replacement can coincide with other work. Given that maintenance of the top side of production wells are very costly and typically occur rarely (~5 year intervals)[4], the probes mounted here should be highly durable.

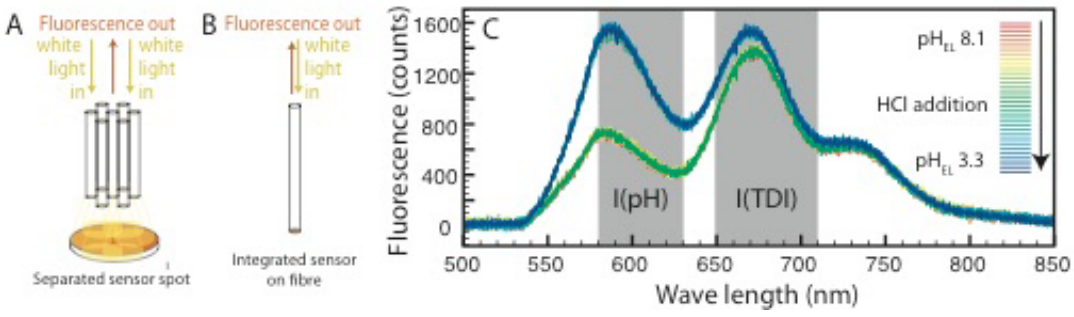

Figure 1. A. Probe geometry with separate sensor spot and optical fibers used for biotech application. B. Developed integrated probe geometry with fluorescent molecules mounted directly on optical fibers. C. 39 spectra of the fluorescence measured every 10 second using separated sensor spot and optical fibers during a cycle in which pH was varied from pH$_{EL}$ of 8.1 to 3.3.

Fully functional probes could significant reduce costs caused by scaling and corrosion by allowing accurate prediction of the processes. This would enable intervention in due time and aid the mitigation of scale and corrosion, increasing the time that production can be profitable. Calcite, barite and many other minerals have growth rates that depend on the degree of supersaturation, i.e., the difference between actual activities and those defined by the solubility.[5] Given that the solubility of calcium and iron carbonates is highly dependent on pH,[1] meaningful modelling of their formation rates during scaling and corrosion is extremely complicated. Development of fully functioning pH probes sets the stage for modelling the formation rates of these materials. In addition, the reaction rates of barite is weakly pH dependent.[6] Thus, modelling of barite scaling in oil wells would become increasingly accurate.[7] Implementation of the probes in injection wells would allow monitoring of DO, securing that pre-injection treatment has adequately removed DO so that aerobic corrosion is minimal. Finally, probe implementation in the produced water treatments where chemical addition risk lowering the pH to levels harmful to the facilities,[4] could allow automatic quality control and lower maintenance costs. Additionally, monitoring DO and pH can also help understanding of microbial activity in process systems causing corrosion, fouling etc. Thus, successful development of a fully functional optical probe opens several avenues for cost reductions.

Validation of technology

One aim of this project was to eliminate the most critical technical risks in the development optical probes for in situ, real time measurement of pH and DO in injection wells. To do so, we redesigning the probe geometry so that fluorescent molecules were mounted directly on the optical fiber and tested the performance. Furthermore, fluorescent dyes often decay as a result of multiple exposures to light. This significantly limits the lifetime or the measurement frequency competing probes (the major drawback of currently available optical probes for pH that can be used in no more than 14 days or 50,000 measurements whichever comes first). Specifically, the goals were to i) test the long term performance of the optical probe using the existing, separated probe design by determining if the fluorescent molecule can be exited more than 200,000 times without decay of pH signal and if it still works after 5 weeks of operation, ii) demonstrate using the separated probe design that the pH probes perform in seawater and waters from oil production (with and without exposure to crude oil), and iii) test if the fluorescent molecules can be mounted directly onto optical fibers to produce a functional optical pH probe with an integrated design that can be further developed to yield a highly robust probe for in situ measurement at high P and T. This technology would then have to be validated at increasingly realistic conditions and eventually tested in the field. In the section "Proposed way forward" we outline the roadmap for such endeavours.

Validated during sprint

To test the performance of the optical probes a range of experiments were performed. During many of the experiments, pH was also recorded using a regular pH electrode (InLab Expert Pro electrode connected to a Mettler-Toledo SevenCompact pH meter). pH measured with an electrode will be referred to as pH_{EL}, whereas pH measured with the optical probe will be refers to as pH_{OP}.

Long term performance. To determine the long term performance of the optical probe, experiments were performed in which i) a sensor spot over 5 weeks was exposed to 64 consecutive cycles of rapid pH change

from 3-8 in a 0.02 M HEPES buffer solution using HCl and NaOH, and ii) three sensor spots were exposed to light with wavelengths from 360 to 800 nm for 80 hours. Figure 1C shows an example of the fluorescence measured during a cycle where pH_{EL} was varied from 8.1 to 3.3. In the figure, the red, yellow and green spectra correspond to pH_{EL} = 8.11. Upon addition of HCl to produce a solution with pH_{EL} = 3.3, spectra (coloured blueish green, blue and magenta) show that the fluorescence increase at a wavelength of about 580 nm. To determine the spectral changes, two parameters are calculated. Firstly, the signal in the wave length range 580 to 630 is integrated. This value will be denoted I(pH). Secondly, the signal at wavelengths of 650 to 710 nm is integrated for normalisation purposes. The determined value is denoted I(TDI).

Figure 2A and B show examples of recorded I(pH)/I(TDI) for the last two cycles during the repeated cycling of the pH. After each addition of NaOH or HCl, the sensor reacted quickly. The response time of the sensor t_{90}, representing a signal conversion of 90%, was typically 15-30 s, and < 1 min for all 64 cycles in the 5 week experiment. Note that these pH jumps corresponds to a change in proton concentration of fiver orders of magnitude, the sensor responds much faster to small changes in pH. After 3 weeks of experiments during which the pH had been episodically cycled, a period of continuous measurements were for 66 hours in a solution with pH_{EL} = 8 to determine drift. Figure 2C shows the measured I(pH)/I(TDI) as a function of time. Clearly, the amount of drift is small.

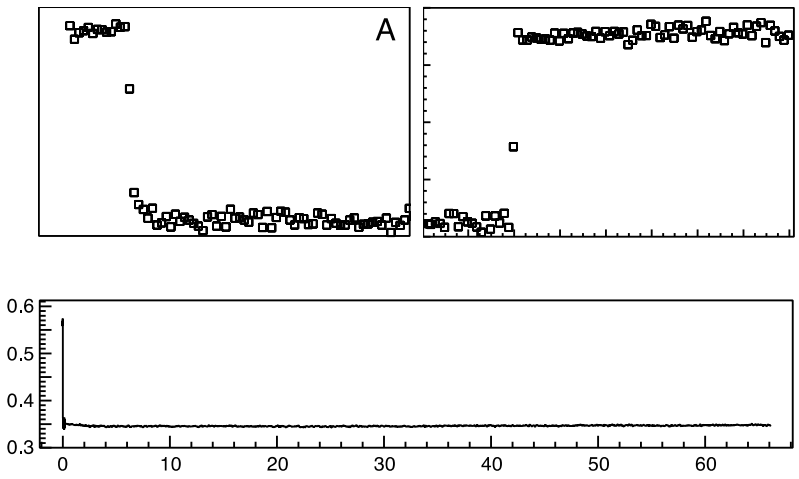

Figure 2. A and B. I(pH)/I(TDI) recorded for the last two cycles (cycles 63 and 64 after 5 weeks of experiments) of repeated cycling of the sensor between pH 3 and pH 8. Each vertical line indicates addition of acid or base. B. I(pH)/I(TDI) recorded in a pH_{EL} 8 solution over 66 hours of constant operation after 3 weeks.

At the end of the 5 week test period, a calibration curve was measured for the used sensor spot by titration with first HCl and then NaOH. The calibration curves were fitted to a sigmoidal function of the type:

$$I(pH)/I(TDI) = y_0 + \frac{a}{1+e^{-k(pH_{EL}-pK_a)}} \qquad (1),$$

where y0, a, k and pK_a are fitted calibration parameters. The pK_a refers to the negative logarithm of the constant for the deprotonation reaction for the fluorescent molecule. The calibration curve and the derived parameters form the fitting are shown in Figure 3A. Based on the fit, the average accuracy of the pH measurement is determined to ~0.03 (all uncertainties refer to 2 standard deviations) in the pH range 4.2 -

7.8. Given the shape of the calibration curve, higher accuracy is expected around the pK_a value. To give an alternative impression of the precision of the optical probe, only the first titration with HCl was used in the calibration. For the second dataset from titration with NaOH, the calibration parameters were used to recalculate I(pH)/I(TDI) into optically determined pH (pH_{OP}) in pH 4.2 - 7.8 using Equation 1. The derived pH_{OP} is shown in Figure 3B as orange squares, whereas green squares represent the pH_{OP} determined similarly for a pristine sensor spot (calibration curve in Figure A1 in the Appendix). Note that uncertainties for both pH_{OP} and pH_{OP} contribute to the slight differences and that the accuracy of the calibration is slightly decreased, because only one dataset was used.

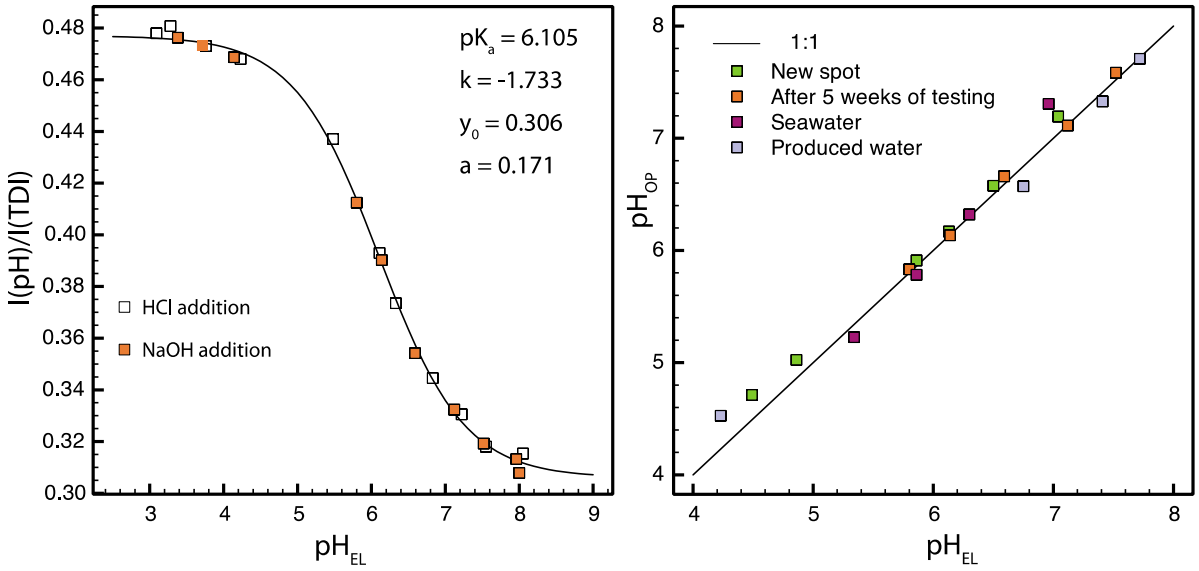

Figure 3. A) Calibration curve and fit for the sensor after 5 weeks of testing. B) Determined pH_{OP} as a function of pH_{EL} during titration for a pristine spot, the spot after 5 weeks of experiments, seawater and produced water. The values were determined using only portions of the datasets for calibration and the rest for determination of pH_{OP}. The line in the insert refers to pH_{OP} = pH_{EL}.

To determine if the fluorescent molecules decay as a results of exposure to light, similar to what is seen for competing molecules, three dry sensor spots were exposed to a broad spectrum of light (360 to 800 nm) for 80 h. As control, three different sensor spots were stored in darkness. The measured I(pH) for the six sensor spots (Figure 4) show no statistical variation as a function of time or light exposure. Thus, we conclude that the fluorescent molecules do not degrade measurably during 80 hours of light exposure. This exposure corresponds to ~300,000 seconds or one hourly measurement of 1 s over 30 years of operation.

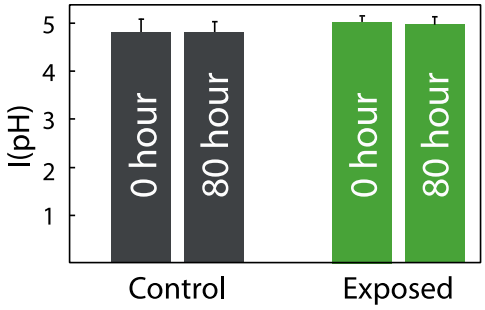

Figure 4. I(pH) for three sensor spots measured before and after exposure to light for 80 h (green) and three other sensors that had been stored in darkness. Error bars denote to 1 standard deviation uncertainty.

Performance in seawater and produced water. A pristine sensor spot was mounted and soaked in 250 ml seawater for one hour. Initial pH_{EL} was measured to 7. To determine the probe performance, the seawater was then titrated with first HCl and then NaOH. The resulting calibration curve and the calibration parameters is shown in Figure A2 in the appendix. Based on the curve fitting, the accuracy of the pH measurement is ~0.03 in the pH range 4.2 - 7.8. Using only one part of titration data for calibration and the other part for pH_{OP} determination yields the data points shown as red squares in Figure 3B.

To determine the pH of produced water, the water portion of a crude oil sample was separated, which resulted in an aqueous solution that was slightly brown, turbid and with a surface that was covered with an oil film. A pristine sensor spot was soaked in 50 ml of the separated production water for one hour yielding pH_{EL} of 7. pH_{EL} was then adjusted to 8.0 using NaOH and a calibration curve was generated by titration with HCl (Figure A4 in appendix). Based on the calibration, the average accuracy of pH measurement in produced water is 0.03 in the pH range 4.0 - 8.0. Excluding every second measuring point in the calibration in the pH range 4.0 - 8.0 and using those data points for calculation of pH_{OP} results in values represented by blue squares in Figure 3B. To determine the response time in produced water, the sensor spot was cycled from pH_{EL} 8.2 to 2.2, and then to 7.8. The I(pH)/I(TDI) from the measured spectra is plotted as a function of time in Figure 5A. The response time of the sensor, t_{90}, was < 60 s.

Performance after contact with oil impurities. In an additional experiment, the sensor spot was washed with pure water, exposed to crude oil, washed quickly with water, and re-immersed in the produced water. Figure 5B shows the measured I(pH)/I(TDI) of the produced water as a function of time. Addition of HCl resulted in a decrease of pH_{EL} from 7.6 to 2.3 (Figure 5C), to which the sensor spot reacted quickly. Subsequent addition of NaOH resulted in pH_{EL} of 7.2. This pH change (Figure 5D) was picked up slower by the sensor spot, requiring ~5 minutes for stabilisation of the fluorescence signal. The reason for the slower response is currently unknown. However, we note that the pH electrode required more than 7 minutes, before it produced a stable value, suggesting that the change in response time might related to the composition of the complex mixture and not the optical sensor.

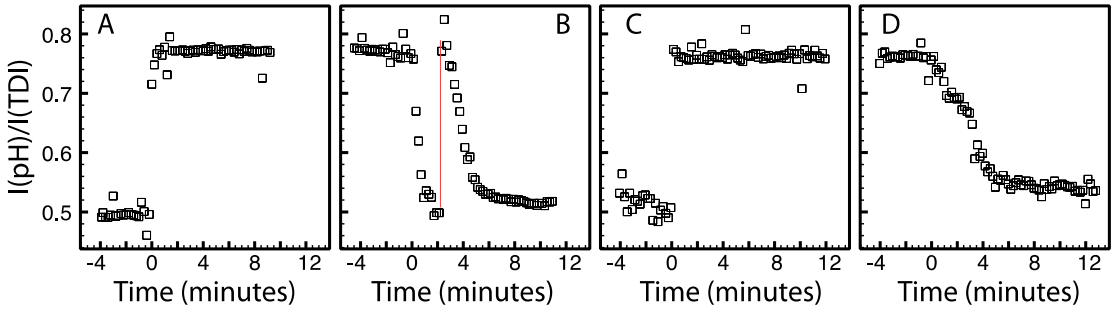

Figure 5 A and B) Response from the sensor spot in production water. In Fig. 5B, two cycles were performed because of pH overshoot (red line marks the start of the second cycle). The last NaOH additionto resulted in pH_{EL} to 7.8. The sensor responded promptly to the pH changes. C and D) Response of the sensor spot in produced water after exposure to crude oil. In the test, pH_{EL} was adjusted to 2.3 and then to 7.2.

Direct attachment of fluorescent molecules to optical fibers. To determine if the fluorescent molecules can be directly attached to optical fibers, two avenues of attachment were tested. In the first of the tests, the composite polymer material used in the sensor spots for bioproduction was deposited on the cleaned optical fiber ends. This material is composed of the fluorescent molecules embedded in a polymer matrix. Initially, the attachment was attempted to a 1000 µm fiber of poly-methylmethacrylate (PMMA). However, curing for hours at 110°C resulted in deformation of the fiber, presumably because the glass transition temperature of PMMA was exceeded. Furthermore, the sensor material became sticky after cooling. Consequently, mounting of the composite material was instead tested using a 1500 µm glass fiber. After removing 1 cm of the jacketing on glass fiber, the bared end of the fiber was cleaned in 1 M HNO3 for 24 hours and washed with water. The fiber was then dip coated with the composite material and cured for 4 hours at 140°C. No deformation or stickiness was observed after curing.

To evaluate the performance of this integrated sensor, the fiber was immersed in a 0.02 M HEPES buffer and pH was cycled between 3 and 8 by addition of HCl or NaOH. Fluorescence spectra for the first two cycles yielded a good signal (top right corner of Figure 6). Furthermore, a fast response was observed upon pH change with t_{90} < 1 minute. Figure 6 shows I(pH) for the cycles as a function of time. Clearly, the signal decreased over the 2 hours of measurement, indicating detachment of fluorescent molecules. However, the signal to noise at the end of the experiment, when the signal from fluorescence had become more stable, remains so low that reasonable pH measurements are feasible. The decrease of fluorescence is most likely caused by i) lack of rinsing of the glass fiber sensor in buffer after curing, the sensor spots are post-treated whereby unbound sensor material is removed; or ii) The dip-coating technique resulting in a thick film of sensor composite material. Normally very thin films are deposited allowing fast response and no decrease in fluorescence. Most likely, optimization of deposition and post-treatment procedure will alleviate the problem.

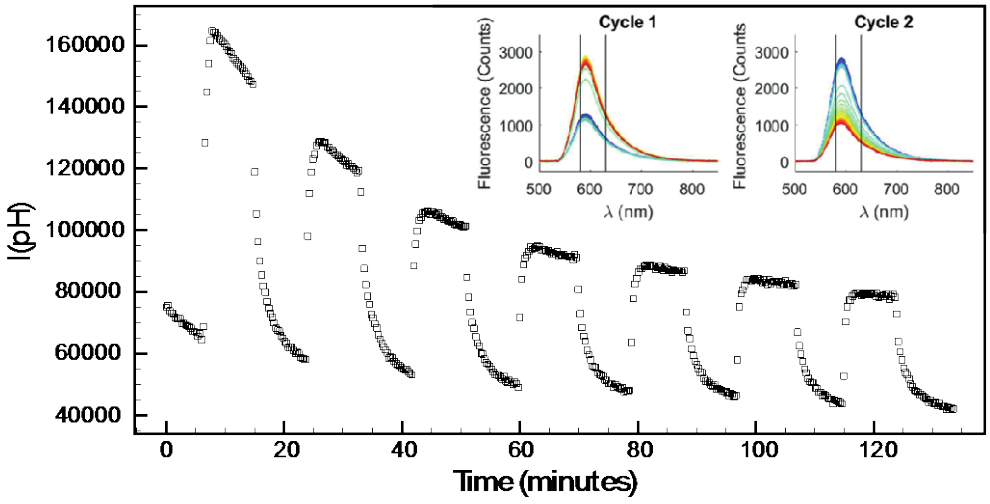

Figure 6. Measured I(pH) during the repeated cycling between pH_{EL} 3-8. Insert at top right corner: Fluorescence measured for the direct mounting of the composite material (fluorescent molecules embedded in a polymer matrix) to glass fiber (first two cycles). Vertical lines indicate the wavelength range for the integration.

To determine if the fluorescent molecule on its own could be attached directly to the glass fiber, a bared end of a fiber was immersed into an ethanol solution containing the polymerizable fluorescent molecules for 5 minutes to bind the molecule to the fiber through acid catalyzed condensation. The resulting probe

was then cured for 4 h at 140°C. The performance of the probe was evaluated by measuring the fluorescence during sequential cycling of pH_{EL} from 3 to 8. Fluorescence spectra for the first two cycles are shown in Figure 7 (insert to the right). Compared to the sensor material, a weaker fluorescence was observed, most likely because a much thinner film had been deposited. The probe response to variation in pH is very fast with t_{90} < 15 s, which is the resolution of the test setup. Measurement of I(pH) during pH cycling is shows that direct attachment of the fluorescent molecules on fiber results in drift that is below the detection level at the recorded signal-to-noise (Fig. 7). To increase the signal from the probe, more fluorescent molecules would have to be attached to the fiber. This could be achieved by mechanical modification (i.e., roughening by sanding) by which the fibers surface area increases. Alternatively, the glass fiber could be manipulated to expose more reactive quartz surfaces or chemical modified through hydrolysis of the SiO_2 using oxidative reagents or O_2 plasma treatment.

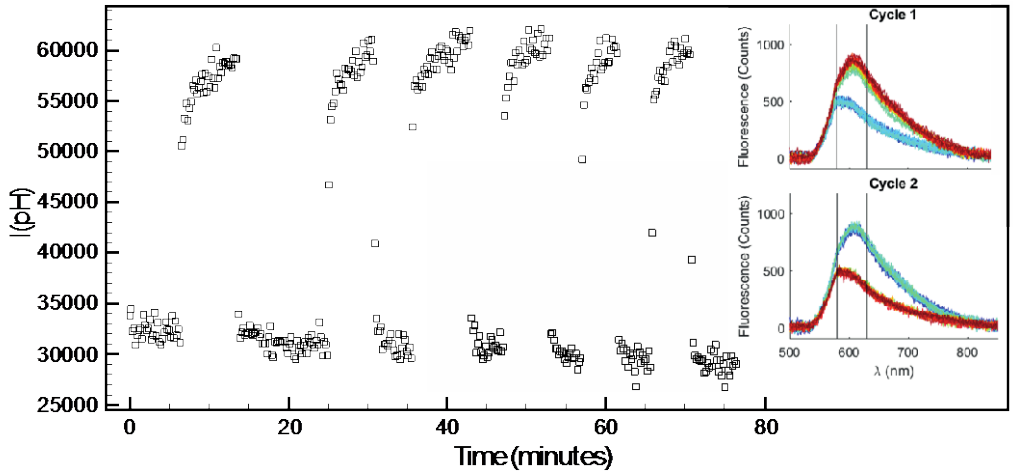

Figure 7. Measured I(pH) for directly mounted fluorescent molecule to glass fiber during repeated cycling between pH_{EL} 3-8. Insert to the right shows the fluorescence spectra for the first two cycles. Vertical lines indicate the wavelength range for the integration.

Conclusions of validation. Our tests shows that the fluorescent molecules do not degrade during 5 weeks of operation, that they are capable of extensive light exposure, corresponding to nearly 300.000 1 second measurements. Furthermore, changes in fluorescence during a 66 hour test is undetectable. The probes are full capable of measurement of pH in seawater and produced water. Assuming worst case, exposure of the probes to oil increase the response time (~5 minutes), but not the measured fluorescence once the signal has stabilized. The fluorescent molecules can be attached to glass fibers both alone and as a composite material, where they are imbedded in a polymer matrix. The signal for the composite material decays with time, but performance is likely to improve if the treatment after attachment is optimised. For the fluorescent molecules attached by themselves, the signal did not vary measurably as a function of time. However, the detected fluorescence was lower. Most likely, more fluorescent molecules can fairly easily be made to attach by mechanically or chemically increasing the surface area of the glass fiber. Thus, the two tests shows that the fluorescent molecule can be attached to glass fibers to yield a functioning pH probe and that the performance of the developed probes most likely can be improved significantly and fairly easily.

Comparison to existing alternatives for pH measurement. A method to measure pH optically has been developed by Schlumberger. It relies on injection in the production well of dye molecules, whose optical

properties are pH dependent.[8] The resulting mixture is then diverted to a spectrometer where the variation in optical properties is detected, allowing pH to be determined with 0.1 pH unit accuracy. Compared to the optical probes we aim to develop, the Schlumberger product features certain advantages, because the dye molecules are only present in the well for a short time. For example, the molecules need not be highly stable. On the other hand, the product requires intervention for each measurement. Thus, continuous monitoring of pH would be very labour intensive. Nevertheless, we note that their product could be used in our development project if needed for testing of the performance of fluorescent probes installed in places that are hard to access.

Proposed way forward

Through discussions with Maersk Oil and Gas, we have identified areas where the probe could be useful within the corporation.[4] and been informed of the specifications for probes in produced water systems and injection wells (given in Table A1 in the Appendix).[9] Given the promising results of this Radical Sprint Project (Phase I), we will apply for additional funding for a second phase (Phase II) of development of the optical probes (schematic given in Fig. 8). To advance the technology past major game stoppers, our immediate aim would be to improve the integrated probe design by i) refining the procedures for attachment of the sensor material and ii) develop the methods for post attachment treatment and coating of the sensor material. The performance developed probes would then be validated through longer term experiments at iii) higher P and T and iv) during formation of $CaCO_3$, the most common scale at the top side of production wells where implementation could occur in the near future. This work would resolve many of the uncertainties associated with the probe development and advance the This work would resolve many of the uncertainties associated with the probe development and advance the technology readiness towards level 3 on many technical aspects for the full pH sensor system. A 1-year project will take us to end-user testing of the sensor system. In addition, the next project phase would through more detailed discussions with Maersk oil and Gas include identification of risks during implementation of the probe at different sites in their operation. Furthermore, we will identify other industries in Denmark, where the probe technology could increase or help maintain their position as state of the art. Possible industries include Danfoss, whose aim to designing intelligent pumps is in harmony with our vision of a robust pH sensor.

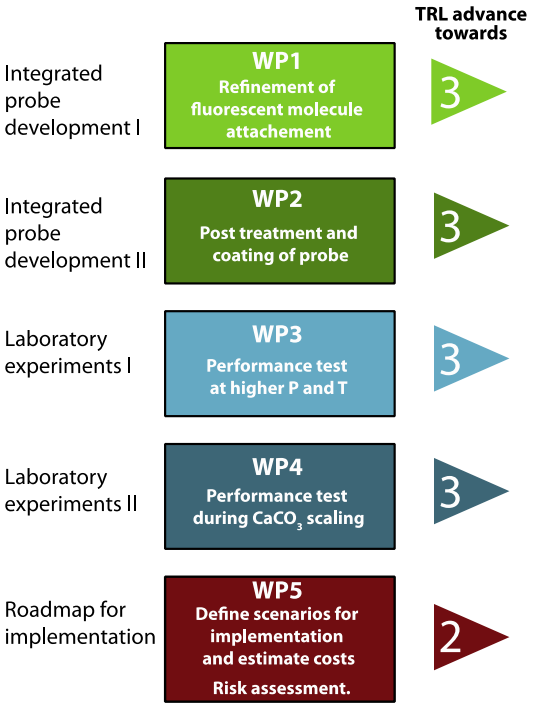

Figure 8. Schematic representations associated with Phase II of the project.

Because conditions and accessibility differ greatly for the sites in oil production, where we aim to mount our probe, the technical complications entailed in implementation of the technology are highly variable. Our intention is to test the technology initially at places where both risks and costs are minimal and then move on to more complicated environments as we refine our product. Thus, we foresee a

third phase (Phase III) project prior to commercialisation, where the final aspects of the probe design will be locked based on lessons learned during Phase II. The laboratory validated system, including documentation of shear stress tolerance, are then ready for end-user testing. A range of sites for testing are available to this project: i) a low temperature, highly accessible contaminated test site owned by the Capital Region of Denmark where we can at minimal costs hook up the probe to existing pump and treat facilities; ii) at Maersk Oil and Gas facilities for treatment of produced water, where our technology could be accessed and modified with relatively little cost; iii) at water injection wells in the hydrothermal energy production of Reykjavik Energy; and iv) the production and injection wells Maersk Oil and Gas. Such a sequence could minimise risk, lower costs, introduce our technology to potential customers and advance the Technology Readiness Revel (TRL) to 5 on the scale used by DHRTC. The project team includes the SMV FRS-systems ApS that will bring the pH sensor system to the market, taking over the TRL5 system and bringing it to TRL7 within a year. The progression from TRL7 to a commercial system is limited by the long-term (6+ months) tests that the commercial system must undergo before market release. The DO sensor and integrated pH/DO sensor is not included in this project and require separate development.

Final conclusion

In this project, we have demonstrated the existing optical probe technology, which features separated sensor spot and optical fiber is fully capable of long term performance and that it can measure pH in seawater and produced water. Moreover, the optical response of the sensor is reliable when the sensor has been preexposed to oil prior to measurement, albeit the response time might be increased. Proof-of-concept was achieved for as an integrated sensor, where the fluorescent molecule by itself or within a polymer were attached directly to a glass optical fiber, provided an adequate fluorescent signal. Further refinement of the pre-deposition, deposition and post-deposition treatment is highly likely to result in a final prototype of an optical probe for pH measurement.

References

[1] Stumm W. and Morgan J. J. (1996) Aquatic Chemistry : Chemical Equilibria and Rates in Natural Waters (3rd Edition). John Wiley & Sons.

[2] Brantley S. L., Kubicki, J. D. and White A. F. (2008) Kinetics of Water-Rock Interaction. Springer.

[3] Cox L. L. and Roetheli (1931) Effect of Oxygen Concentration on corrosion Rates of steel and Composition of Corrosion Products formed in Oxygenated Water. *Ind. Eng. Chem.* 23, 1012–1016.

[4] Discussions about the optical probe implementation with Freddy Oliviera Martinez and Jan Michael Kristensen from Maersk Oil and Gas conducted on the 11th of October as part of this project.

[5] Brantley S. L. (2008) Kinetics of Mineral Dissolution. In: Kinetics of Water-Rock Interaction. Eds: Brantley, S. L., Kubicki, James D. and White, Art F. Springer.

[6] Zhen Wu B. Y., Dideriksen K., Olsson J., Raahauge P. J., Stipp S. L. S. and Oelkers E. H. (2016) Barite dissolution and precipitation rates: Effects of temperature and aqueous fluid composition. *Geochim. Cosmochim. Acta* 194, 193-210.

[7] Dideriksen K. and Stipp S. L. S. (2017) A model for predicting scaling. Report on Sprint project for the Danish Hydrocarbon Research and Technology Centre. 12 p.

Deep Reach Through Acid Encapsulation and Wormhole Propagation

Jyoti Shanker Pandey (Research Assistant-CERE, DTU)

Prof Nicolas von Solms (Associate Professor-CERE, DTU)

Abstract

Acidizing is a common method used in the oil and gas industry to increase oil production by improving the permeability and bypassing the wellbore damage. For a successful acidizing job, dissolution behaviour of formation rock with injected acid needs to be fully understood. At reservoir conditions, dissolution rates of carbonate rocks in injected acid is one of the control mechanisms of wormhole formation and propagation. Corrosion is also an important consideration during acidizing at high temperature. The primary objective of this sprint project was to demonstrate the ability of retarded acid to penetrate deeper into the formation. It was shown in the study that acetic acid and mixtures of acetic and hydrochloric acid penetrated deeper than hydrochloric acid solution alone. Different acidizing fluids including HCl, acetic acid and a blend of HCl and acetic acid was considered for soaking and acid injection using core flooding experiments followed by CT scanning. Experiments were done at standard conditions. Acetic acid, a blend of acetic and HCl were considered for low rock dissolution capacity and HCl was considered for high rock dissolution power. Additional experiments were done to study the effect of cavity, access type, and effect of density increase. Additionally, literature review was done to study the current encapsulation techniques to retard the acidic fluid. Developing a recipe to encapsulate acidic fluid, while extremely interesting and relevant, was considered beyond the scope of this sprint project due to schedule and funding constraints.

Experimental evidence in this research shows that cavity size influences the acid penetration and retarded acid penetrates deeper than stronger acid for the same size cavity. The concept was to mimic radial jet drilling, since radial jet drilling would create a cavity and allow acid to reach deep into the formation, increase seepage area and create conductive flow. Selection of a suitable retarded acid could play an important role. Based on a literature review alone, encapsulated acids may be a better alternative than HCl for deep reach. Emulsified acid is an attractive and viable option for future research with possible field application in the Danish North Sea. Emulsified acids are shear thinning, non-corrosive, require lower treating volume and less pumping power and help in cost reduction by reducing the cost of equipment/machinery replacement and maintenance.

Technology vision

What can the technology do?

Conventional acids such as 15% HCl are very popular acidizing fluids due to easy availability and very low price. However, due to key disadvantages such as high dissolution rate and corrosion, researchers have developed and industry is adopting many alternative options to either reduce dissolution rate of HCl or replace HCl with another retarded acid. Organic acid, gelled acids and encapsulated acids, additives and chelating agents are being used to retard the rock dissolution in acidic medium to achieve deeper acid penetration as well as control the corrosion and iron precipitation.

Our Lab results show that acid would be able to create deeper conductive channel if it has retarded nature compare to regular 15% HCl. We have also found that pre-existing cavity would accelerate the acid penetration because it is easier for acid to collect in cavity rather create conductive channel from surface. Increase in injection rate leads to higher acid penetration and permeability enhancement. For Danish North Sea chalk, 15% HCl has strong chalk dissolution capacity, which increases at higher reservoir temperature. To control these high dissolution rates at higher temperature, additional toxic, non-eco-friendly additives are mixed with HCl. Our research shows that for deeper acid penetration while keeping the cost low, there is a need to adopt retarded environment friendly less corrosive acidic fluid system as an alternative to regular HCl. For ongoing Radial Jet drilling Research, deeper penetration could be achieved by replacing HCl with another alternative acidic fluid.

One of the alternatives could be developing an emulsified acid. Emulsified acid is based on an encapsulation concept, which controls the acid diffusivity. Therefore, emulsified acids can be used in lower volumes. In emulsified acid, smaller droplets are surrounded by a liquid hydrocarbon layer until it reaches the formation and releases acid which then reacts with the formation. Encapsulated acid has additional advantages in that it is less corrosive compared to a regular acid system, which means less consumption of toxic corrosion inhibitors.

What does the technology look like when it is installed/used in oil and gas production in the North Sea?

The proposed innovation does not require changes in existing infrastructure. Innovation proposed is to replace conventional HCl acid fluid system in radial jet drilling by retarded acid preferably encapsulated acid such as emulsified acid. This change does not require any additional innovation or arrangement in logistical arrangement and existing logistical arrangement should be sufficient. Encapsulated acids are preferred over Organic acid because organic acids produce precipitation, which can cause formation damage and choking of conductive path. Our research shows the precipitation caused by Acetic acid at room temperature.

However, emulsified acids are prepared using diesel, which is external phase or carrier fluid. Initially emulsified acids would be expensive alternative option compare to HCl however overall benefits such as lower treating volume, lower corrosion, lower replacement/maintenance cost and improved permeability make overall option, more attractive.

How to implement / install the technology?

Further lab research is needed to select the best possible acidic replacement, which is more environment friendly, less corrosive, retarded nature and not very expensive. Once the lab experiments are over and final selection is made. It is easier to adopt this technology without any additional investment.

What actions can be taken when the technology is installed?

Presently, using HCl during the acid treatment require additional action such as permit and clearance to use, handling and transport. Additional safety to Crewmembers. Additional use of various hazardous and toxic chemicals with HCl to retard it and control the corrosion, sludge formation etc. We propose to use alternative acidic fluid system, which would remove all these steps and make the operation more smooth and efficient while getting deeper acid penetration and lower corrosion. Deeper penetration through emulsified acid would require lesser resources such as lower pump rate, lower storage volume and lower use of corrosion inhibitors as well as lower cost of replacement of well tube or surface equipment.

How can the technology be maintained/ repaired if it breaks down?

We have used 10% Acetic Acid as a proxy for retarded acid. Acetic acid, at lower temperature does not react full and remain unspent. On the other hand, stability of Emulsified acids are connected with temperature at wellbore conditions. It is recommended to conduct lab experiment to understand the effect of North Sea crude oil on key properties such as stability, viscosity and droplet size as well as quantity of emulsifier agent.

Questions

How far will capsules go?

Capsule release depends on the well bore temperature. Literature based evidence shows that emulsified acid could remain stable up to 5 hours at 121˚C (Lynn et al, 2001, US Patent US2689009A, US2721174 A). Another research has shown the stability up to 72 hours at 24˚C (Al Anazi et al, 1998). Encapsulation based Emulsified acids are thermodynamically unstable system and stability depends on the many factors such as mixing method, type of external phase, volume ratio of internal vs external phase, concentration of emulsified agent and concentration of internal phase acid. Research is continued to make emulsified acid, a stable system for longer duration at higher temperature and less expensive by replacing diesel with other form of available liquid hydrocarbon such as Xylene (Fattah et al, 2010) and refinery based waste oil (Sidaoui, Z et al, 2017) to address stability and rheological behaviour, which would in fact increase the capsule reach. Xylene is used as effective agent to remove Asphaltene deposition. There has not been extensive research (Patent US20120090845A- indicate the use of Nano particle for stabilizing Emulsified acids) or evidence available regarding the development of emulsified acid and its application in context of Danish North Sea. Existing literature suggest (Ziauddin et al, 2007) that different rock types will have different dissolution patens for similar acids. These differences could be caused by the difference in permeability, porosity and pore structure in the sample. Most of the existing

emulsified acids related experimental results are based on limestone formation. Hence, as a first step, chalk dissolution behaviour in different acidic fluids including emulsified acids need to be fully understood. Service companies have a range of products including emulsified acids (Patent US 2689009A, US 2721174A) and IP may cover all geographical areas. However, it would be worthwhile to see the effect of North Sea crude oil on droplet size, viscosity and stability of either In house developed Emulsified acid or commercial available alternative option.

How do we make sure the wormholes are connected?

Limestone- acid reaction leads to many dissolution patterns within formation, which directly depends on the injection rate, reaction kinetics, flow geometry and the fluid loss rate. Wormholes are formed in mass transfer regimes and key dissolution patterns are face dissolution, conical wormholes, dominant wormholes, ramified wormholes and uniform wormholes (Al-Harthy et al. 2008). At optimum injection rate, dominant wormholes are developed. Dominant wormholes correspond to minimum pore volume to breakthrough, higher depth of acid penetration and higher reduction in skin (Al-Harthy et al. 2008). At injection rates equal or higher than optimum rate, acid is forced into smaller pores, which leads to more branching and higher volume of acid consumed. Theoretical model shows that the optimal injection rate depends on the reservoir condition, rock mineralogy and properties pore size distribution, and reaction rate. (Wang, Hill, and Schechter 1993).

Risk of plugging?

Crude oil also forms precipitate or sludge in presence of regular acids, which can be experimentally assessed as it, depends on crude oil chemistry and gross composition. This sludge can clog the formation and block the flow path results into reduction in the permeability. These are irreversible effects and to avoid, additional chemical are required to add to the acids. (Houchin et al. 1990). Some of these additional additives are in the watch list of environmental agencies for not passing the standards developed for oil and gas industry. (String fellow et al. 2017).

Apart from strong acids, weak acids are also popular acidizing fluids specially for high temperature wells and where longer acid pipe contact happen such as horizontal wells. Due to very low reaction rates and reversible in nature, organic acids do not completely react and large quantity is left unspent after the well treatment. This limit its application. Organic acids are more expensive and the risk of product precipitation due to the low solubility of calcium acetate and format salt limit their use at high concentration. (Chang et al. 2008, LePage et al. 2009). In few experiments where we have used 10% Acetic acid as proxy for weaker acid, we could see the calcium acetate formation as given in Figure 1

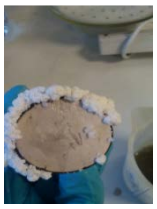

Figure 10 Acetate precipitation during the lab test

Risk of emulsions?

According to Fredd et al (1996), In the presence of strong acid, crude oil forms asphaltene sludge and rigid film emulsions, which can lead to partial or complete plugging of the formation after acidizing. Risk of sludge formation risk increases with increase in acid concentration. To avoid risk of unnecessary emulsions and sludge precipitation into the formation as well as Iron control, many acid additives are added such as de-emulsifier agent or anti sludging additives, iron control additives and micro emulsion surfactant. According to Global Harmonized Systems (GHS) of Classification and Labelling of Chemicals, toxicity level of Corrosion inhibitor and Iron Control are reported to be in Level 2 and Level 3, respectively. (Stringfellow et al. 2014) which is very high. List of key additives along with their GHS Category and commercial quantities are given in the Table 1

Table 3 Description of Various Chemical additives

Type of Additives	GHS Category	Per thousand gallon
Reducer Iron control additive	3	3 gallon
PlexBreak 150 non emulsifier additive	Not available	2 gallon
CRONOX ™ Ak-50 Corrosion Inhibitor additives	2	2 gallon
Plexsurf 285 micro-emulsion surfactant	Not available	1 gallon

Validation of technology

Pumping rates, reservoir conditions such as temperature and formation type has direct impact of deep reach of the acid. During the project, we have tested in laboratory, how to get acid deep into formation and improve permeability through the acid injection. To understand deeper penetration through wormholes propagation, multiple lab experiments including soaking and acid injection through core flood set up were conducted and effect of variables such as cavity design, density difference, access type, retardation and injection rates on permeability enhancement were studied. Dominant wormholes are only formed at optimal injection rates however micro channel are formed as rock dissolved reacting with acid inside pores and such pore start connecting generating micro wormholes. Presence of such micro wormholes are confirmed by increase in permeability after acid injection however, it is hard to observe them on CT scan and additional techniques such as NMR are getting popular. Experiment results show that increase in permeability was achieved by retardation, increase in injection rate, lower concentration, cavity presence however, increase in density did not lead to increase in permeability. Set of soaking experiments have confirmed that presence of cavity stimulate deeper acid penetration and smaller cavity compare to bigger cavity, allow deeper penetration.

Validated during sprint

Which part of the technology has been validated?

Deep reach through wormholes propagation

There are two ways to achieve deeper reach through acid. First way is to create fracture and another way is to create wormholes. Fractures are created when fluid is injected above the formation fracture pressure. If Fluid is acid, it is called acid fracturing, if fluid is another fluid, it is called hydraulic fractured.

When the acid is injected below the formation fracture pressure, method is called carbonate matrix acidizing. In case of carbonate, regular acid 15% HCl is used. When acid react with carbonate rock at injection pressure below the formation fracture pressure, there is possibility of many dissolution patterns. These dissolution structure depends on, injection rate, reaction kinetics, flow geometry and the fluid loss rate. Key dissolution patterns are face dissolution, conical wormholes, dominant wormholes, ramified wormholes and uniform wormholes (Al-Harthy et al. 2008). At lower injection rate, dissolution pattern is face dissolution and at high injection rate, dissolution pattern becomes uniform dissolution. At intermediate flow, known as optimum injection rate, dominant wormholes are developed. Dominant wormholes results into minimum pore volume to breakthrough, higher depth of acid penetration, higher reduction in skin and maximum increase in permeability (Al-Harthy et al. 2008). Factors like temperature, formation type & mineralogy, reaction kinetics and pore size distribution decides the optimal injection rate for each acid-formation type pair. Literature suggest that wormholes could be 6 meter long in good acidizing job.(Economides et al., 1994)

Connection of dominant wormholes with optimal injection rate are best explained by Damkholer number (Da) theory. According to this theory (Hoefner and Fogler 1988), Da controls the wormhole formation process. Da is calculated as the ratio of the net rate of acid dissolution to the rate of acid transport by convection. For wormholes, the net rate of dissolution is equal to the rate of dissolution calculated under the mass transfer regime. An optimum Da of 0.29 was suggested in literature based on prior knowledge of wormhole dimensions. (Fredd and Fogler 1996). Later research suggested that optimum Da varies between 0.28 and 0.35. (Golfier et al. 2002). The formula for Da (Fredd and Fogler 1996), (Equation 1) suggests that Da is proportional to the overall dissolution rate and inversely proportional to the flow rate.

$$Da = \frac{\pi * d * L * k}{q} \qquad \text{Equation 1}$$

Where d and L are the diameter and length of the wormholes, q is the flow rate in the wormholes and k is the overall dissolution rate depend on the mass transfer and surface transfer coefficients.

Acid penetration inside carbonate rocks could further improved by retarded acids. Acid rock reactions are mass transfer controlled reaction in lower injection rate and during this regime, increase in injection rate leads to increase in dissolution rate and wormhole initiation. During the matrix acidizing, high rock dissolution rate in acid are not preferred as acid doesn't have enough time to react and penetrate deeper. Therefore, in place of regular strong acid 15% HCl, many alternatives are considered to chemically retard acid-rock reaction. Such alternative include use of lower concentration of acid, use weaker acid such as acetic acid, use chemical additives to retard or apply encapsulation of acid to control diffusion.

Experimental Objectives

Our objective under this research was to see how to achieve deeper acid penetration. We have evaluated the following,

- Effect of cavity
- Effect of access type
- Effect of density
- Effect of retardation
- Effect on injection rates

Key experiment were acid injection using core flooding and soaking experiments and followed by CT scanning of the acid treated cores.

Results & Discussion

Soaking Experiments

Cavity create an entry space for acid to reach and collect in place that is easier process in comparison to wormhole initiation and propagation. Uniform access and Controlled access through lab experiment could be described in Figure 2

Figure 11a) Uniform access b) Controlled access.

Uniform access corresponds to open hole arrangement where formation surface including cavity is equally accessible. Controlled access is arrangement-having similarity to controlled access liner, which means acid can go into formation through designated area and whole formation cannot be acidized at once. It is worth notable that horizontal wells in Maersk oil are based on CAJ liner based however, potential radial jet application would lead to open hole inside the formation.

One of the experimental observation was that the cavity initiate the deeper acid penetration that in turn would improve the permeability. It is not always possible to create dominate wormhole detectable by CT scanner and increase in permeability support the creation of micro wormholes when acid react with carbonate formation. Effect of cavity geometry is also checked on acid penetration. Geometry of cavity is controlled by changing the diameter and depth of the cavity. Results from soaking experiment are summarized in Table 2

Table 4 Experimental results based Soaking experiments

Objective	Without Controlled entry	Controlled Entry
Effect of Cavity depth on Acid penetration	Lower depth promote deeper acid penetration	Same
Effect of Cavity diameter on Acid penetration	Smaller diameter promote deeper acid penetration	Same
Effect of Acid Strength on Acid penetration	Weaker acid penetrate deeper than stronger acid	Stronger Acid penetrate deeper than weaker acid.

Experimental results highlight difference in acid penetration for both weaker and strong acid based on change in cavity geometry and access type. In open hole, it is recommended to use retarded acid because acid would have higher time to react due to slower diffusivity. For controlled access, it is recommended to use the stronger acid for deeper penetration. Results also suggest that smaller diameter and lower depth leads to deeper acid reach.

Another set of experiments were done using High-density regular acid blended though adding acid into high density concentrated halide brine. Final selection of the salt is based on cost effectiveness and desire acidic property. It has also proven that, by increasing the density of acid, there is no significant change in dissolution rates however, there would be increase in corrosion strength of acid due to increase in concentration of halide ions responsible for damaging the protective layer. Cheng et al (2011) has tested heavy acids in lab and results show $CaCl_2$ increased acid corrosion substantially due to presence of excess free chloride ions as it dissolves the protective Cr_2O_3 layer which results in extreme corrosion during acidizing (De Wolf et al. 2012). Therefore, selection of appropriate corrosion inhibitor and friction reducer is crucial while using heavy acids. Table 3 highlight the different brines and their density.

Table 5 Different Brines and their density at 25˚C

Type	26% KCl	26% NaCl	33% NaBr	27.5% $CaCl_2$	40% NaBr	45% NaBr	21% NaBr+ 15%NaCl	44% NaBr+4% NaCl
Density (g/cm3)	1.17	1.19	1.32	1.26	1.41	1.48	1.34	1.514

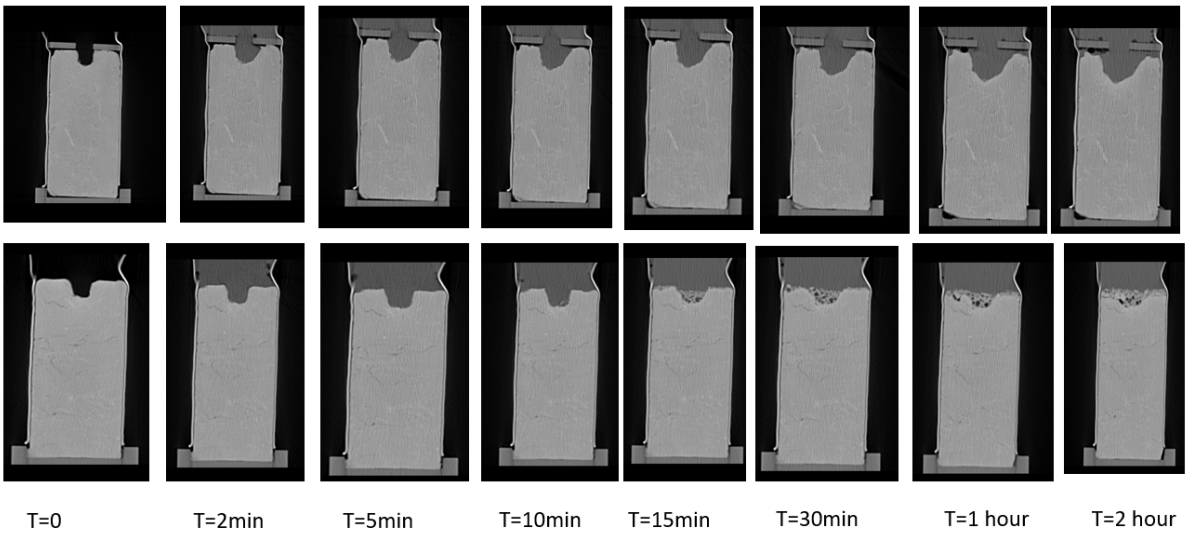

Figure 8 Heavy Density Acid penetration for 5% HCl (With cover (Top) and without cover (bottom))

Figure 3 Compare the acid penetration of 5% HCl saturated with $CaCl_2$ brine. System density was measured to be 1.24 gm/cm3 at 25 degree C. From the figure, it is visible that there are different dissolution behavior in case of controlled entry and uncontrolled entry. It is clear from the comparison that controlled entry case, acid is able to penetrate deeper than the uniform access case.

In Figure 4 below, 10% Acetic acid penetration was compared between saturated core and dry core. Results suggest that, dry core allow acid to go deeper compare to saturated core. Experiment was done for controlled entry case only. Dry cores and poured acid has density difference in the order of 1000 g/cm3 whereas in case of saturated core, density difference is close to zero. It is evident that density difference of such order resulted into higher acid penetration.

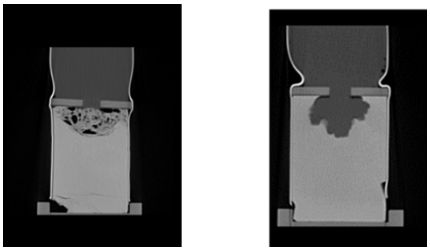

Figure 13 CT scan comparison of Weak acid (10%AA) penetration after 2 hours for saturated core (left) and dry core (Right)

Core Flooding Experiments

Core flood setup is used to simulate matrix acidizing process in the laboratory. It provides experimental evidence related to ability of the acidizing sample fluid to generate wormholes, and to examine the core sample after it comes to contact with the acid. The setup can be used to study the influence of temperature, injection rate, Fluid type and concentration and back pressure. The core flood setup can be used to measure the core permeability. Thus the setup is an ideal tool to first

perform the matrix acidizing and then to find the change in permeability of the rock sample. The permeability is calculated by using the Darcy's law.

$$k = -\frac{q\mu L}{A\Delta P}$$

A	=	Cross sectional area (cm^2)
k	=	Permeability (D)
L	=	Length (cm)
ΔP	=	Pressure difference (atm)
q	=	Flow rate (mL/s)
μ	=	Viscosity (cp)

Backpressure is maintained at 1000 psi during the acidizing to ensure that CO2 produced from the reaction during matrix acidizing remained in the solution thus ensuring a single phase flow system. The main objective of this experiment was to compare the increased permeability by injecting different acidic sample solutions through the Chalk core samples at various conditions. In all experiments 2 PV of the acid was injected and permeability before and after the acid injection was measured. Key variable in core flooding experiments are acid type and strength, injection rates, density difference and presence of cavity Injection rate varied from 0.5 ml/min to 1.5 ml/min, for weak acid, 10% AA was considered, to see the effect of concentration, 15% HCl and 5% HCl was considered, for density, 5% HCl with density equal to 1.25 gm/cm3 was selected. To see the effect of cavity, 8 mm dia X 5 mm depth cavity was created. Chalk Cores from Stevns Klint with average porosity equal to 40% and low initial permeability equal to 2 mD were used. Average core diameter was 37.4 mm and average Initial length was 51.9 mm. Results of Core flooding experiments are listed in Table 4. During the calculation, it is assumed that length and area of the core is not changed due to core flooding experiments.

Table 6 Core Flooding Experiments results

Core Id	Acid Type	Injection Rate m1/min	Cavity	Delta K
CF-1	5% HCl	0,5	No	98%
CF-2	5% HCl	1	No	171%
CF-3	5% HCl	1,5	No	364%
CF-5	10% AA	0,5	No	0%
CF-7	5% HCl +$CaCl_2$	1	No	179%

CF-11	5% HCl	0,5	Yes	85%
CF-12	5% HCl	1	Yes	253%
CF-13	10% AA	1	Yes	674%
CF-15	5% HCl +CaCl2	1	Yes	17%
CF-4	15% HCl	0,5	No	Sample destroyed.

Results for the experiments are following.

One of the first observation we had was that 15% HCl is very strong acid for chalk formation as the core was fully damaged to calculate. Effect of other parameters were studied as below.

Effect of Injection rate on change in permeability for no cavity

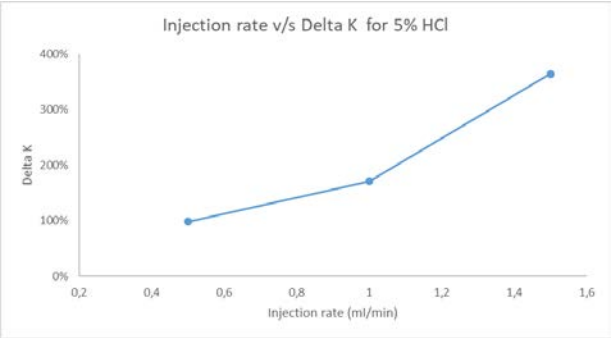

Figure 10 Effect of injection rate on change in permeability for strong acid

Figure 5 shows that for strong acid, increase in injection rate leads to higher increase in permeability.

Effect of cavity on the change in permeability

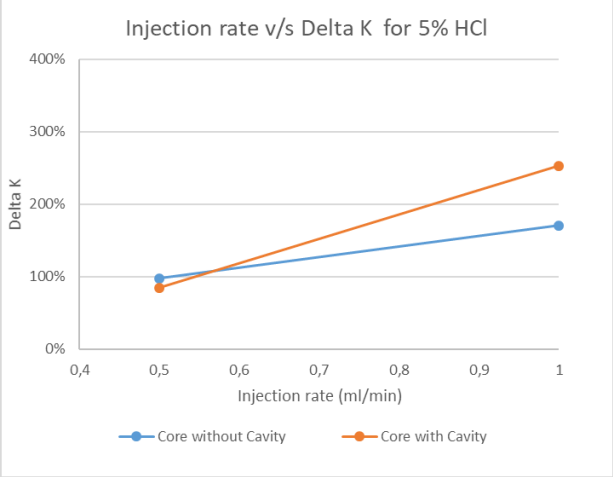

Figure 11 Effect of Injection rate vs change in permeability when cavity present

Figure 6 shows that for cavity accelerate the change in permeability and higher injection rate, there is higher increase in permeability

Effect of cavity on high-density acids

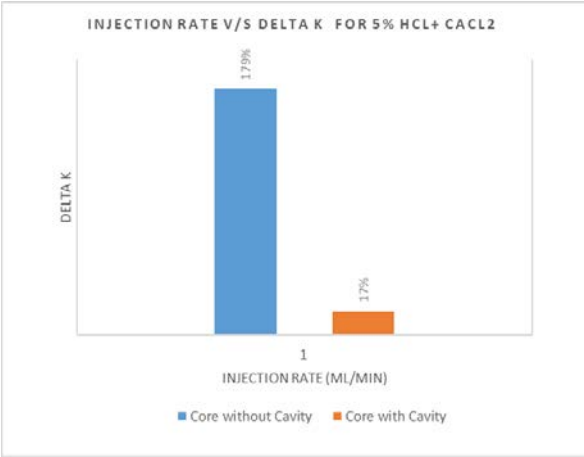

Figure 12 Effect of Cavity on permeability change for heavy density

Figure 7 show that for heavy density, presence of cavity reduces the permeability.

Effect of acid strength on permeability change when no cavity present

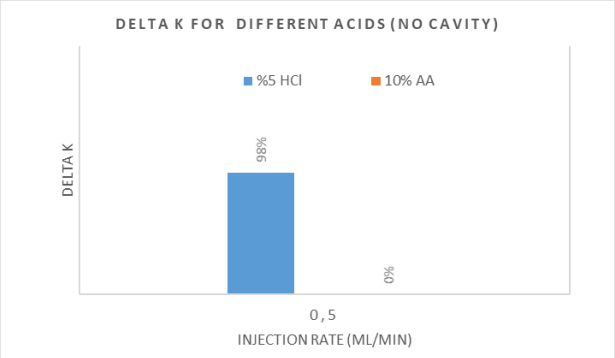

Figure 13 Effect of Acid type on permeability when no cavity

Figure 8 shows that stronger acid are more effect and enhance permeability better than the weaker acid when no cavity present.

Effect of acid strength on permeability change when cavity present

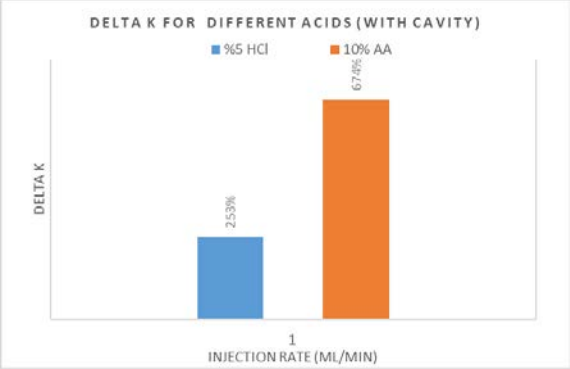

Figure 14 Effect of Acid strength on permeability when cavity present

Figure 9 shows that stronger acid are more effect and enhance permeability better than the weaker acid.

Effect of Acid density on permeability with cavity present

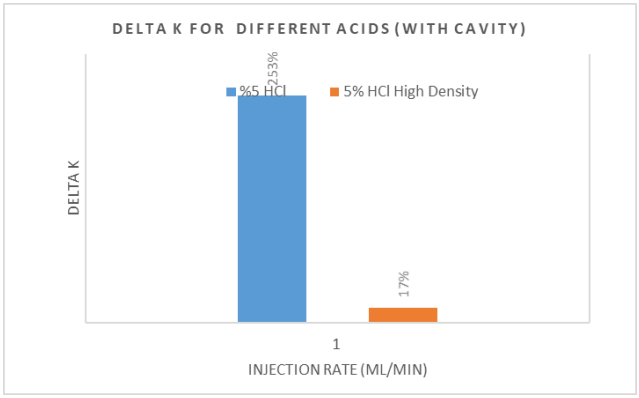

Figure 15 Effect of Acid density on permeability when cavity present

Figure 10 shows the increase in density reduce the permeability when the cavity is present.

Effect of Acid density on permeability with no cavity present

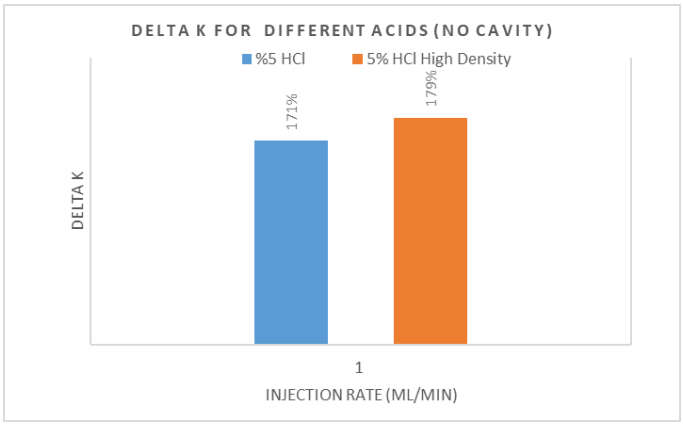

Figure 16 Effect of Acid density on permeability No cavity

Figure 11 shows the density increase does not have effect of permeability when there is no cavity

Deep Reach through Encapsulation Technology (only literature review)

Most popular form of encapsulation-based acid is emulsified acid. Emulsified acid is HCl in Diesel emulsion. There are more than 30 SPE papers on Emulsified Acid and many patents and commercial applications are documented (Al Anazi et.al, 1998). It has numerous benefits over regular HCl. Key advantage are that it offer best chemical retardation through decrease in acid diffusion, which allows live acid to penetrate rock matrix deeper and more uniform ally (Hoefner et al,1987). This acid system has smaller treating volume and has lower corrosion damage to pumps and downhole equipment. Usually Emulsified acids are non-Newtonian, shear-thinning fluid, which means as the shear increase, viscosity decreases. Such fluids follow power law model and their apparent viscosity has an inverse relationship with temperature explained through Arrhenius equation (Sidaoui et al, 2017) however there are some exceptions (US Patent 20120090845).

Emulsified acid is thermodynamically unstable system and by combining mechanical and chemical method will results into stable emulsion. Stable emulsified acid shows stable viscosity, which does

not increase, or decrease even over elevated temperature and at expected pumping shear. Many researchers have prepared the emulsified acid with 70:30 acid to diesel volume ratio, 15% wt HCl and upto 2% volume of emulsifier agent. Some researchers have successfully replaced diesel with Xylene to have dual benefit of asphaltene precipitation removal along with acidizing. Al-Mutairi et al, 2007 & Al-Mutairi et al, 2009 studied effect of emulsifier concentration on droplet size, stability, acid diffusion, and viscosity. Their research shows as emulsifier concentration increases, the droplet size decreases, viscosity increases, acid diffusivity decreases and emulsion stability increases. It could be important for the delivery as smaller drops may also means quick delivery. Recently few studies have focused on replacing diesel with waste oil from refinery to make emulsified acid economical cheaper product. Emulsified acid cause less corrosion damage to pumping equipment and downhole tubulars as external phase is hydrocarbon. Due to shear thinning property, emulsified acid has lower viscosity inside well and higher viscosity in to the formation. Increase in viscosity inside the formation would increase the acid rock contact time and allows acid more time to react and improve acid sweep efficiency thus create Christmas tree type branched wormholes. This would overall improve acid distribution in heterogeneous formation and seepage area near well bore area. Emulsified acids would require less pumping power due to their shear thinning nature and retarded nature as retarded acids have better stimulation at lower injection rates compare to stronger acids (Fredd et al, 1996)

Proposed way forward

As a way forward from this study, clear overview is required for all patents available and based on input collection from service companies. Existing lab tests results are available for limestone and therefore knowledge of chalk formation dissolution rates for different acidizing fluids including emulsified acids at reservoir condition would be an interest prospects for future modelling and simulation works. Either a novel emulsified acid compatible with North Sea crude oil can be developed or few selected ones offered by services companies can be lab tested for effect on chalk and compatibility with crude oil. Lab studies will provide an idea about different parameter such as droplet size and stability. Experiments such as Core flooding, dissolution test, Turbiscan for emulsions or microbalance experiments can be performed in the lab

- To study the effect of North Sea crude oil on droplet size, viscosity, acid volume fraction and stability of Emulsified acid.
- To study the chalk dissolution rates and Injection Rate vs PVBT for Emulsified acid-chalk combination and development of CO_2.

Final conclusion

According to Giovanni et al, 1995, key reasons for failure of acidizing job include failure resulted from incorrect field procedures, insufficient injection pressure and pump rates and selection of wrong stimulation fluid. This makes laboratory-based experiments of great importance to gather data to see if very negative results are obtained during lab work that would discourage stimulation or what are lab results in case there are negligible previous field experiences.

Experimental evidence show that that cavity size influence the acid penetration and retarded acid penetrate deeper than stronger acid for same size cavity. Radial Jet drilling would create cavity, allow acid reach deep into formation, and create conductive flow. Selection of suitable retarded acid would play an important role.

We also believe that encapsulated technique based emulsified acid would be better candidate compare to regular 15% HCl as jetting fluid during radial jet drilling application. It has many advantages over 15% HCl and is more economical as well as environment friendly option to choose during the radial jet drilling application. Emulsified acid is retarded, shear-thinning fluid which means it require lower pumping power than stronger acid and small treating volume. Shear thinning behaviour also make the jet drilling less turbulent during the operation, which improve the effectiveness of jetting.

References

Al-Mutairi, S. H., Nasr-El-Din, H. A., Hill, A. D., & Al-Aamri, A. (2009, December 1). Effect of Droplet Size on the Reaction Kinetics of Emulsified Acid With Calcite. Society of Petroleum Engineers. doi:10.2118/112454-PA

Al-Mutairi, S. H., Hill, A. D., & Nasr-El-Din, H. A. (2007, January 1). Effect of Droplet Size, Emulsifier Concentration and Acid Volume Fraction on the Rheological Properties and Stability of Emulsified Acids. Society of Petroleum Engineers. doi:10.2118/107741-MS

Al-Anazi, H. A., Nasr-El-Din, H. A., & Mohamed, S. K. (1998, January 1). Stimulation of Tight Carbonate Reservoirs Using Acid-in-Diesel Emulsions: Field Application. Society of Petroleum Engineers. doi:10.2118/39418-MS

Al-Harthy, Salah, Oscar A Bustos, Mathew Samuel, John Still, Michael J Fuller, Nurul Ezalina Hamzah, Mohd Isal Pudin bin Ismail, and Arthur Parapat. 2008. "Options for high-temperature well stimulation." Oilfield Review 2009 (20):4.

Brainerd, H. W., Jr. (1954). U.S. Patent No. US2689009A, . Washington, DC: U.S. Patent and Trademark Office.Acidizing wells.

Brainerd, H. W., Jr. (1952). U.S. Patent No. US2721174. Washington, DC: U.S. Patent and Trademark Office. Emulsified acids for high temperature wells

Chang, Frank Fakuen, Hisham A Nasr-El-Din, T Lindvig, and XW Qui. 2008. "Matrix Acidizing of Carbonate Reservoirs Using Organic Acids and Mixture of HCl and Organic Acids, SPE-116601-MS." SPE Annual Technical Conference and Exhibition.

Cheng, X., Li, Y., Ding, Y., Che, M., Zhang, F., & Peng, J. (2011, January 1). Study and Application of High Density Acid in HPHT Deep Well. Society of Petroleum Engineers. doi:10.2118/142033-MS

Chatelain, JC, IH Silberberg, and RS Schechter. 1976. "Thermodynamic limitations in organic-acid/carbonate systems." Society of Petroleum Engineers Journal 16 (04):189-195.

De Wolf, Corine, Hisham A Nasr-El-Din, Arjen Bouwman, Edwin Bang, and Ed Naylor. 2012. "A new, low corrosive fluid to stimulate deep wells completed with Cr-based alloys, SPE-152716-MS." SPE International Conference & Workshop on Oilfield Corrosion.

Economides, M.J., Hill, A.D., and Ehlig-Economides, C. 1994. "Petroleum production systems". United States.

Fredd, CN, and H Scott Fogler. 1996. "Alternative stimulation fluids and their impact on carbonate acidizing, SPE-31074-MS." SPE Formation Damage Control Symposium.

Fattah, W. A., & Nasr-El-Din, H. A. (2010, May 1). Acid Emulsified in Xylene: A Cost-Effective Treatment To Remove Asphalting Deposition and Enhance Well Productivity. Society of Petroleum Engineers. doi:10.2118/117251-PA

Fredd, CN, and MJ Miller. 2000. "Validation of carbonate matrix stimulation models, SPE-58713-MS." SPE International Symposium on Formation Damage Control.

Frenier, Wayne W, and Donald G Hill. 2002. "Effect of acidizing additives on formation permeability during matrix treatments, SPE-73705-MS." International Symposium and Exhibition on Formation Damage Control.

Golfier, F, Cesar ZARCONE, B Bazin, R Lenormand, D Lasseux, and Michel QUINTARD. 2002. "On the ability of a Darcy-scale model to capture wormhole formation during the dissolution of a porous medium." Journal of fluid Mechanics 457:213-254. doi: https://doi.org/10.1017/S0022112002007735.

Huang, T. (2010). U.S. Patent No. US20120090845. Washington, DC: U.S. Patent and Trademark Office. Stabilizing Emulsified Acids for Carbonate Acidizing

Houchin, L. R., Dunlap, D. D., Arnold, B. D., & Domke, K. M. (1990, January 1). The Occurrence and Control of Acid-Induced Asphaltene Sludge. Society of Petroleum Engineers. doi:10.2118/19410-MS

Hoefner, ML, and H Scott Fogler. 1988. "Pore evolution and channel formation during flow and reaction in porous media." AIChE Journal 34 (1):45-54. doi:

Hoefner, M. L., & Fogler, H. S. (1987, February 1). Role of Acid Diffusion in Matrix Acidizing of Carbonates. Society of Petroleum Engineers. doi:10.2118/13564-PA

LePage, James N, Corine De Wolf, Josine Bemelaar, and Hisham A Nasr-El-Din. 2009. "An environmentally friendly stimulation fluid for high-temperature applications, SPE-121709-MS." SPE International Symposium on Oilfield Chemistry.

Lynn, J. D., & Nasr-El-Din, H. A. (2001, January 1). A Core Based Comparison Of The Reaction Characteristics Of Emulsified And In-Situ Gelled Acids In Low Permeability, High Temperature, Gas Bearing Carbonates. Society of Petroleum Engineers. doi:10.2118/65386-MS

Mumallah, NA. 1991. "Factors influencing the reaction rate of hydrochloric acid and carbonate rock, SPE-21036-MS." SPE International Symposium on Oilfield Chemistry.

Paccaloni, G., & Tambini, M. (1993, March 1). Advances in Matrix Stimulation Technology. Society of Petroleum Engineers. doi:10.2118/20623-PA

Rabie, Ahmed I, and Hisham A Nasr-El-Din. 2011. "Measuring the reaction rate of lactic acid with calcite using the rotating disk apparatus, SPE-140167-MS." SPE Middle East Oil and Gas Show and Conference.

Sidaoui, Z., Sultan, A. S., & Brady, D. (2017, June 1). A Novel Approach to Formulation of Emulsified Acid using Waste Oil. Society of Petroleum Engineers. doi:10.2118/188116-MS

Stringfellow, William T, Mary Kay Camarillo, Jeremy K Domen, Whitney L Sandelin, Charuleka Varadharajan, Preston D Jordan, Matthew T Reagan, Heather Cooley, Matthew G Heberger, and Jens T Birkholzer. 2017. "Identifying chemicals of concern in hydraulic fracturing fluids used for oil production." Environmental Pollution 220:413-420. doi: https://doi.org/10.1016/j.envpol.2016.09.082.

Stringfellow, W. T., Domen, J. K., Camarillo, M. K., Sandelin, W. L., & Borglin, S. (2014). Physical, chemical, and biological characteristics of compounds used in hydraulic fracturing. Journal of hazardous materials, 275, 37-54.

Wang, Y, AD Hill, and RS Schechter. 1993. "The optimum injection rate for matrix acidizing of carbonate formations, SPE-26578-MS." SPE Annual Technical Conference and Exhibition.

Ziauddin, M. E., & Bize, E. (2007, January 1). The Effect of Pore Scale Heterogeneities on

Carbonate Stimulation Treatments. Society of Petroleum Engineers. doi:10.2118/104627-MS

Treatment of produced water - recovery of salts and fresh water

Cejna Anna Quist-Jensen, Henriette Casper Jensen, Morten Lykkegaard Christensen,
Department of Chemistry and Bioscience, Aalborg University
Aamer Ali, Institute on Membrane Technology – National Research Council Italy

Abstract

A new membrane technology called membrane crystallization has been tested for produced water treatment with the aim of recovering valuable salts from the stream, which can be used as modified injection water or can be sold to other industries. During this radical sprint project, NaCl and fresh water have been recovered at a lab-scale membrane crystallization plant. In the experimental studies, synthetic produced water containing crude oil has been tested. The performance of the membrane filtration proved a stable flux even with a high oil content (> 100 ppm). Moreover, the produced NaCl crystals had the same quality as crystals, which have been recovered from produced water without oil.

Some preliminary estimations on thermal energy consumption and footprint have also been carried out during the sprint project. It is shown, that the feasibility of membrane crystallization is highly dependent on available thermal energy. Since produced water is often at high temperatures (40°C-80°C) when leaving the well, it can, through optimization of energy recovery and module design, become a feasible treatment technology for produced water. Moreover, the compact size of membrane modules makes it a strategic process for turning produced water into a valuable product – in terms of salts and fresh water.

Technology vision

Imagine if an oil and gas platform can recover – beside oil and gas – the various valuable compounds present in produced water as for example magnesium, lithium, barium, strontium etc. and simultaneously produce fresh water (Figure 1).

In future, minerals and water will be scarce resources and therefore, there is a clear motivation to turn waste into products. In this regard, the oil and gas industry is an interesting case where produced water-a mineral-rich liquid stream- is considered as a waste product. Growing volume of produced water and increasingly stringent environmental regulations are making the proper management and treatment of produced water a challenging issue.

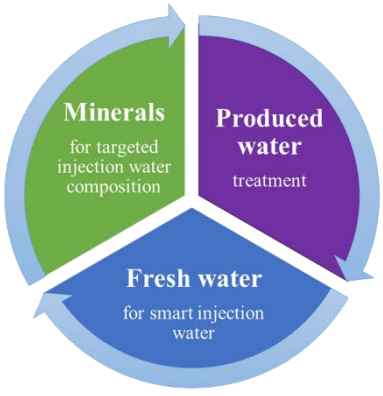

Figure 21: Technology vision

The conventional treatment techniques for produced water are mainly aimed at meeting the discharge criteria. If produced water has to be treated, why not create some value out of it, at the same treatment cost.

The current sprint project provides an alternative treatment option where produced water is considered as a source of freshwater and minerals. There are several possibilities to consider produced water as a supply of salt and fresh water:

1) It can be used for modified injection water – it requires that some salts (mainly scale components) are removed from solution.

2) It can be used as a fresh water resource – a water resource for smart injection water, drinking water, cooling towers etc.
3) It can be used as a mining resource if the valuable salts in produced water are recovered – these salts can eventually be considered as an additional salable product or some of the salts can be dissolved in fresh water to create smart injection water modified according to the specific well.
4) In certain cases, the final concentrated stream can be used directly as a raw material for certain industrial sectors such as chlor-alkali industry when produced water mainly consists of sodium chloride

Objective of radical sprint project

The main limitation for treatment of produced water and many other waste streams is the unavailability of efficient treatment technologies and/or high treatment costs. Several technologies have been suggested for produced water treatment, but the main problem is the high salt content and oil residues [1], [2] which limit the treatment options.
In this radical sprint project, a new membrane process (i.e. membrane crystallization) is applied for the treatment of produced water. Membrane crystallization (MCr) has some outstanding features compared to other technologies:

- *It can treat solutions independently of their concentration.*
- The process can be operated with *low-grade heat* generally available with produced water during its production
- *From one waste stream it can produce several products – fresh water and the salts present in solution – without the need of other processes*

Comparison with state-of-the-art desalination technologies

MCr is not a pressure driven membrane processes, but it is based on a temperature gradient (Figure 2). It only allows volatile compounds such as water to go through the membrane, due to the hydrophobic nature of the membrane and therefore, it can produce a high-quality fresh water stream. Since it is not pressure driven, MCr is less prone to fouling and is marginally affected by the feed water salinity. Moreover, it does not require the use of anti-corrosion agents - an essential part of thermal processes used for desalination - thus the operation itself is more environmental friendly.
State-of-the-art desalination plants are based either on thermal technologies (multi-stage flash (MSF), thermal evaporators with mechanical vapor compression units, brine crystallizers etc.) or membrane operations. Thermal desalination technologies are known for their operational reliance upon high-grade energy, large foot prints, bulky equipment, scaling issues and, in certain cases (for instance MSF), limited recovery factor.
Membrane based desalination is mainly carried out by using reverse osmosis (RO), which cannot go beyond twice the concentration of seawater. Since produced water is often at much higher concentration, this limits the use of RO and therefore, other technologies have to be developed for the treatment of produced water. MCr has significantly smaller footprints compared to thermal desalination techniques. Also the use of polymeric (or possibly ceramic membrane) allows getting rid of corrosion issues. Thus, the technology represents a compact, lightweight and corrosion-free treatment of produced water to yield freshwater and minerals.

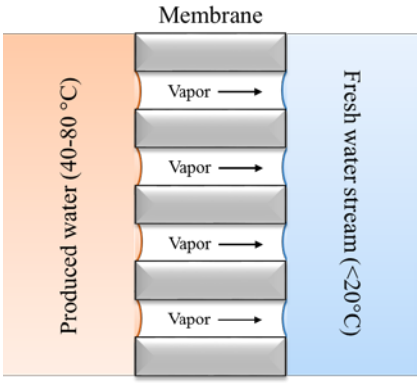

Figure 18: Illustration of membrane crystallization membrane

Membrane crystallization at large scale

The technology can be installed in form of a compact unit consisting of a heat exchanger to heat the feed to the set feed inlet temperature, a cooling arrangement (possibly a heat exchanger using seawater as the cooling media) to condense the vapors, membrane modules and two pumps, each for feed and permeate. The cooling arrangement can be avoided if air gap membrane crystallization is used.

Several small companies (such as Memsys, Aquatsill, AQUASEP etc.) have recently emerged which provide the build-in MCr plants with varying capacities. These units are customized to treat the feed solutions with a wide range of salinities. MCr is installed in form of modular structure which allows easy scaling up of the technology if needed. The overall recovery factor can be tuned by changing the operating conditions or by adding/bypassing some of the module stages. The technology is expected to be suitable for the rapid start-up and emergency shut-down.

MCr technology can possibly face the scaling, fouling and wetting issues. In case of fouling/scaling, the washing of membrane with freshwater or another appropriate solvent (such as dilute acetic acid solution) might be needed. In case of wetting, the additional requirements of membrane drying may also be needed. Due to the modular structure of separation unit, in case of wetting or breakage of some membrane, it is easy to replace the damage modules.

Validation of technology

Validated during sprint

In this sprint project, initial lab-scale testing of MCr to treat synthetic produced water has been performed. Some crude oil has been added in the produced water to test whether MCr can treat the oil-containing produced water. Moreover, a thermodynamic modeling of produced water has been carried out to estimate which valuable minerals can be recovered from produced water (and in which amount) and to evaluate the volume of associated freshwater that can be produced. In this regard, preliminary estimations on footprints and energy consumptions have also been estimated.

Validation method

The technology has been tested experimentally by using the lab-scale setup shown in Figure 3 and the composition of synthetic produced water given in Table 1. Two compositions have been tested – a low concentrated solution, which is similar to the composition found in Denmark and a higher concentrated solution to prove the efficiency of MCr under extreme conditions [2].

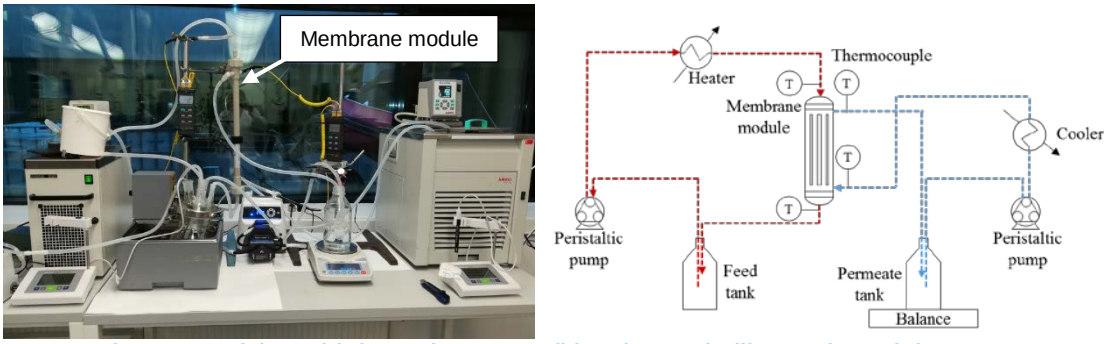

Figure 19: (a) real lab-scale setup, (b) schematic illustration of the setup

Table 7: composition of produced water

Composition	Low concentration (mg / L]	High concentration (mg / L]
Crude oil	100	100
Na^+	15000	97000
Mg^{2+}	1000	6000
Ca^{2+}	1000	25800
Cl^-	35000	200000
SO_4^-	2000	1650
Sr^{2+}	1000	1000
Ba^{2+}	0.5	650
K^+	100	4300
Li^+	-	50

Results and discussion

The aim of the sprint project has been to validate the technical potential of the MCr technology for freshwater and salts recovery from the synthetic produced water containing oil. High oil content can interfere with the hydrophobic character of the membrane, which is essential for the operation of MCr, and therefore can destroy the process stability. For this reason, 100 ppm of crude oil has been added in the produced water. OSPAR regulations require a maximum of 30 ppm dispersed oil in produced water prior to discharge and hence 100 ppm accounted for expected worst-case scenario. However, as evident from the stable flux over time shown in (Figure 4a), the oil content (higher than 100 ppm) did not negatively affect the stability of the process. The long term experimentation (several weeks) is necessary to further prove the strength of this observation to ensure that a slow build up does not affect membrane efficiency.

The MCr process, applied in current study, rejects non-volatile components from a solution and produces freshwater and salts from the mixture. Oil, being a volatile component, cannot be completely rejected and therefore cannot be removed from produced water by using MCr. However, MCr can be integrated after the hydrocyclone or other membrane based operations, such as micro/ultrafiltration, which is investigated in other DHRTC projects.

The average flux is around 0.5 L/m^2/h, which might be too low for large-scale applications. The same flux has been measured using distillate water before any produced water treatment and therefore not due to either oil content or salt concentration. The reason is a non-optimized flow rate for this membrane module, which can be optimized by increasing the flow rate slightly, ensure that air is not inside the membrane module and by optimizing the module configuration.

Figure 4b illustrates the fresh water recovery factor versus time for the MCr experimentation performed on the produced water. For the low concentrated solution, the operation was terminated at recovery factor of 60% due to low volume of solution left in the feed tank, but it is possible to go much further. To prove this claim, a higher concentrated solution has been tested and the similar flux has been achieved. The high-concentrated solution was used to finish the experimental campaign within the time allocated for the sprint project. For the high concentrated solution, the crystallization started at around a recovery factor of 30%, which proves the potential of MCr to achieve supersaturation and thus crystallization from the produced water. It should also be noticed that a high initial concentration of crude oil (100 ppm) has been added in the produced water. This highlights, that despite high oil content, MCr is still functioning and providing a stable flux.

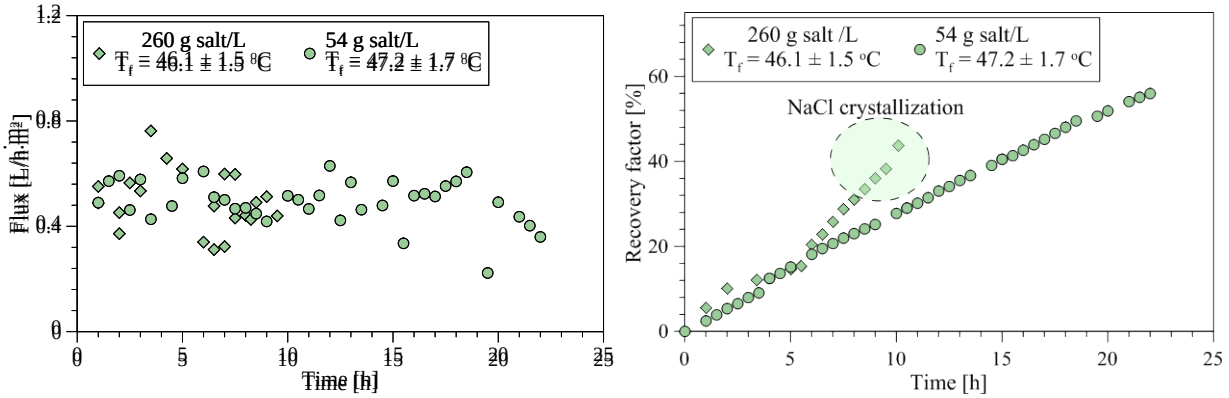

Figure 20: Performance of MCr, (a) fresh water productivity per unit of membrane area (Flux), (b) fresh water recovery factor versus time

The influence of oil on the purity of NaCl crystals has been studied by using XRD analysis. As shown in Figure 5, the quality of NaCl with oil present is similar to crystals without oil in the produced water. Until now, we have been able to recovery 13 g/L of NaCl. Crystallization by MCr normally produces a high-quality product. The main concern is if heavy metals will be incorporated into the crystal structure. In this study, the peaks from XRD analysis shows a high-purity NaCl product. However, this can be further confirmed by inductively coupled plasma (ICP) analysis if the project is continued.

Another perspective on produced water treatment, is regarding the heavy metals, which might be easier to remove from the solution after MCr treatment. There could be two possible options to address this issue. If recovery of multiple salts is considered from the solution, heavy metals can also be recovered in form of pure crystals. However, heavy metals have not been considered in this study and needs further investigations. At high water recovery factor, with possible salts recovery, the volume of the rejected stream (which also contains heavy metals) will be very less and therefore, can be disposed at significantly lower cost due to the reduced volume.

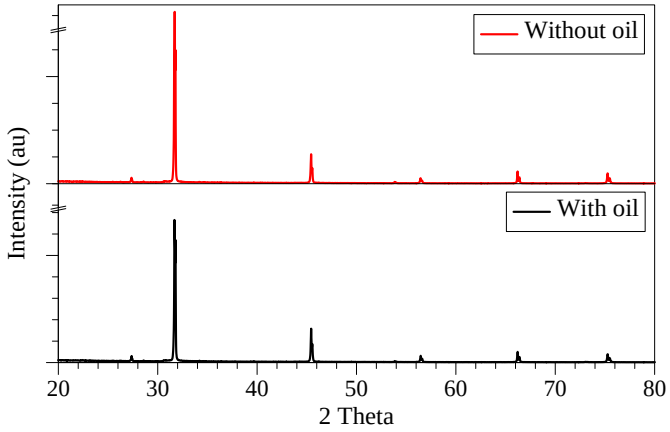

Figure 21: Quality of produced NaCl crystals

In the sprint project, recovery of NaCl has only been obtained, but in future projects, the recovery of more valuable salts can be targeted. Thermodynamic modeling can be used to estimate recoverable salts from produced water. An example of such modeling is shown in Figure 6. This can also give estimations on which salts can cause scaling issues during the treatment and whether the produced water can be re-injected into the well without proper treatment.

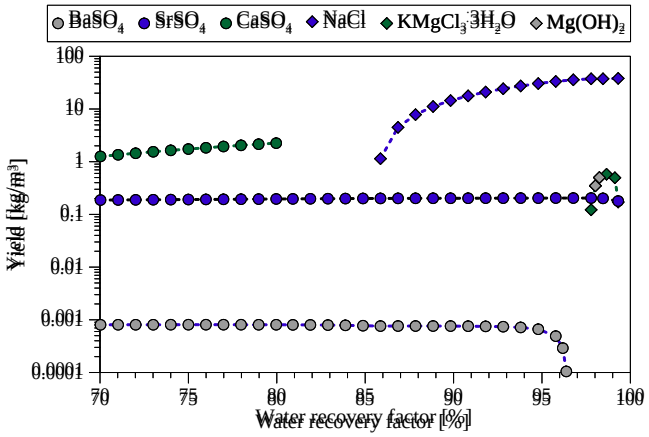

Figure 22: Thermodynamic modeling of the low concentrated produced water

Energy and foot print estimation

In the sprint project, MCr technology has been validated experimentally, but we have also performed some preliminary estimations of energy consumptions. The model has been developed according to our previous work [3]. The MCr technology is highly dependent on availability of waste heat or that the produced water is already coming from the well with a sufficient temperature. In Figure 7, the energy consumption has been estimated according to a temperature between 40-80°C, which we consider realistic for real scale plant.

There are two ways of considering thermal energy consumption in MCr. The heat required if produced water from the well needs to be heated before inlet to the module and when the solution needs to be reheated and recirculated back to module inlet. The latter is caused by the temperature loss within the membrane module. As noticed in Figure 7, thermal energy consumption is very high if no heat is available and increases with increase in the required solution temperature. However, for produced water, where the heat is available, the energy consumption will be low and the target is to have 100% availability of thermal energy. Moreover, these energy consumptions are based on the membrane and module characteristics, which we have utilized during the lab-scale testing and therefore, not meeting the large-scale standards. At industrial level, better

membranes and optimized module length and configuration will be used, which will decrease the energy consumptions significant. Moreover, no heat recovery has been considered in this study, which will always be considered during industrial-scale treatment.

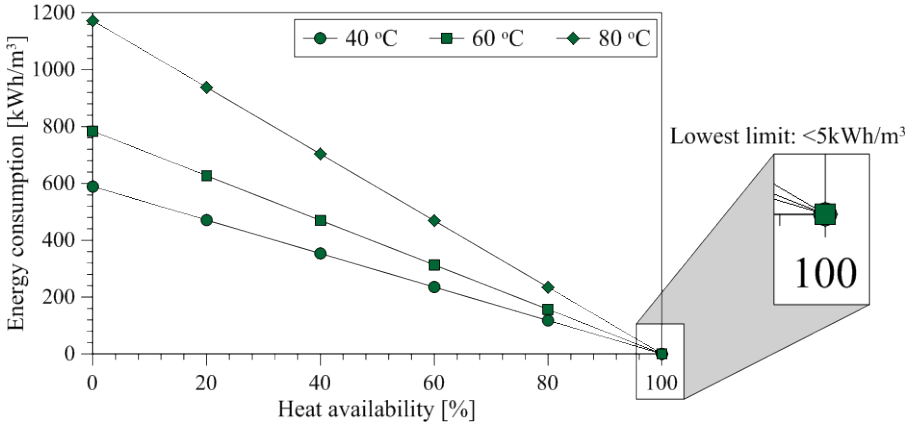

Figure 23: Energy estimations of MCr technology

We have also roughly estimated the size for a plant having a capacity of 100 m^3/h (Figure 8). The capacity is the volume of fresh water produced from the plant and not the produced water volume. The flux has been calculated based on a model developed in our previous work [3], where it has also been validated for seawater. The plant size has been estimated according to industrial large-scale RO modules with a membrane area of 34.4 m^2/module and a length of 1.02 m [4]. A correlation factor of two has been used to account for the volume needed in between the modules, thus the take-up volume of the membranes has been multiplied by two. As seen in Figure 8, the plant size is highly dependent on flux and reduces from 127m^3 to 21m^3 depending on the flux.

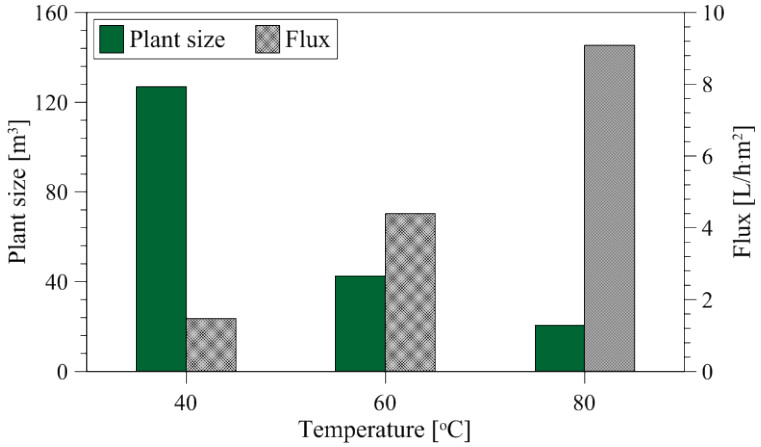

Figure 24: Plant size (volume-based) at different produced water temperatures together with the corresponding water flux. Assumptions are a capacity of 100m^3/h, module area of 34.4m^2/module and module length of 1.02 m.

Proposed way forward

The sprint project has proven the ability of membrane filtration of synthetic produced water with an added oil residue. Bringing the technology further with respect to application in the Oil and Gas Industry would be to:

- Build a pilot scale setup facility

- Using the pilot scale facility to test the design of the membrane for most optimal flux.
- Testing initially with synthetic water with different concentration and different oil residue
- Testing over longer period of time
- Test with actual produced water
- Test if small gas bubbles affect performance
- Work on how the valuable minerals are crystalized and recovered and how the products are commercialized.
- Propose exact MCr facility design and capacity for an actual oil field.
- Link the project to existing smart water compositions and investigate additional requirements to the abovementioned facility.

Dependency on other technologies

The MCr technology depends mainly on the available footprint, load capabilities and surplus thermal energy supply on existing platforms. All though this can appear as an obstacle for the cost benefit of applying MCr novel solutions need to be considered due to increased amounts of produced water and the potential of decreasing the oil residue limit. Approximately 10 years ago the residue limit was reduced from 40 ppm to 30 ppm, and environmental focus may push the industry further also due to increased amounts of produced water. Hence, the MCr technology is available but not researched sufficiently within Oil & Gas application.

Proposal for next project

A six months feasibility research project within the DHRTC program has been applied for in order to further validate the MCr technology. In a next project, the main focus will be to specific modify produced water to meet the standards of smart injection water. In this regard, the following tasks will be accomplished:

1) Longer duration tests of MCr are required to fully validate the technology and to develop a cleaning scheme of the membrane. In this regard, in-depth analysis of the quality of fresh water and oil interaction during crystallization will also be carried out. The membranes utilized in the sprint project will be compared with other membranes from Aquastill in order to make the MCr process more energy and time efficient.
2) Another work package will be devoted to investigate the potential to modify produced water to meet injection water quality. An enhanced crystal recovery system will be developed to harvest the crystals and suggestions on how to separate the salts from each other will be given. This will be performed together with partners from Italy and, furthermore, contact to DHRTC and GEUS employees will be established in order to understand the composition and changes of produced water for smart injection water.

Final conclusion

During the three months sprint project, we have performed initial feasibility tests of membrane crystallization technology. We have shown, that it is possible to recover 60% of fresh water from synthetic produced water with 100 ppm oil residue. Moreover, NaCl crystals have been recovered, which have the similar quality as crystals recovered from produced water without oil.
Estimations on specific thermal energy consumption in membrane crystallization application, highlights the need of having thermal energy available in order to be feasible for industrial applications. This study also shows that the footprint is highly dependent on water flux through the membrane. Plant size in terms of volume has been estimated between 21m^3 to 127m^3 for a plant producing 100 m^3 fresh water per hour. However, both energy estimations and footprint have been calculated based on the membranes and membrane configuration utilized at lab-scale, thus it can be decreased significant by optimizing the design of the plant at pilot and large-scale.

References

[1] E. Drioli, A. Ali, Y. M. Lee, S. F. Al-Sharif, M. Al-Beirutty, and F. Macedonio, “Membrane operations for produced water treatment,” *Desalin. Water Treat.*, 2015.

[2] A. Fakhru’l-Razi, A. Pendashteh, L. C. Abdullah, D. R. A. Biak, S. S. Madaeni, and Z. Z. Abidin, “Review of technologies for oil and gas produced water treatment.,” *J. Hazard. Mater.*, vol. 170, no. 2–3, pp. 530–51, Oct. 2009.

[3] A. Ali, C. A. Quist-jensen, F. Macedonio, and E. Drioli, “Optimization of module length for continuous direct contact membrane distillation process,” *Chem. Eng. Process. Process Intensif.*, vol. 110, pp. 188–200, 2016.

[4] GE Water & Process Technologies, “AD HR Series, Seawater RO High Rejection Elements.” [Online]. Available: http://www.lenntech.com/Data-sheet/GE-Osmonics-AD-HR-series-Sea-Water-RO- %0AHigh-Rejection-Desalination.pdf.

ShipNet

Cosmin Avasalcai, Research Assistant at DTU Compute
Paul Pop, Prof. at DTU Compute

Abstract

The goal of this “sprint project” is to perform a research study on how to use supply vessels to implement a seamless high-bandwidth communication link.

The Oil and Gas (O&G) industry must take advantage of all modern technologies risen with Industry 4.0, such as the Internet of Things and Industrial Internet of Things. This will enable to use efficiently Cloud Computing to better store and analyse the collected data, data that enables new applications like *Predictive Maintenance, Process Optimization* and *Remote Control* to be used on the platform. These applications and more can bring huge benefits to the O&G Industry by helping to perform all actions on the platform in an efficient way.

The “digitalization vision” is nice but even though many old platforms are connected via a communication link with each other and then with a shared fiber link to shore, still only selected data is transferred to be analysed onshore and a huge part of data is discarded. Thus, thorough data analysis and application of control algorithms are applied only to roughly 1% of collected data. To a high extent, simple cause and effect logic is incorporated in the SCADA systems offshore and relies heavily on the interaction of the control room operator.

Additionally, newer installed and highly advanced equipment e.g. centrifugal compressors are not set up to transfer all collected data to the SCADA system and the full utilization of data analytics of this equipment is not achieved. The main reason for this lays in the fact that prior to implementation through data analysis is necessary and will initially take up time, money and more importantly bed space. Especially bed space limits and/or hinders investments, upgrades, and modifications. This is also the case for the facilities of the Danish Norths Sea. Furthermore, applying IoT requires continuous monitoring of all data parameters by specialists and onshore support and as such minor delays in data transfer can be accepted. However, this should not extend into years or months as the utilization of IoT will not be valuable to the operator.

In conclusion, this project addresses the key parameter of all facilities to start utilizing the benefits of all applications presented in the "digitalization vision", by providing a solution that enables the possibility of transferring huge amount of data in a safe and reliable way, between multiple platforms and to shore. This method can be used to backup data onshore and to move it to Cloud in a timely manner. Furthermore, it can be used as a backup for the communication link when the fiber-link is down. Finally, this method offers the possibility to upload data from onshore to a certain platform.

Technology vision

As in many other industries to embrace the Industry 4.0, the digitalization vision, the infrastructure most often must be changed and updated such that will accommodate all these new applications. O&G industry is no different, in contrast, the infrastructure will need a bigger change in order to converge to this new vision because 40-year-old technology still dominates the offshore platforms. Furthermore, if we take the last 10 years as an example, this industry has already started to slowly embrace emerging new technologies to improve its production operations. However, the O&G industry have a long road ahead to achieve fully digitalization, starting by overcoming the challenges of the limitations in today's infrastructure and systems.

All the challenges of today are related to systems that are used from the beginning when the platform first started operating. In the past, the technology was not so advanced making a real challenge to design, deploy and maintain robust data connectivity. This is the reason why on such offshore rigs the fundamental telecommunications infrastructure today is extremely limited, and they were never built to support high fidelity data streams and analytics. Some of the communication approaches used today are: third party data transfer devices, hard-wires connected equipment, radio devices plus towers for a line of site communications, wireless broadband, satellite, as well as no connectivity to the central system. Additionally, all real-time decisions are based on the expertise on the problem of the engineer. This approach is neither scalable or proactive or capital efficient. Besides the telecommunications challenge, other limitations can be found in the SCADA systems that are used for control and in the asset management [1].

O&G infrastructure today

The SCADA systems have evolved in capabilities in the last years, but still, have some critical limitations that could enable O&G companies to improve data insights. Some of these limitations are: data structures are typically not optimized to handle complex statistical approaches used for recognizing and predicting tasks; it presents a relatively low fidelity of collecting and storing the data reading a data measurement every 10 minutes to an hour long; also, sometimes it cannot reach all devices due to the connectivity problems. This is because industries still implement their monitoring and control systems using the traditional method of wired control networks that make use of conventional communications protocols like 4-20 mA, Highway Addressable Remote Transducer (HART), FOUNDATION Fieldbus and PROFIBUS among others. This approach has led to a significant increase in complexity in the planning and installation stage, due to the inflexibility of the wiring and the need of accommodating future possible changes during project execution. Moreover, because the use of wired connection will limit the number of measurements (there are inaccessible areas on the platform that cable trays cannot reach), frequent layout changes such as addition/deletion or reallocation of measuring nodes, change in instrument types, etc. and maintenance of the cables will drastically impact the project time and cost. The current trend, that will provide a cost-efficient and improved solution, is to use a wireless sensor network (WSN) approach.

The asset management presents some limitations as well that will slow the advancement to IoT and analytics such like: there is a lack of integration between procurement systems and asset management systems resulting in inaccurate or outdated data being stored and analysed. Moreover, there is no communication between the maintenance processes of an equipment and the asset management system that will allow tracing all the historical interactions of a certain machine. Finally, the biggest drawback is the

use of Microsoft Excel as a tracking mechanism in the field making it hard to analyse this valuable data due to the lack of accessibility. In the end, without having an accurate asset and well profile data, it is very difficult to recognize, predict and react to issues that impact production in a correct manner. This results in increased costs, planning, and maintenance costs and more.

The situation at Maersk Oil platforms in the North Sea is not so different from what was described above. The operations technology is still old working from the 70s and 90s, but there are some improvements on how data is collected and a stable connection to the shore. First of all, all platforms are connected in some way to each other using communication cables of different bandwidths and then there is a shared fiber-link used to communicate onshore. Doing so, it gives the possibility of collecting measured data at a period of 9 seconds via SCADA systems and store it in an Onshore Historian (OH). This historian has a capacity of 4-5 TB and requires a link of 2-3 Mbit to collect what is considered important data from the platforms. With this data, an Integrated Operation Monitor (IOM) represents a full process model of the offshore rig that can at some extent predict and an Integrated Virtual Metering (IVM) representing the first attempt to use data and creating a digital twin of a well estimates. All this data is collected via SCADA making it impossible to have information from all machines because new challenges arise when trying to connect new machines to SCADA. Furthermore, the sampling rate is not enough to perform more complex analysis like vibrations test for example. In this case, the frequency of collecting data should be at the level of milliseconds, hence making the current bandwidth and the OH obsolete. Regarding maintenance strategies, currently in the industry RM and PM are used.

O&G infrastructure in the future

However, if the O&G industry will decide to embrace the "digitalization vision" the benefits will be tremendous, both from the perspective of costs savings and from operations efficiency. By investing in digital trends such as Big Data and Analytics, IoT, Cloud, Mobile device, Artificial Intelligence and so on, new application can be applied to offshore rigs like Predictive Maintenance that will reduce the unplanned shutdowns and prevent doing unnecessary maintenance by predicting when an equipment will fail; Operation optimization that will improve the extraction of oil and Remote Operations Centre giving the possibility to explore parts of the world where the working environment is too harsh for humans. All of these applications and more can improve the safety and health of workers, can extend the life of a platform and at the same time making the oil extraction more efficient [2]. An example can be seen in Figure 1:

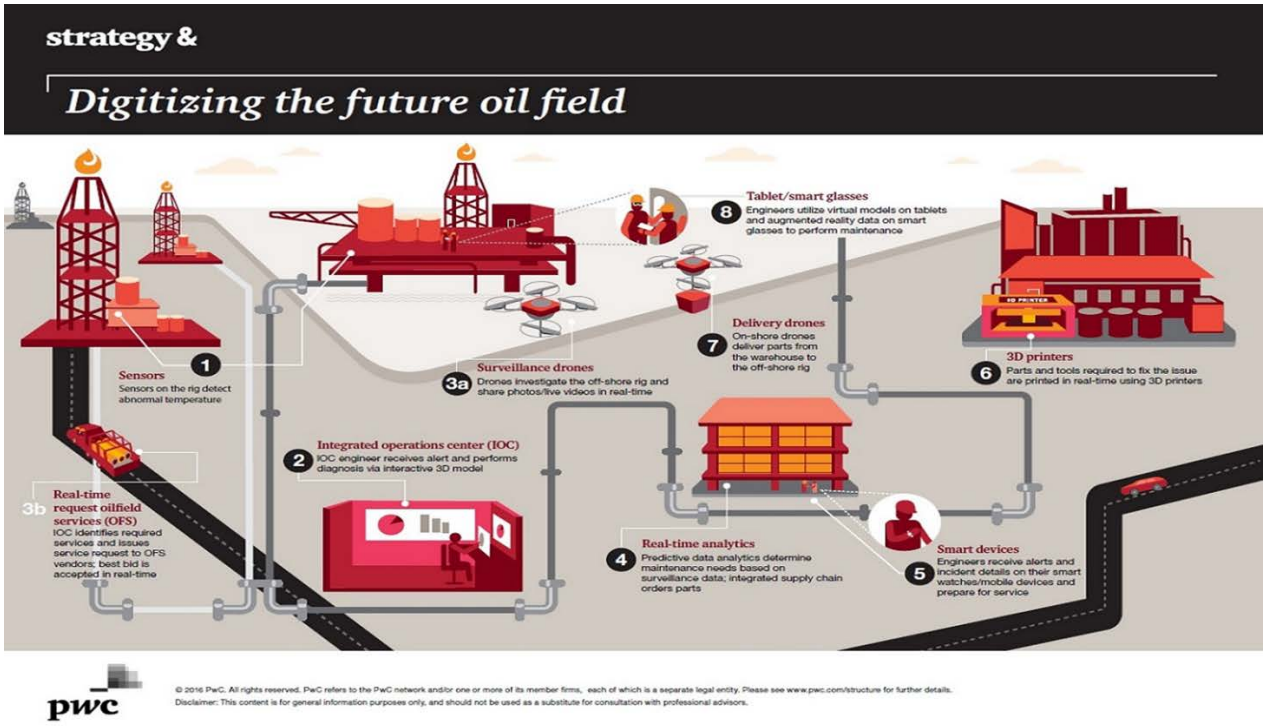

Figure 1: The future of Oil and Gas Industry [7].

These applications are based on data collection. Thus, the first limitation the O&G must conquer is using a WSN that will offer the possibility to collect data from hard spots to reach and be more cost efficient compared with a more traditional wired communication, for maintenance purposes. The wireless technology used in WSN is one of the most demanded technologies in the industry today and guarantees to provide the same maintenance and control services or even better compared to the wired solution [3]. Some advantages introduced by such a network are: the increased complexity, cost, and maintenance related to the wired counterpart are eliminated and extends the capability of measuring inaccessible areas. However, concerns about security, reliability, safety, and integrity have caused great delay in adoption of this strategy. The main reason behind this is the maturity of such a network and the absence of an open standard that meets the requirements of the industry. Today, there are two open standards suitable for industrial automation on the market: IEC 62591 which is based on WirelessHART and IEC 62734 which is using ISA100.11a, both very similar in terms of specifications. Although, one of them is more suitable, and this is WirelessHART. WirelessHART is the first complete interoperable and open WSN standard designed for process measurement and control application is WirelessHART [4]. WirelessHART is a WSN technology based on HART industrial protocol maintaining its simplicity and robustness. Moreover, it offers backward compatibility, meaning that it will offer the possibility of transparent adaptation of HART compatible control systems and configuration tools to integrate new wireless networks and their devices, as well as use of proven configuration and system-integration work practices [5]. Hence, making easier and cheaper to use HART technologies, which already is one of the most popular industrial protocols today according to Emerson [6]. Furthermore, it is a true mesh topology structure ensuring an increased reliability of 99.999%, keeping at the same time data secure [3].

WirelessHART has a wide variety of applications in all process industries, and even though it was created for control purposes also, the standard is limited today to monitoring application only such as process monitoring and measurements, equipment health monitoring, environmental monitoring, energy management, asset management, diagnostics and predictive maintenance.

ShipNet

The digitalization vision will require, as I mentioned above, a big change on how things are performed at the moment by using future applications to make more efficient the process of extracting oil and gas. Moreover, adopting these applications will require to change or upgrade the current communication infrastructure of offshore rigs because everything is focused on how the data is collected and the correctness of it. Of course, it will become very costly to change the entire communication infrastructure of an old platform. This is why it is imperative to find a solution that will be cost-effective, and it will help do this upgrade in an efficient way by using also the existing equipment.

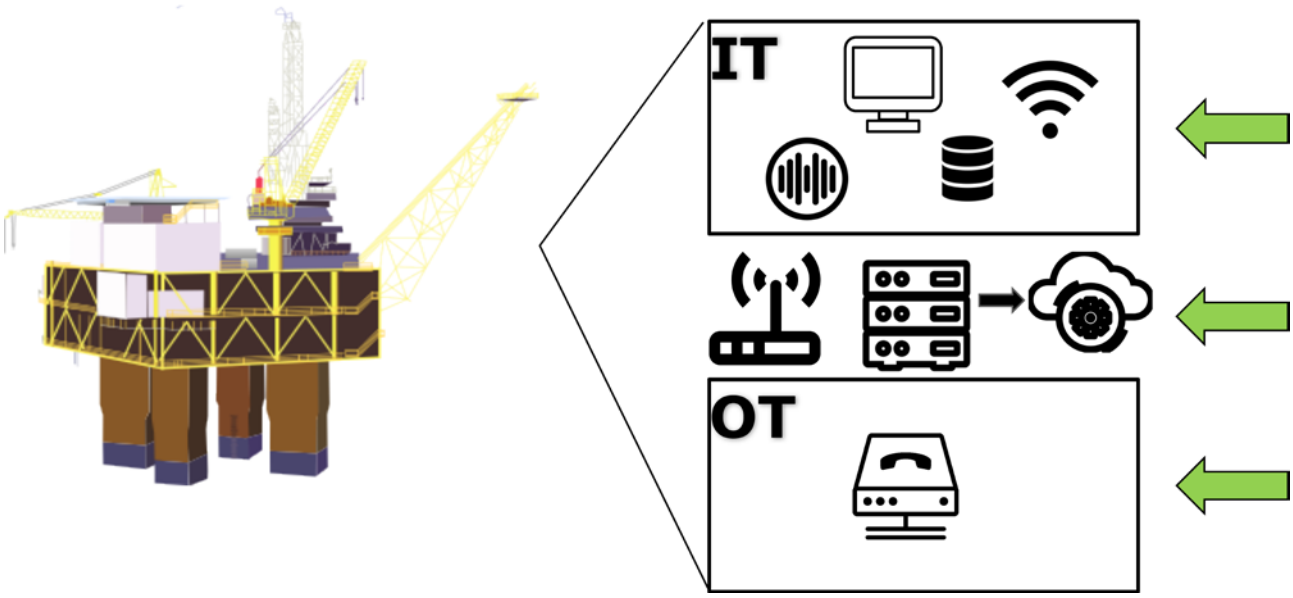

Figure 1: Infrastructure required for new use cases

An example of such a scenario can be viewed in Figure 1 where we desire to apply three new application to our offshore rig. These three applications are robotics, predictive maintenance, and structural health monitoring. In order to be able to use them we will need special equipment such like: a database to store some collected data on site and process it for real-time decisions and then it will be moved to Cloud for further analysis; a new WSN to collect data in a more cost-efficient way and also from hard to reach zones; a gateway; sensors and a docking pad for the drones among others. Some of these already exist on a platform and some don't, therefore a proper analysis prior to deployment of such projects is required.

Data availability is at the centre of Industry 4.0 being an enabler to all future applications. Hence, to be able to collect vast amounts of data correctly and send them to Cloud to be further analysed it is a very important aspect of the whole digitalization idea. However, today the current communication infrastructure cannot handle to transport such vast amount of data to shore on a daily basis because even

though there is a shared fiber link connecting the platforms to shore the generated data on a day from a single platform can surpass the amount of 2 TB. At this rate, the current communication infrastructure is becoming obsolete. Hence, new solutions must be found to move this huge amount of data to shore for further analysis.

ShipNet is such a solution for the purpose of transporting in a reliable and efficient way a vast amount of data onshore for future analysis by using the vessels. The idea is presented in the next Figure 2:

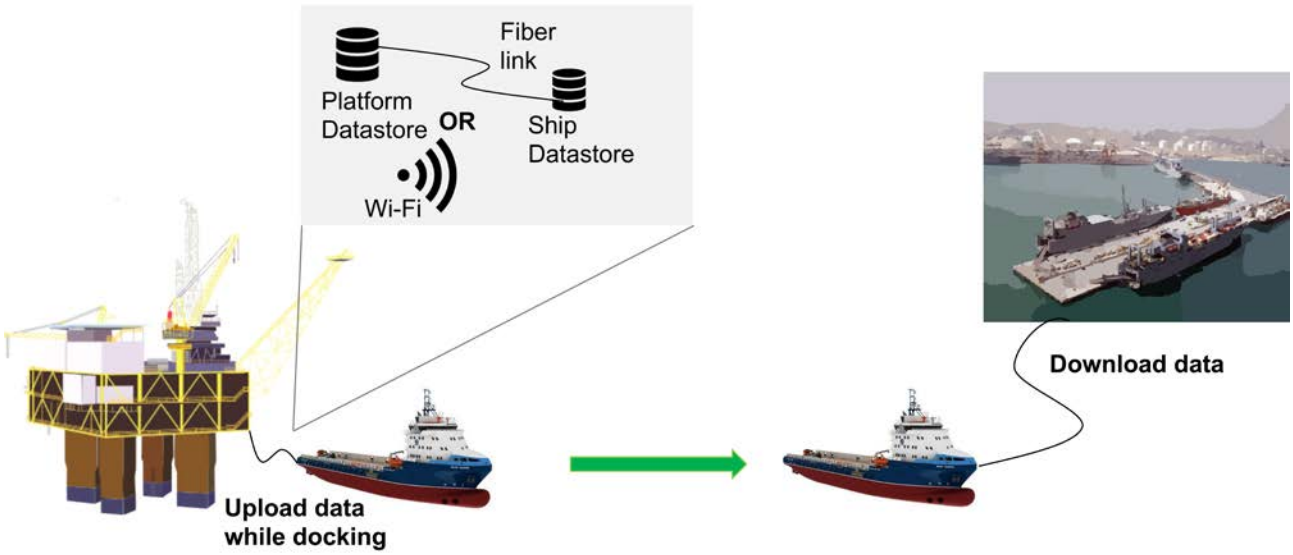

Figure 2: ShipNet solution

This transfer of data can be realized in multiple ways: one solution could consist of making an engineer taking out the hard drives from the local database on the platform and move them to the ship. This method is fast enough, and it could be used also with the helicopter. But it is highly dependent on how much data is stored and transferred. A second solution can be to use a wireless data transfer that will start downloading data to the ship from the minute it docked. This had the advantage that it requires no interaction with the staff, but it could be more time-consuming. A third solution is to take a fiber link cable from the ship and connected directly to the servers on the platform. Furthermore, there could be a solution where you transfer automatically data when two vessels pass by each other.

In it important to specify that ShipNet can be used for backup purposes as well, both for storing all data to shore and as a backup solution in case that the shared fiber link connection is down. Also, this can be applied to both old and new platform and can be used at some point to upload data to the platforms. Furthermore, it is easy to maintain or repair the technology because half of it will be on the ship, making it more accessible and giving the possibility of doing the repairs onshore and the other half can be repaired while the ship is docking by an engineer. Also, this is true when the technology is installed.

Validation of technology

Big companies onshore face the same problem of moving their stored data from a local server to the Cloud in a reasonable amount of time. This is a problem even for the very advanced internet connections. Hence, big Cloud providers like Amazon, Google and Microsoft considered other possibilities to solve this problem and came up with a solution that will enable such companies to transfer data to the Cloud offline. For example, Amazon has proposed two solutions: the first solution is called Snowball which is a box full of hard drives that is shipped via mail to the client and after the download is done the box is shipped back to an Amazon data centre where the data is uploaded to the Cloud [8]. A second solution proposed to consist of using an actual truck that will be driven to the client, connect to its database, download the data and then drive it back to Amazon [9]. Also, Microsoft and Google have accepted normal hard drives shipped by the client with its data to be uploaded to Cloud. Furthermore, Google has a new solution like Amazon's Snowball that is currently in beta [10].

Moreover, a more appropriate example of such a solution that is working in the same remote and harsh environment as Oil and Gas industry is coming from the Mining Industry [11]. In this case, in order to perform vibration monitoring of an electric shovel, data was stored locally and at a scheduled time a pickup truck will park nearby and via wireless, the data will be stored on it. Then the truck will go and make available the data for analysis on a more suitable location.

Validated during sprint

During the “sprint project” we validated our idea by conducting meeting with Maersk Oil to understand the current infrastructure of an offshore platform, see if there is any value in this approach and if there is a place for this technology in the North Sea. Alongside these meeting, we performed a research on the subject to see what solutions were proposed in other industries and digitalization in O&G.

Once the infrastructure was understood and that the data is at the centre of future applications that needs to be applied to platforms in the future, we concluded there is value in our approach. So, we discussed how the technology could be implemented.

Proposed way forward

The next step will be to validate this on a real case, by choose one of the methods and collect some data from a platform. Once this is done, more test will be conducted with the solutions that were identified during this project. In the end, comparing the results and applying the best one.

Final conclusion

In conclusion, this is a solution that offers the possibility to move huge amounts of collected data to Cloud without having to online, connected at all times. It is a good approach for collecting data but not for real-time processing due to the delay introduced by the vessels. Therefore, for real-time purposes it is advised to use the shared fiber link connection already available or to have an edge computing locally that will process this data and make decisions based on it in real time.

References

[1] I. I. Consortium, *Beyond digitization: The convergence of big data, analytics and intelligent systems in oil gas*, October 2015.

[2] A. World Economic Forum, *Digital transformation initiative oil and gas industry*, January 2017.

[3] Sabo M. Hassan et. all., *Application of wireless technology for control: A WirelessHART perspective*. IEEE International Symposium on Robotics and Intelligent Sensors, IRIS 2016, December 2016.

[4] Song, J., Han, S., Mok, A., Chen, D., Lucas, M., Nixon, M., et all., *WirelessHART: Applying wireless technology in real-time industrial process control*, Real-Time and Embedded Technology and Applications Symposium, RTAS'08, 2008.

[5] Wikipedia. WirelessHART. https://en.wikipedia.org/wiki/WirelessHART , June 2017.

[6] Emerson, *Emerson proves advancements in eddl (electronic device description language) technology*, https://goo.gl/uq9i1D .

[7] N. Clark, A. Abraham, *Improving oil and gas efficiency through digital*, https://goo.gl/agbzxA , 2016.

[8] Jeff Barr, AWS Import/Export Snowball – Transfer 1 Petabyte Per Week Using Amazon-Owned Storage Appliances, https://goo.gl/CaUHjf , 2015.

[9] Amazon, *AWS Snowmobile*, https://goo.gl/6uv3jN .

[10] Google, *Google Transfer Appliance,* https://goo.gl/X54q7B .

[11] Dan Nower, *Online Vibration Monitoring on Electric Mining Shovels*, MaintWorld, May, 2013.

Use of Tracers in Oilfield Scale Squeeze Treatments to Estimate Placement

Oscar Vazquez, Heriot Watt University

Abstract

Oilfield scale is common name for the solid deposits formed by the precipitation of inorganic mineral scale in producing wells, being one of the biggest production challenges of the oil and gas industry. One of the most common techniques to prevent mineral scale deposition is squeeze treatments, which involves the injection of scale inhibitor chemical slug in producer wells under risk of scale deposition. Squeeze treatments normally consists of the following stages: a pre-flush to condition the rock formation, main treatment where the main chemical slug is injected, an overflush to push the chemical slug deeper into the formation and a shut-in stage to allow the chemical to adsorb on the rock formation. Then the well is put back in production and the scale inhibitor chemical will be slowly released into the produced brine. The well will be protected, i.e. the chemical will prevent scale deposition, if the scale inhibitor chemical concentration is above a certain threshold concentration, commonly known as Minimum Inhibitor Concentration (MIC), normally between 1 and 20ppm.

Placement is critical for the effectiveness of squeeze treatments, there might be situations where although the concentration of scale inhibitor back produced is above the MIC, evidences of scale precipitation are found, such as reduction of production or evidence of scale deposition. This may be due to the fact that there might be sections of the well that remained unprotected, such as in long horizontal wells, where might be difficult to reach the toe of the well. Normally, in order to evaluate any placement issues, a PLT (Production Logging Tool) is used to provide a pressure log (or injection/production flow rate log), although it can be prohibitively expensive. A much cheaper alternative involves the injection of a tracer slug and then produced at different rates until all the tracer is back produced. In normal circumstances, it is expected to be fully produced back in less than 48 hours. The resulting tracer return concentration profile will have particular features that can be used to estimate chemical placement, (Vazquez, Mackay, et al. 2014).

The objective of this research project is to identify a fit for purpose tracer that could be deployed as part of a squeeze treatment, in particular in the overflush stage. One advantage of this approach will be that there is no significant increase in the operational expense (OPEX); the only additional expense will be the cost of the tracer and subsequent analysis. It is envisaged that the cost will be less than 5% of the total squeeze treatment cost.

Technology vision

Including a tracer program in the squeeze treatment design has never been proposed; the closest study in the literature involved the injection of a KCl (Sodium Chloride) slug to determine the layer flow-rate profile along a producer well in the Norne field (Vazquez, Mackay, et al. 2014). KCl was deployed because it is a common tracer and known to be compatible with inhibitor chemical species. Although the study was

successful, the chemical slug was not part of the squeeze treatment, and the use of KCl required futher interpretation. The potassium concentration was used to determine the tracer return concentration profile, where the background concentration had to be removed.

This technology is innovative in two aspects: a) including a fit for purpose artificial tracer with low presence in the formation brines to avoid further interpretation, and b) demonstrating that including the tracer into squeeze treatments will not hinder the performance of scale inhibitor chemicals. In addition, it has the potential to revolutionise how squeeze treatments are designed. Including a tracer program will provide invaluable information to monitor and evaluate the placement of scale inhibitors during a squeeze treatment, thereby avoiding expensive production logging. As a result squeeze treatments designs could be optimised to maintain oil and gas production free of setbacks, where potentially significant cutting cost can be achieved. Finally, adding the tracer slug in the squeeze treatment is estimated to add less than 5% of the total squeeze treatment cost.

How the technology addresses zonal contribution

To calculate the zonal flow contribution, or in other words where along the completion interval the chemical will be placed at the injection stage. For example, in long horizontal wells, if the chemical slug is bull-headed, there is a degree of uncertainty if the toe of the well is reachable. If all the contributing zones of the well are protected the squeeze treatment will be successful, the well will be protected and the production flow will be maintained. If the toe of the well is unreachable at injection, the tracer return profile will be characteristically different. Assuming that the toe of the well is not reachable, but flows at production. The tracer return concentration will be lower than the injected concentration, and secondly to fully deplete the tracer from the reservoir will take significant longer time, see Figure 1.

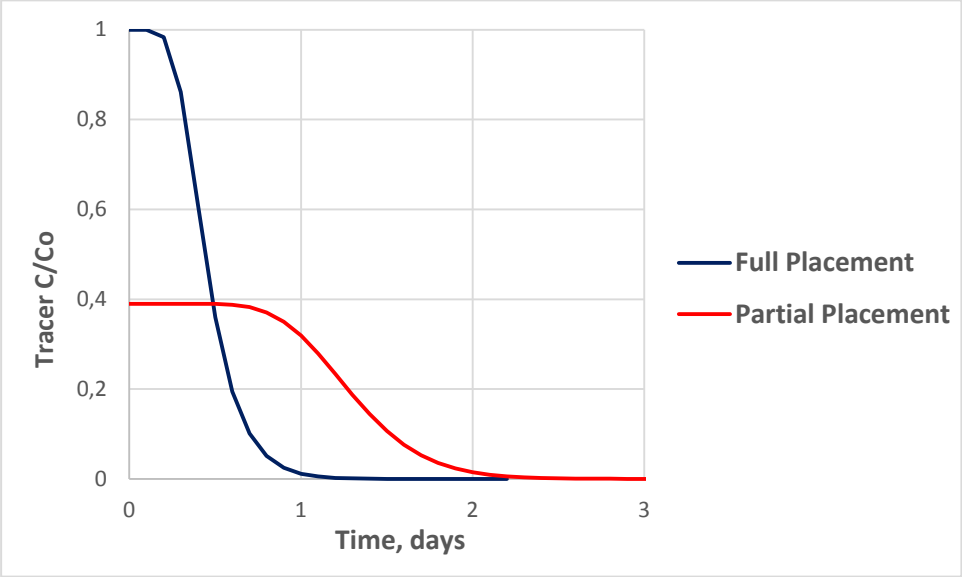

Figure 25 Return Tracer profile in a long horizontal well, assuming reaching the toe of the well (Full Placement) and not (Partial Placement).

How the technology will be implemented in oil and gas production in the North Sea

The tracer slug is recommended to be injected during the overflush stage, due to a number of reasons. First, the tracer should be sequentially injected and then produced, so the desired features in the return

concentration profile can be as clear as possible. If the tracer was injected before the treatment, the tracer will be transported deep in the reservoir, where the tracer will be naturally dispersed, and the desired features might not be clearly identifiable. Secondly, although a buffer between the tracer and the scale inhibitor chemical is not strictly necessary, it is preferable to avoid any unexpected incompatibilities with the scale inhibitor or other chemicals part of the squeeze treatment.

In operational terms, the technique is not significant different from a squeeze treatment, so it is expected that the crew responsible for the squeeze treatment will find adding the tracer not very disruptive. In addition, adding other additives in squeeze treatments is relatively common. The main obvious difference is the sampling regime after the well is back in production, which is necessary to be at higher frequency than in conventional squeeze treatments

Which tracer is the most suitable?

Tracers have been commonly used in the oil industry for the last 50 years, they can be classified as artificial and natural tracers (Zemel 1995; C. Serres-Piole et al. 2012; Huseby et al. 2010). Radioactive tracers were actively used over the past years, combined with logging tools. However, due to strict regulations and advances in chemical technology, are gradually substituted by chemical ones (Agenet, Moradi-Tehrani, and Tillement 2013; Brichart et al., n.d.; Sanni et al. 2015). They can also be further classified as passive or partitioning. Passive tracers do not interact with the system fluids and just follow the path of the injection. Active tracers on the other hand, are mostly used for the estimation of residual oil saturation and are a useful tool in the design of EOR methods (Huseby et al. 2015; Deans 1971). Passive tracers can be further classified as natural and artificial tracers. Natural tracers have been used to evaluate inter-well communication between injectors and producers and a source of information for reservoir characterisation and a valuable tool when trying to optimise reservoir simulation models (Huseby et al. 2008, 2005; Vazquez et al. 2015; Vazquez, Young, et al. 2014) and to evaluate and optimize scale squeeze treatments in the Norne Field (Vazquez, Mackay, et al. 2014).

There are great variety of artificial chemical tracers, (C. Serres-Piole et al. 2012), among them fluorinated benzoic acids (FBAs) that were developed in 1990's are commonly used for hydrothermal, geothermal and oilfield applications(Huseby et al. 2010; Meza et al. 2007; Pritchett et al. 2003; Seccombe et al. 2010)., they are highly soluble in water, they are characterised by high thermal stability (250-300^{o}C), low presence in formation brines and low level of detectability, as low as ppb (parts per billion (Mike C Adams et al. 2004; Michael C. Adams et al. 1992). These desirable characteristics make FBAs a very promising candidate.

Analysis of Tracer effluent

A number of analytical methods with level of detection as low as ppb (parts per billion) has been reported. This is a clear advantage for field applications as the mass of tracer required is in the order of kilograms to achieve few ppm, well above the detection level. Since the tracer is recommended to be deployed in the overflush, and based on the fact that the volume of tracer is minimal, the impact in terms of operations and logistics is almost negligible. The main difference is the sample frequency, in particular, at the beginning of production. Although, typically in squeeze treatments this is not critical, for the personnel responsible for the collection of samples, it should not imply a major impact on their normal working routines. The only difference is the frequency of sampling, which is envisaged to be between 30 and 60 mins for the first 24 to 48 hours after the well is back in production.

Analysis of 4-FBA by UV

The tracer 4-FBA (4-fluorobenzoic acid) is detectable by UV, at wavelength of 230nm which shows a peak of high UV absorbance in seawater, see Figure 2, and the corresponding calibration in Figure 3.

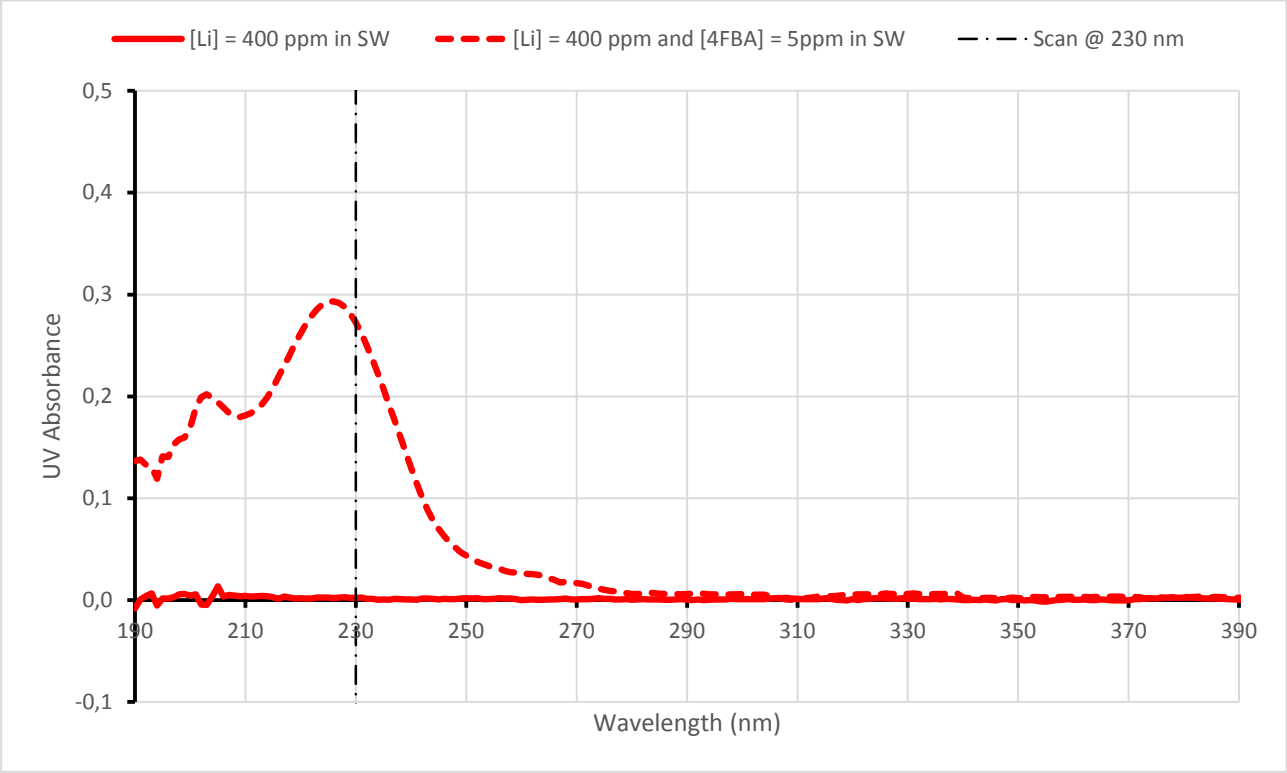

Figure 26 Multi-Wavelength Scans for 400 ppm Li in SW with and without 5 ppm 4-FBA.

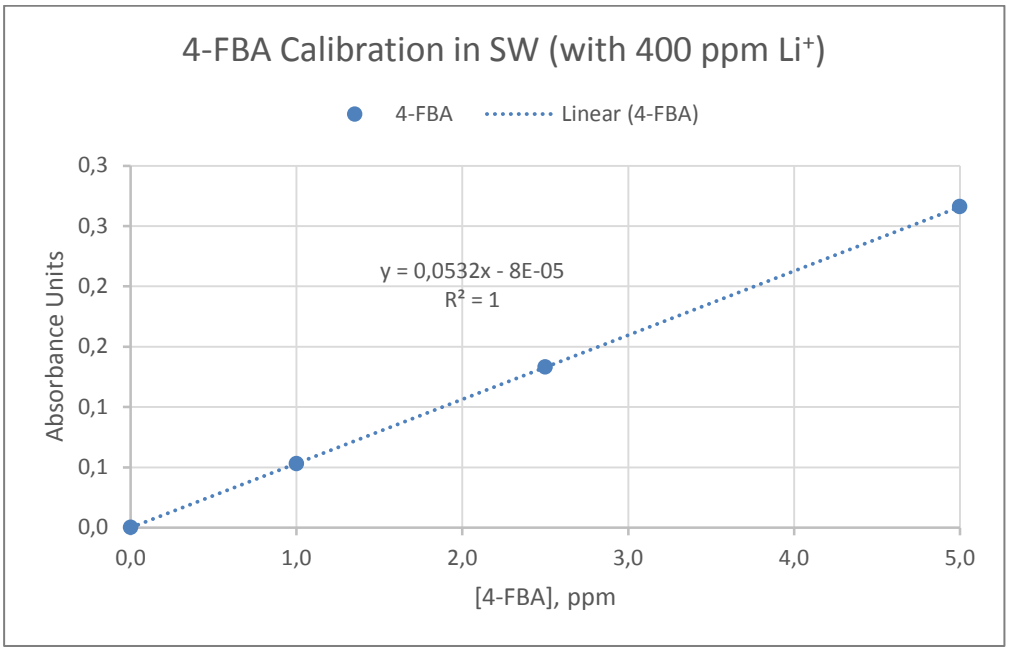

Figure 27 4-FBA UV calibration in SW with 400ppm Li.

Environmental rating of artificial tracers

15 artificial tracers were under study, among these 2-FBA has the best Norway/Denmark environmental rating, yellow chemical, as can be seeing in Table 1. The Red coding is as a consequence of low biogradation.

Tracer	Chemical name	Environmental coding – Norway	Environmental coding – UK
2-FBA	2-fluorobenzoic acid	Yellow	HQ Band Gold
4-FBA	4-fluorobenzoic acid	Red	HQ Band Gold
2,6-DFBA	2,6-difluorobenzoic acid	Red	HQ Band Gold
2,4,5-TFBA	2,4,5-trifluorobenzoic acid	Red	HQ Band Gold
IFE-WT-1	Proprietary	Red	HQ Band Gold
IFE-WT-5	Proprietary	Red	HQ Band Gold
IFE-WT-7	Proprietary	Red	HQ Band Gold
IFE-WT-8	Proprietary	Red	HQ Band Gold
IFE-WT-10	Proprietary	Red	HQ Band Gold
IFE-WT-11	Proprietary	Red	HQ Band Gold
IFE-WT-16	Proprietary	Red	HQ Band Gold
IFE-WT-42	Proprietary	Red	HQ Band Gold
IFE-WT-44	Proprietary	Red	HQ Band Gold

Table 8 UK and Norway environmental coding.

Validation of technology

The technology has been validated performing two type of experiments, in one hand, static experiments, designed to validate the suitability of the FBA's tracers for squeeze treatments. Static test are further categorised as compatibility and efficiency. Secondly, dynamic tests designed to evaluate how these chemical behave as inert tracers.

Static experiments

The static experiments focused on assessing the compatibility of a number of tracers with DETPMP and PPCA, two of the most common scale inhibitors used in the North Sea, and the effect on scale inhibition efficiency in the presence of tracer. The experiments mimic what would happen if tracer mixes with the scale inhibitor chemical at injection or production. Although this is unlikely to occur, rationale behind was

to represent the conditions if mixing occurred. Two different type of experiments were performed, the first focus on the compatibility and the second on the efficiency in the presence of tracer.

To mimic the possible scenarios for injection and production, North Sea Seawater and Nelson Forties Formation Water was used, see Table 2. A number of combination of scale inhibitor concentration and pH was considered to mimic a number of possible situations. At injection stage, in the main treatment stage the concentration of chemical is high and the pH is low, to prevent the dissociation of the acids and so preventing early precipitation. At production, if there was any mixing between the tracer slug (injected in the overflush stage) and the main treatment, the concentration of chemical will be lower and the pH closer to neutral.

	NSSW	**NFFW**
Na^{+}	10,890.0	31,275.0
Ca^{2+}	428.0	2,000.0
Mg^{2+}	1,368.0	739.0
K^{+}	460.0	654.0
$SO4^{2-}$	10,890.0	269.0
Li^{+}	50.0	771.0
Cl^{-}	20,029.3	50.0

Table 9 NSSW and NFSW compositions.

Table 2 shows the combination of pH and scale inhibitor concentrations for the incompatibility experiments for DETPMP, in all the experiments the concentration of tracer was 5ppm. The results for the incompatibility tests are shown in Table 3, where only at pH close to neutral, there seems to be some incompatibility. The precipitation is thought not to be a consequence of adding the tracer, but to the fact that the experiment conditions are close to supersaturation of the complex Ca_DETPMP (Sorbie et al. 1993), in particular at neutral pH and high temperature, conditions at which the polyacid will be deprotonated and likely to be bound to free cations, such as calcium or magnesium.

Bottle No.	**[SI], ppm**	**Matrix**	**pH**
3	100,000	NSSW	3
4	100,000		3
5	50,000		3
6	50,000		3
7	10,000		3
8	10,000		3
11	25,000	NFFW	5
12	25,000		5
13	5,000		5
14	5,000		5

Table 10 Compatibility test for DETPMP and tracers at 5ppm.

Bottle No.	No Tracer RT	Tracer RT	pH Adjustment (Target = 3.00)	Tracer 95°C	pH Adjustment (Target = 5.00)
3	N	N	2.96	N	5.50
4	N	N	2.99	N	5.55
5	N	N	3.03	N	5.49
6	N	N	3.01	N	5.47
7	N	N	3.04	Y	5.53
8	N	N	2.99	Y	5.54
11	N	N	3.04	Y	5.54
12	N	N	3.02	Y	5.49
13	N	N	3.01	Y	5.49
14	N	N	3.00	Y	5.51

Table 11 Incompatibility experiments results for DETPMP and tracers at 5ppm.

Table 4 shows the combination of pH and scale inhibitor concentrations for the incompatibility experiments for PPCA, in all the experiments the concentration of tracer was 5ppm. The results for the incompatibility tests are shown in Table 5, where only at pH close to neutral there is some incompatibility. The precipitation is thought not as a consequence of adding the tracer, but to the fact that the experiment conditions are close to supersaturation of the complex Ca_PPCA (Farooqui 2015). At high pH and temperature PPCA will be deprotonated and likely to be bound to free cations such as calcium or magnesium.

Bottle No.	[SI], ppm	Matrix	pH
3	50,000	NSSW	3
4	50,000		3
5	10,000		3
6	10,000		3
7	5,000		3
8	5,000		3
11	1,000	NFFW	5
12	1,000		5
13	500		5
14	500		5

Table 12 Compatibility test for PPCA and tracers at 5ppm.

Bottle No.	No Tracer RT	Tracer RT	pH Adjustment (Target = 3.00)	Tracer 40°C	pH Adjustment (Target = 5.00)
3	N	N	2.95	N	5.54
4	N	N	2.97	N	5.53
5	N	N	3.00	N	5.51
6	N	N	2.96	N	5.52
7	N	N	2.95	N	5.53
8	N	N	2.95	N	5.49
11	N	N	2.98	Y	5.54
12	N	N	2.97	Y	5.51
13	N	N	2.95	Y	5.52
14	N	N	3.05	Y	5.51

Table 13 Incompatibility experiments results for PPCA and tracers at 5ppm.

The efficiency of DETMP and PPCA inhibiting $BaSO_4$ was evaluated by evaluating the level of barium left in solution in supersaturated solution, with and without the presence of 5ppm tracer concentration. To estimate the efficiency a solution of 60% NSSW and 40% NFFW was prepared, where the final solution is supersaturated against $BaSO_4$. The concentration of barium remaining in solution was measure at 2 and 24 hours at pH 5.5 and 95°C. The concentration of scale inhibitor was close to the MIC at these conditions, around 20ppm for DETPMP, for PPCA two concentrations were considered 15 and 150 ppm, due to the fact that PPCA inhibition depends on the molecular weight distribution, (Farooqui 2015), therefore to guaranty efficiency at 22 hours the concentration should be around 150ppm. Figure 4 shows the inhibition efficiency for DETPMP and Figure 5 for PPCA, as expected the presence tracer did not seem to have a negative effect on the scale inhibition efficiency.

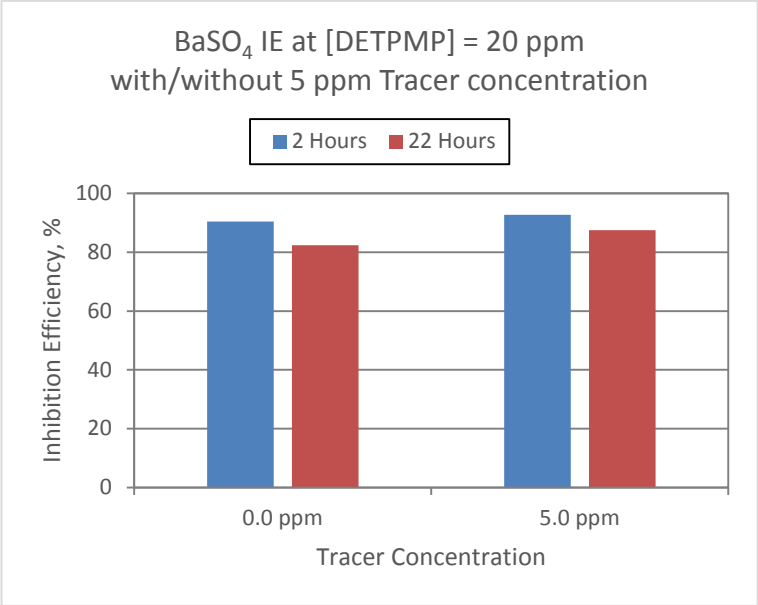

Figure 28 DETPMP scale inhibition efficiency with and without tracer concentration.

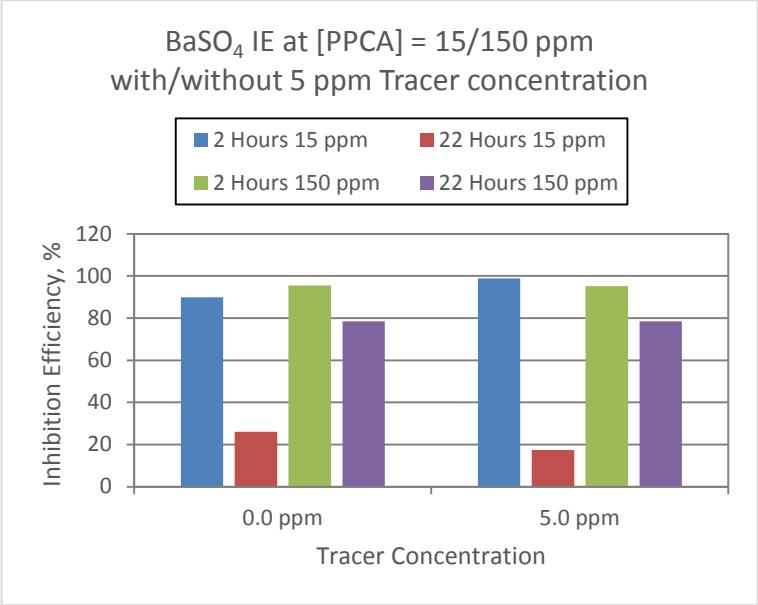

Figure 29 PPCA scale inhibition efficiency with and without tracer concentration.

Dynamic experiments

Dynamic experiments were focused on evaluating FBA as inert tracers. The experiments involved the characterisation of two pack columns, one packed with sandstone and the other with calcite, to have a broader representation of the type of reservoir found in the North Sea. Carbonate reservoirs are significantly more reactive than sandstone. All the pack flood experiments were carried out in NSSW at pH 5.5.

The characterisation of column packs or core consist in injecting an inert tracer, in lab conditions, normally iodide or lithium, which are known to be inert and easy to detect. The characterisation implies the estimation of the pore volume, which is equivalent to the effective porosity. The technique involves the injection of a tracer until the pack is fully saturated, i.e. the concentration at the effluent is the same than the inlet, followed by a postflush stage at zero tracer concentration. Essentially, two stages tracer in and tracer out. The goal is to compare FBAs tracers against conventional inert tracer.

Figure 6 shows the results for the sandstone pack flood experiment, the results show the injection and subsequent postflush for one of tracers 4FBA (4 Fluorinated Benzoic Acid), which is UV detectable at ppm level, (for lower detection levels other techniques are available). From the results, it is concluded that 4FBA behaves as inert tracer.

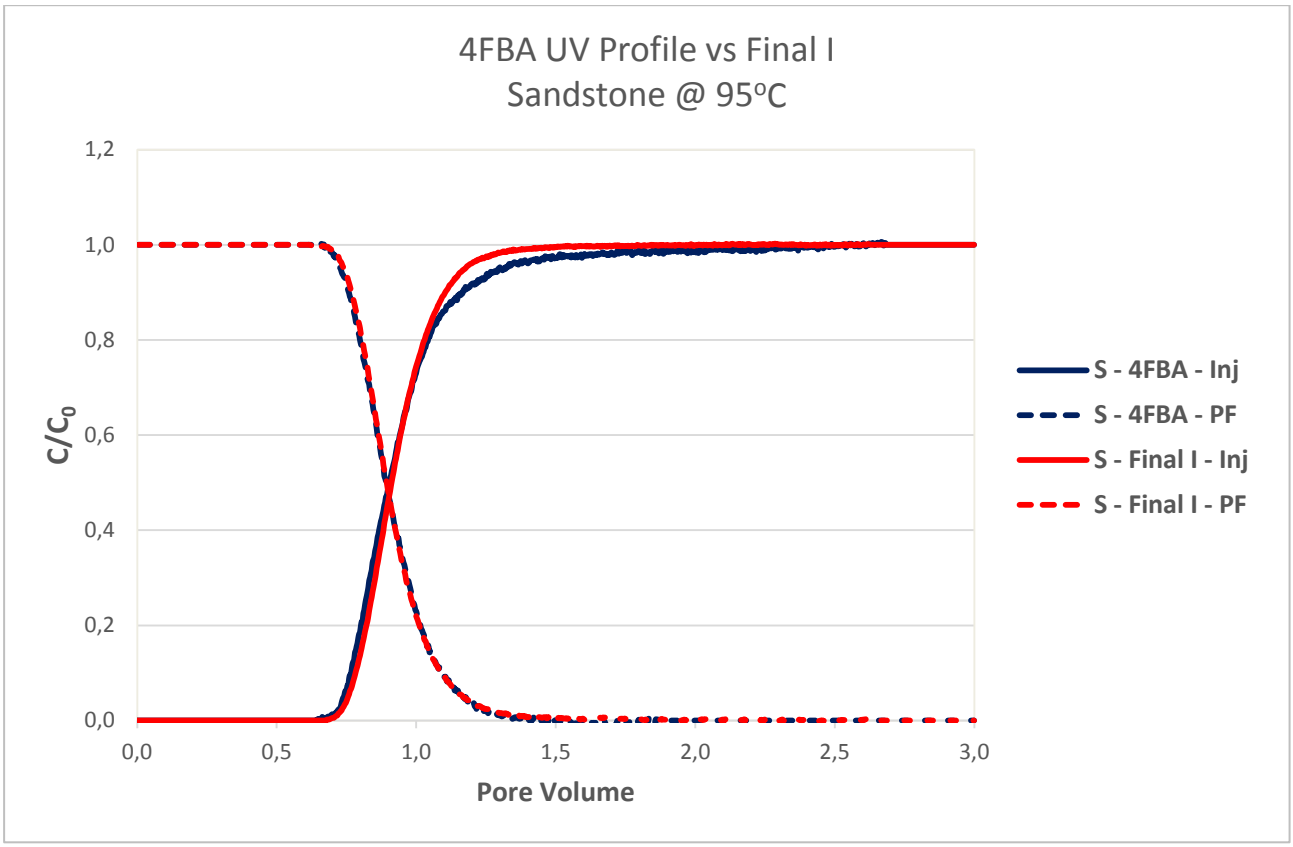

Figure 30 Sandstone pack injecting 4FBA detected by UV versus Iodide at 95°C.

Figure 7 shows the results for the carbonate pack flood experiment, the results show the injection and subsequent postflush for one of tracers 4FBA. Although the flood was performed injecting NSSW at pH 5.5, due to dissolution of calcite, a significant void visible in the pack was observed. As a consequence the porosity change, and so the tracer effluents. Despite the dissolution, both tracers' profiles, i.e. 4FBA tracer and Lithium, are very close. The offset is due to the fact that UV reading is recorded at different location than the lithium samples.

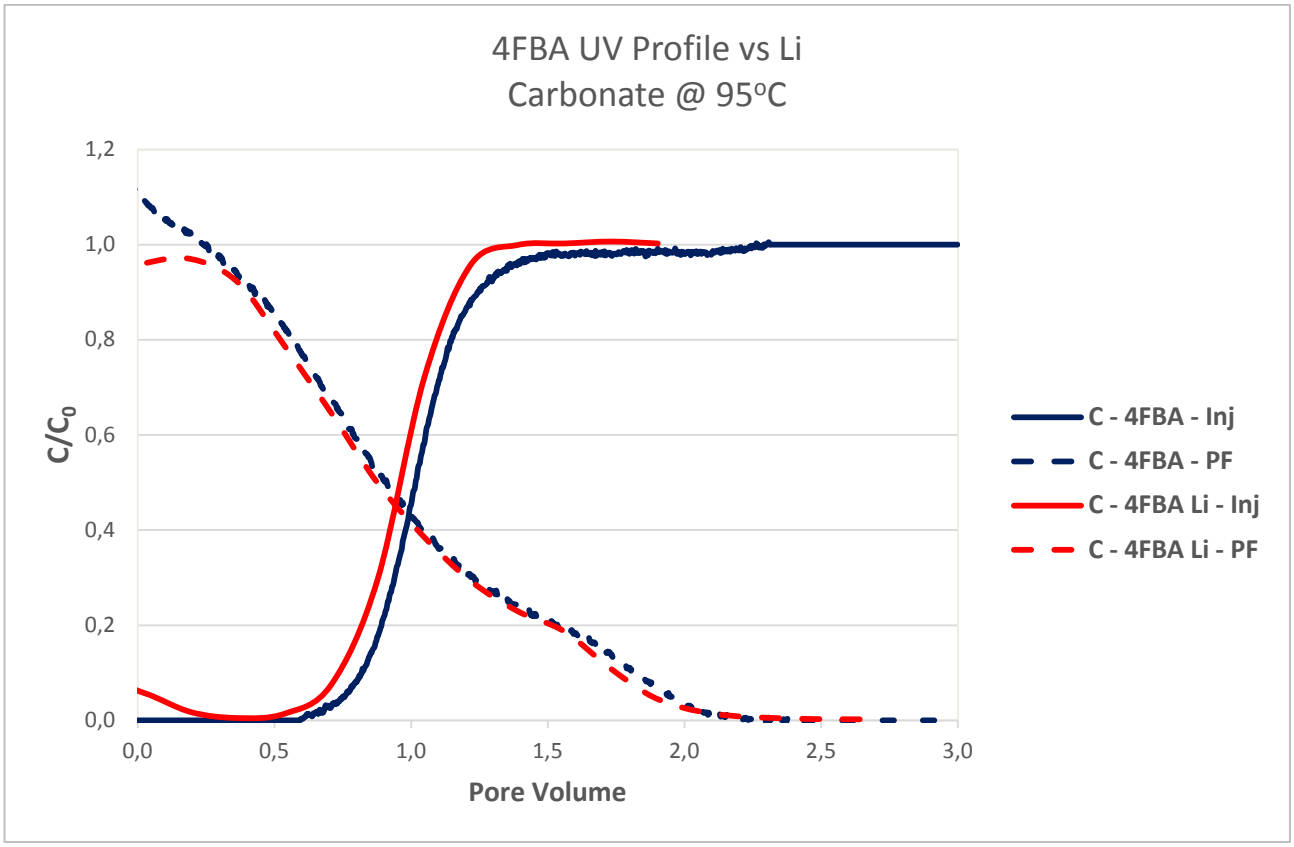

Figure 31 Carbonate pack injecting 4FBA detected by UV versus Lithium at 95°C.

The other tracers under study showed a similar behaviour to 4-FBA in sandstone pack (Figure 8) and carbonate (Figure 9). The large variance of 2-FBA as tracer (Yellow chemical), when compared to the Lithium profile, is believed to be caused by the interference by another compound in the matrix, 2-FBA was blended with other tracers. However, 2-FBA is expected to have a similar behaviour as 4-FBA and detectability using UV.

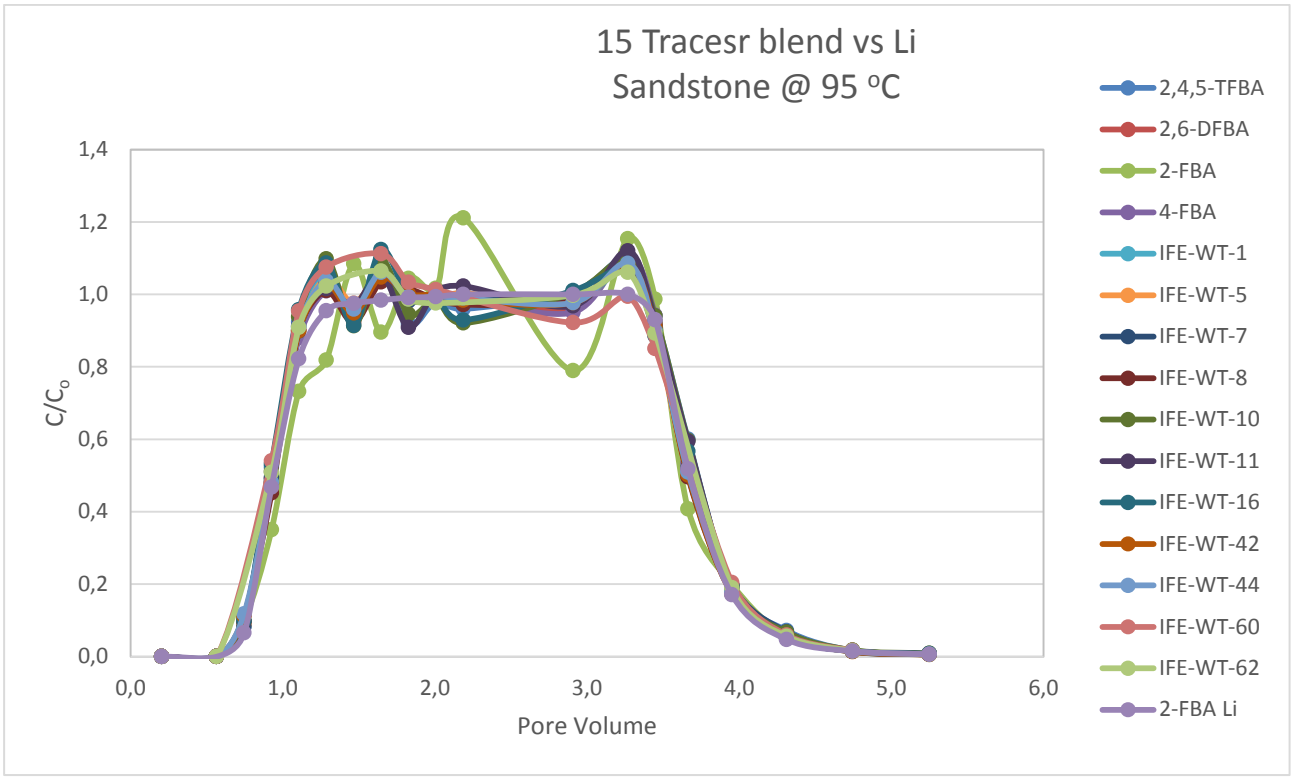

Figure 32 Sandstone pack injecting 15 tracers blend versus Lithium (2-FBA Li) at 95°C.

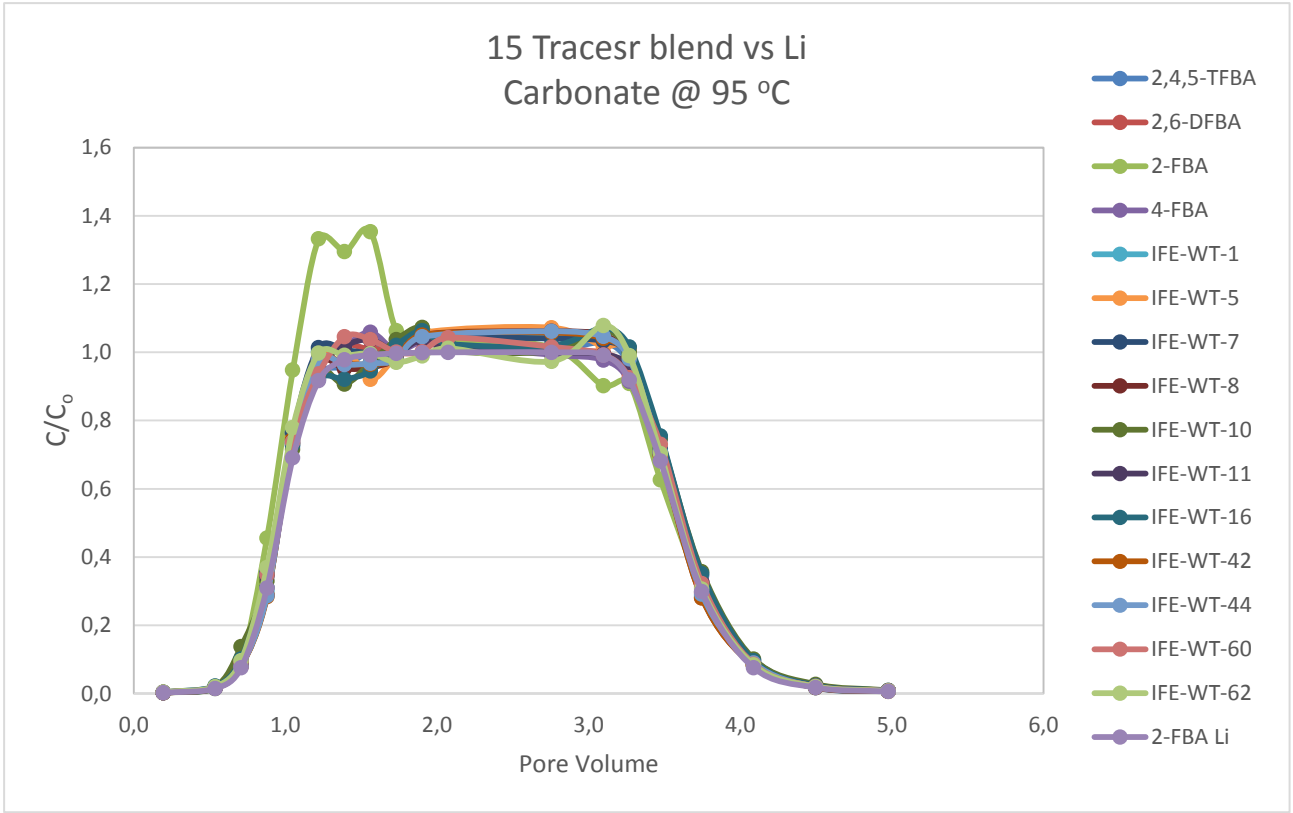

Figure 33 Carbonate pack injecting 15 tracers blend versus Lithium (2-FBA Li) at 95°C.

Validated during sprint

Which part of the technology has been validated?

During this project, the inclusion of a fit for purpose artificial tracer in oilfield scale squeeze treatments was validated. The artificial tracers selected are fluorinated benzoic acids, which are referred as FBAs. They have been commonly used in oilfield applications since the 1990s. They thermally stable up to 175^{o}C and detectable at ppb (parts per billion) concentration levels, and finally, the presence of FBAs in oil reservoirs is very low. In conclusion, all these characteristics make the FBA tracers as a very good option as an inert tracer.

To fully validate the use of FBAs as tracers in squeeze treatments, two set of experiments were performed. First, static tests, the objective of these tests was to assess the effect of the tracer in the presence of scale inhibitors, where the compatibility and efficiency in the presence of scale inhibitors was studied. Secondly, a number of pack columns experiments were performed to investigate the level of adsorption in sandstone and carbonate substrate, the results from the pack-flood experiments indicated negligible adsorption, i.e. they exhibit a conservative behaviour and behave as inert tracers.

What are the conclusions of the validation?

From the validation studies, it can be concluded that FBA tracers are suitable to injected part of a squeeze treatment, they seem to be compatible with common scale inhibitors, they are low concentration detectable, thermal stable, low presence in reservoir brines and behave as common water inert tracers. The tracer slug is recommended to be injected in the overflush stage, in order to maximise the desired features in the return concentration profile and to minimise any unexpected incompatibilities with scale inhibitors or any other additive.

Proposed way forward

What is next in line to be validated?

Although the FBAs under study showed negligible adsorption in sandstone and carbonate packs, the packs were performed 100% water saturation. The next natural step is to study the interaction of these compounds in the presence of oil. A partition coefficient higher than 3 indicates partitioning behaviour, which implies that the compound will be present in the water and oil phase, (Coralie Serres-Piole et al. 2011). Although there are empirical methods to calculate the partition coefficient, partitioning should be evaluated with a number of oils, as well as the corresponding pack floods to investigate the interaction of these compounds in presence of oil, and assess the level of retardation against pure water tracers. Secondly, any iteration between tracer and the chemical inhibitor should be investigated to evaluate the level of retention of scale inhibitors in the presence of FBA and vice versa. Finally, optimise of squeeze treatment/Tracer program to maximise the potential of both.

How can this be validated?

The full validation of the use of FBA tracers should include a number of pack floods at residual oil saturation. Preceding these experiments, the partition coefficient should be determined in the presence of number of oil phases. Secondly, pack floods should be performed in the presence of scale inhibitors, to evaluate any interaction between them in terms of retention levels. Finally, numerical simulator such as Squeeze software, should be use to optimise squeeze treatments including a tracer package, based on the

optimisation studies of squeeze treatment reported before (Vazquez et al. 2017; Vazquez, Fursov, and Mackay 2016).

Final conclusion

The use of FBA tracers in combination with squeeze treatments to estimate chemical placement has been demonstrated. The FBAs under study are compatible with commonly used scale inhibitors, i.e. DETPMP and PPCA, at a range of concentration, pH and temperature. In addition, the presence of tracer does not seem to have a negative effect on the scale inhibition efficiency.

The FBAs under study seem to be behave as ideal water tracers based on the pack columns under study at 100% water saturation. In these experiments, the injection and effluent results were compared against Iodide and Lithium, commonly used as inert tracers.

References

Adams, Michael C., Joseph N. Moore, Laszlo G. Fabry, and Jong Hong Ahn. 1992. "Thermal Stabilities of Aromatic Acids as Geothermal Tracers." *Geothermics* 21 (3): 323–39. doi:10.1016/0375-6505(92)90085-N.

Adams, Mike C, Y Yamada, M Yagi, C Kasteler, P Kilbourn, and N Dahdah. 2004. "Alcohols as Two-Phase Tracers." *Proceedings 29th Workshop on Geothermal Reservoir Engineering, Stanford University*.

Agenet, Nicolas, Navid Moradi-Tehrani, and Olivier Tillement. 2013. "Fluorescent Nanobeads: A New Generation of Easily Detectable Water Tracers." In *International Petroleum Technology Conference*. doi:10.2523/15312-MS.

Brichart, T.B., M.O.M. Metidji, L.F. Ferrando-Climent, and T.B. Bjørnstad. n.d. "New Fluorescent Tracers for SWCTT." In *19th European Symposium on Improved Oil Recovery*.

Deans, H. 1971. Method of determining fluid saturations in reservoirs. US patent #3623842, issued 1971.

Farooqui, N. 2015. "A Detailed Study of the Scale Inhibitor Phase Envelope of Ppca in the Context of Precipitation Squeeze Treatments." Heriot Watt University.

Huseby, Olaf, Mona Andersen, Idar Svorstol, and Oyvind Dugstad. 2008. "Improved Understanding of Reservoir Fluid Dynamics in the North Sea Snorre Field by Combining Tracers, 4D Seismic, and Production Data." *SPE Reservoir Evaluation & Engineering* 11 (4): 15–17. doi:10.2118/105288-MS.

Huseby, Olaf, C. Chatzichristos, J. Sagen, J. Muller, R. Kleven, B. Bennett, S. Larter, A. K. Stubos, and P. M. Adler. 2005. "Use of Natural Geochemical Tracers to Improve Reservoir Simulation Models." *Journal of Petroleum Science and Engineering* 48 (3–4): 241–53. doi:10.1016/j.petrol.2005.06.002.

Huseby, Olaf, Sven K Hartvig, Kjersti Jevanord, Øyvind Dugstad, and Restrack As. 2015. "Assessing EOR Potential from Partitioning Tracer Data." In *SPE Middle East Oil & Gas Show and Conference*. doi:10.2118/172808-MS.

Huseby, Olaf, Randi Valestrand, Geir Nævdal, and Jan Sagen. 2010. "Natural and Conventional Tracers for Improving Reservoir Models Using the EnKF Approach." *SPE Journal* 15 (4): 1–15. doi:10.2118/121190-PA.

Meza, Edgar, Francisco García, Nancy Muñoz, Carlos Reyes, and Arturo Amador. 2007. “Optimization of Tracer Test Design — Practical Applications.” In *International Oil Conference and Exhibition*.

Pritchett, James, Harry Frampton, Joe Brinkman, Steve Cheung, Jim Morgan, K.T. Chang, Dennis Williams, and James Goodgame. 2003. “Field Application of a New In-Depth Waterflood Conformance Improvement Tool.” *SPE International Improved Oil Recovery Conference in Asia Pacific*. doi:10.2118/84897-MS.

Sanni, Modiu L, Mohammed A Al-Abbad, Sunil L Kokal, Saudi Aramco, Sven Hartvig, Huseby Olaf, and Kjersti Jevanord. 2015. “A Field Case Study of Inter-Well Chemical Tracer Test.” In *SPE International Symposium on Oilfield Chemistry*, 13–15. doi:10.2118/173760-MS.

Seccombe, Jim, Arnaud Lager, Gary Jerauld, Bharat Jhaveri, Todd Buikema, Sierra Bassler, John Denis, Kevin Webb, Andrew Cockin, and Esther Fueg. 2010. “Demonstration of Low-Salinity EOR at Interwell Scale, Endicott Field, Alaska.” *SPE Improved Oil Recovery Symposium* 2008. doi:10.2118/129692-MS.

Serres-Piole, C., H. Preud’homme, N. Moradi-Tehrani, C. Allanic, H. Jullia, and R. Lobinski. 2012. “Water Tracers in Oilfield Applications: Guidelines.” *Journal of Petroleum Science and Engineering* 98–99. Elsevier: 22–39. doi:10.1016/j.petrol.2012.08.009.

Serres-Piole, Coralie, Annie Commarieu, Hervé Garraud, Ryszard Lobinski, and Hugues Preud’Homme. 2011. “New Passive Water Tracers for Oil Field Applications.” *Energy and Fuels* 25 (10): 4488–96. doi:10.1021/ef2007485.

Sorbie, K S, Ping Jiang, M D Yuan, Ping Chen, M M Jordan, and a C Todd. 1993. “The Effect of pH, Calcium, and Temperature on the Adsorption of Phosphonate Inhibitor Onto Consolidated and Crushed Sandstone.” *SPE Annual Technical Conference and Exhibition*, 1–16. doi:10.2118/26605-MS.

Vazquez, O., I. Fursov, and E.J. Mackay. 2016. “Automatic Optimization of Oilfield Scale Inhibitor Squeeze Treatment Designs.” *Journal of Petroleum Science and Engineering* 147: 302–7. doi:10.1016/j.petrol.2016.06.025.

Vazquez, O., E. Mackay, T. Tjomsland, O. Nygård, and E. Storås. 2014. “Use of Tracers To Evaluate and Optimize Scale-Squeeze-Treatment Design in the Norne Field.” *SPE Production & Operations* 29 (1): 5–13. doi:10.2118/164114-PA.

Vazquez, O., Gi. Ross, M. Jordan, D. A. Angga, E.J. Mackay, and C. Johnson. 2017. “Automatic Optimisation of Oilfield Scale Inhibitor Squeeze Treatments Delivered by DSV.” In *SPE International Conference on Oilfield Chemistry*.

Vazquez, O., C. Young, V. Demyanov, D. Arnold, A. Fisher, A. Macmillan, and M. Christie. 2015. “Produced-Water-Chemistry History Matching in the Janice Field.” *SPE Reservoir Evaluation and Engineering* 18 (4).

Vazquez, O., C. Young, V. Demyanov, D. Arnold, A. Fisher, A. MacMillan, and M. Christie. 2014. “Estimating Scale Deposition through Reservoir History Matching in the Janice Field.” *SPE Production & Operations* 29 (1): 21–28.

Zemel, B. 1995. *Tracers in the Oil Field*. Elsevier.

Center for Olie og Gas - DTU
Danish Hydrocarbon Research and Technology Centre
Technical University of Denmark

Elektrovej 375
2800 Kgs. Lyngby
Tlf. 45 25 72 10

www.oilgas.dtu.dk